J. Nannoplankton Res., **39**(1), 2021, pp. 29–75 © 2021 International Nannoplankton Association
ISSN 1210-8049 Printed by The Sheridan Press, USA

Ultrastructure and taxonomy of the family Sphenolithaceae

Richard Howe
Ellington Geological Services, 1414 Lumpkin Road, Houston, TX 77043, USA; richard.howe@ellingtongeo.com

Manuscript received 21st August, 2020; revised manuscript accepted 26th March, 2021

Abstract Coccolith species belonging to the family Sphenolithaceae, in the genera *Sphenolithus* and *Furcatolithus*, are widespread and common throughout most of the Cenozoic. This study details their ultrastructure, emphasising the importance of recognising their major structural components. In *Sphenolithus*, these are: 1) the proximal element cycle; 2) the lower lateral element cycle; 3) the upper lateral element cycle; and 4) the apical structure. In *Furcatolithus*, these are: 1) the proximal element cycle; and 2) the bifid spine, which is derived from the upper lateral element cycle in *Sphenolithus*. The evolutionary transition from *Sphenolithus* to *Furcatolithus* involved loss of the lower lateral element cycle and the apical structure, and upward growth of the upper lateral element cycle into the bifid spine. Here, 65 species are recognised as valid within the Sphenolithaceae (48 in *Sphenolithus* and 17 in *Furcatolithus*) and are described in detail. Two new species—*Sphenolithus shamrockiae* n. sp. and *S. bergenii* n. sp—are introduced. The family Sphenolithaceae, the genera *Sphenolithus* and *Furcatolithus* and the species *S. furcatolithoides* and *S. delphix* are emended. Sixteen species previously assigned to *Sphenolithus* are recombined into *Furcatolithus*––*F. akropodus*, *F. avis*, *F. bulbulus*, *F. celsus*, *F. ciperoensis*, *F. cuniculus*, *F. directus*, *F. intercalaris*, *F. obtusus*, *F. patifunditis*, *F. peartiae*, *F. predistentus*, *F. tawfikii*, *F. triangularis*, *F. tribulosus* and *F. umbrellus*.

Keywords nannofossils, coccoliths, Discoasterales, Sphenolithaceae, *Sphenolithus*, *Furcatolithus*, Cenozoic, Neogene, Palaeogene, taxonomy, ultrastructure

1. Introduction

The family Sphenolithaceae is a group of Cenozoic calcareous nannofossils that originated in the Late Paleocene (Late Danian) and flourished until the end of the Early Pliocene (Zanclean). They are one of the most important groups used in Cenozoic nannofossil biostratigraphy, but differentiating among species is often difficult because many species share the same basic structure, but with varying proportions of the major components. The two genera included in the Sphenolithaceae—*Sphenolithus* and *Furcatolithus*—are clearly related; however, there are major ultrastructural differences between them that have not been fully recognised in previous studies.

This study arose from the realisation that the upper and lower lateral element cycles present in *Sphenolithus* coccoliths have been conserved throughout the geological history of the genus, and hence are fundamentally important characteristics for discriminating between species. Previous studies have tended to consider the lateral element cycles in two fundamentally different ways: 1) as part of the base of the coccolith (e.g. the upper pair of the four basal quadrants of Young et al., 1997); or 2) as part of the upper part of the coccolith (e.g. the lower part of the calyptra of Aubry, 2014). In both instances, the resulting two-part ultrastructural division minimises the importance of the lateral element cycles.

Four distinct ultrastructural components of *Sphenolithus* species were distinguished in this study (Figures 1–4): 1) the proximal element cycle; 2) the lower lateral element cycle; 3) the upper lateral element cycle; and 4) the apical structure. The characterisation and subsequent recognition of *Sphenolithus* species requires that all four of these components are described fully. In this study, all previously described species of *Sphenolithus* were considered, as well as those ascribed to other genera considered to belong to the Sphenolithaceae. The taxonomy was rationalised, and all valid species were described using a common ultrastructural framework and terminology.

Once the importance of the lateral element cycles in *Sphenolithus* species was understood, it was further recognised that, in the lineage that arose with *Sphenolithus kempii,* the upper lateral element cycle underwent a series of modifications through time. The upper lateral element cycle in species of this lineage increased in height vertically over time, with the number of elements in the cycle being reduced, ultimately to two. Concurrently, the apical structure diminished and eventually disappeared.

The modified upper lateral element cycle became a vertically split, two-part spine, here termed the bifid spine (Figures 1H–K, 3B, 4), with a very different appearance to the upper lateral element cycle it was derived from. With subsequent loss of the lower lateral element cycle, the lin-

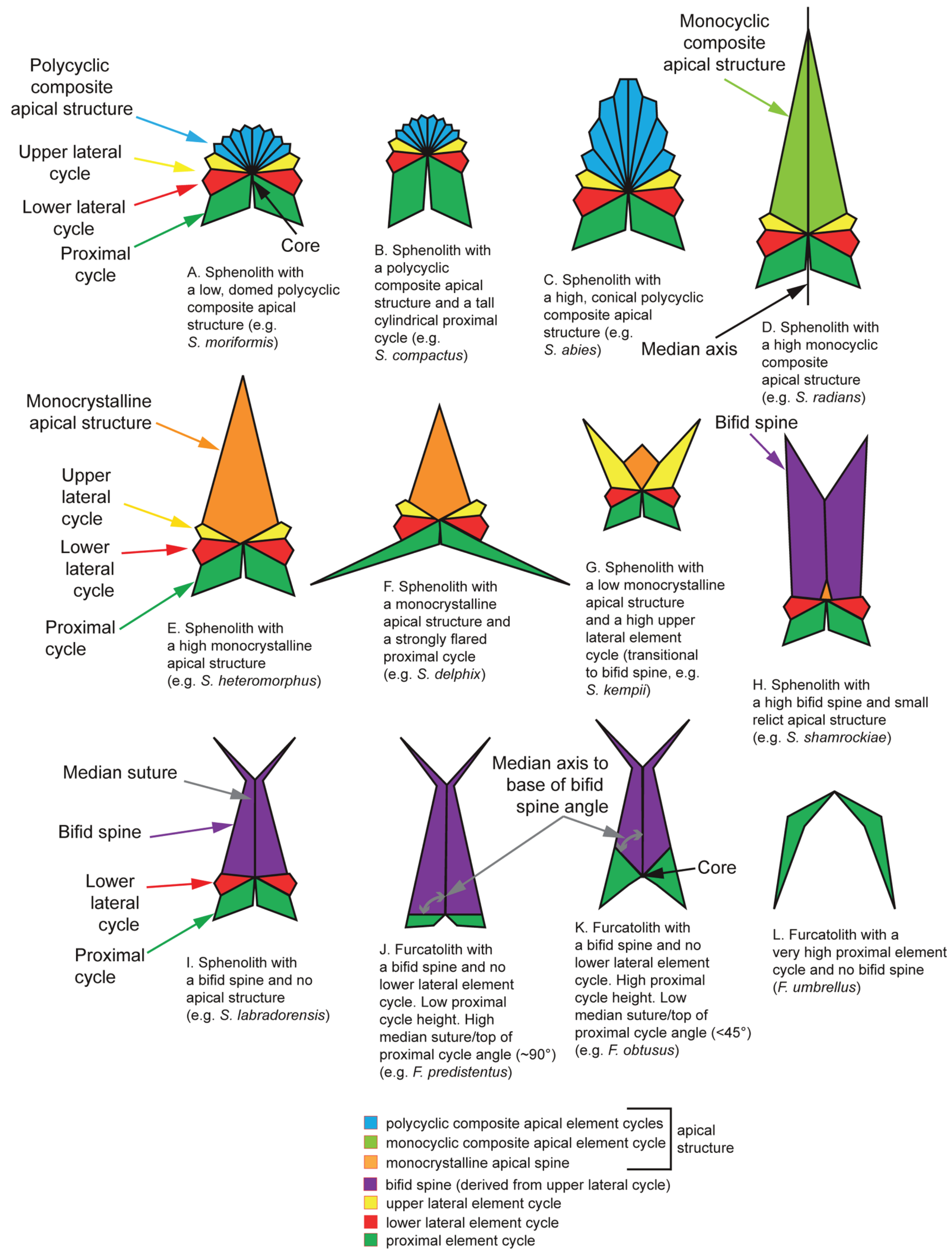

Figure 1: Schematic sketches showing the ultrastructural components of sphenolithid species and variations in their proportions. For each sketch, an example of a species showing the same characteristics is listed. Only elements with the long axes parallel to the plane of the slide are shown

eage that resulted has clear structural differences from the *Sphenolithus* species it descended from. Species in this diverged lineage were recombined here into the emended genus *Furcatolithus*. In clear contrast to the four distinct ultrastructural components in *Sphenolithus*, species in *Furcatolithus* only have two.

2. Origin of the family

Species in the family Sphenolithaceae are considered here to be heterococcoliths in the order Discoasterales. They are constructed of vertically stacked cycles of radially oriented elements, with radial *c*-axes in each element. Aubry (2014) indicated that the earliest known species in the Sphenolithaceae descended from the Danian genus *Diantholitha* Aubry *in* Aubry et al. (2011), based on strong similarities in the proximal element cycles of *Diantholitha* and early specimens of *Sphenolithus primus*. Above the proximal cycle, *Diantholitha* has a single distal cycle of elements, in contrast to the multiple element cycles in *S. primus*.

The addition of extra cycles of elements above the distal cycle in *Diantholitha* is a plausible step in the transition between the two genera. Aubry (2014) considered *Diantholitha* to be descended from the Early Danian genus *Biantholithus*, which has well-documented occurrences of intact coccospheres (Mai, 2001), and is clearly a coccolithophorid. Speculation by Towe (1979, fig. 8) and Aubry (2014, text-fig. 27a, b) that *Sphenolithus* and *Furcatolithus* form coccospheres, with the concave (proximal) surface of the coccoliths being situated adjacent to the living cell, is certainly plausible, although there is little evidence to support the interpretation by Towe (1979, p. 569) that the coccoliths on these coccospheres were polymorphic.

3. Morphology and ultrastructure

Species in the Sphenolithaceae show a range of gross morphologies that are all roughly cylindrical, in contrast to most heterococcoliths, which are approximately disc-

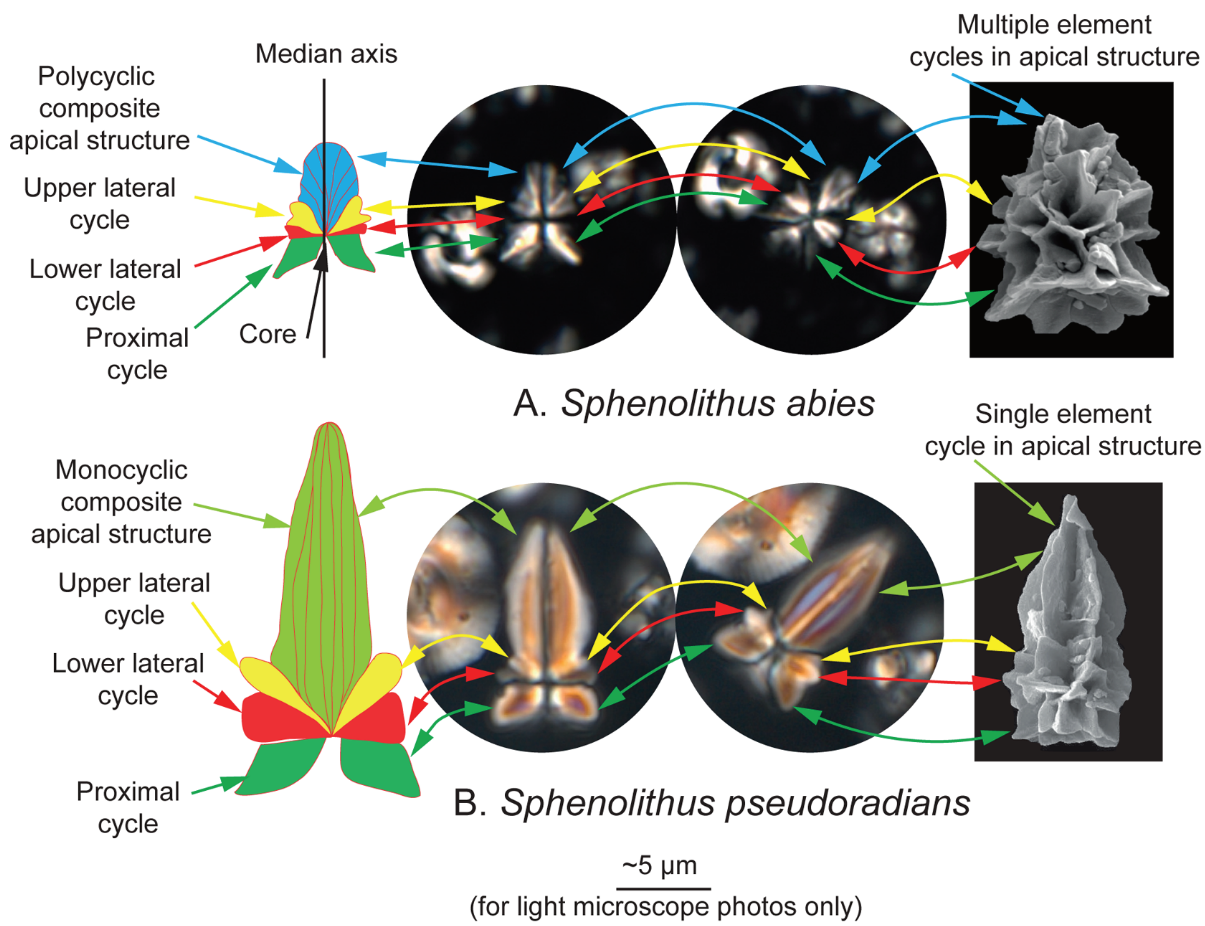

Figure 2: Schematic sketches (based on holotype specimens) showing the major ultrastructural components of (**A**) *S. abies* and (**B**) *S. pseudoradians*. Only elements with the long axes parallel to the plane of the slide are shown

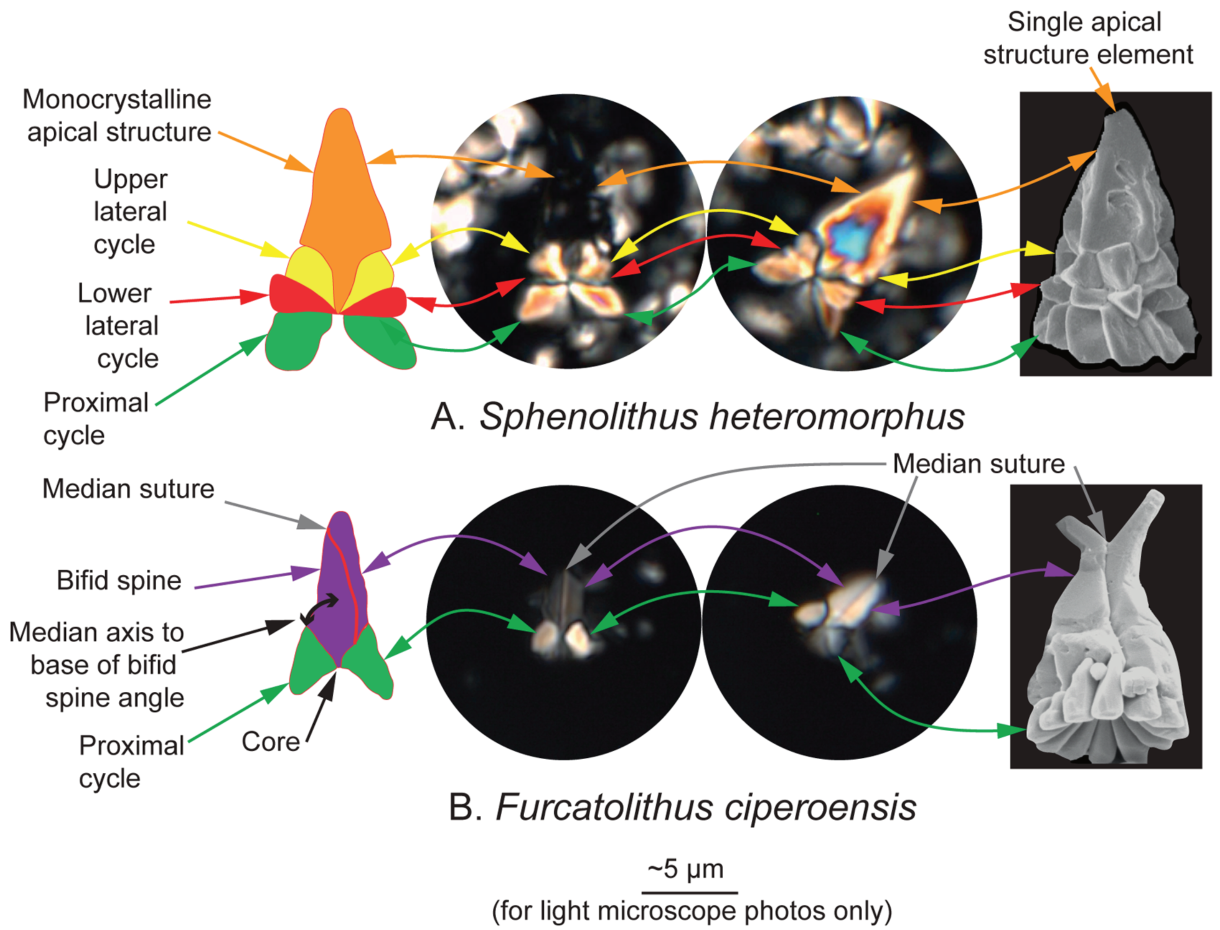

Figure 3: Schematic sketches (based on holotype specimens) showing the major ultrastructural components of (**A**) *S. heteromorphus* and (**B**) *F. ciperoensis*. Only elements with the long axes parallel to the plane of the slide are shown

shaped. Although, without preserved coccospheres, we cannot be sure of the original orientation of such cylindrical coccoliths, the generally broader, concave end is assumed to be the proximal end, with the opposite end assumed to be the distal end. The distal surface of coccoliths in the Sphenolithaceae may be rounded, flat or spinose, conical or flaring, and may bifurcate or be spinose. The basal surface is always concave, above which there is one or more stacked cycles of lath-shaped elements, arranged radially around the median axis of the coccolith. The basal cycle, termed the proximal cycle, is similar in all members of the Sphenolithaceae, reflecting their common origin (Figures 1–4). The upper central point of the proximal cycle, on the median axis, is termed the core (Young et al., 1997), and is the point from which all of the elements in the coccolith radiate (Figures 1–4).

Coccoliths belonging to the genus *Sphenolithus* are termed sphenoliths. Above the proximal cycle, species in this genus have two vertically stacked element cycles—the lower and upper lateral cycles (Figures 1A–G, 2, 3A, 4). Previously, this term has been used for all members of the family, but here it is strictly limited to species that have both lower and upper lateral element cycles and belong to the genus *Sphenolithus*.

Above the upper lateral element cycle in most sphenoliths, there is an apical structure, which may comprise a single vertical or sub-vertical element, termed a monocrystalline apical structure (Figures 1E–G, 3A), or single or multiple cycles of elements, termed monocyclic (Figure 1D) or polycyclic (Figures 1A–C, 2A) composite apical structures, respectively. Some sphenoliths completely lack any apical structure (e.g. *S. labradorensis*, Plate 2, figs 7–10).

Species in the Sphenolithaceae that lack a lower lateral element cycle belong to the genus *Furcatolithus* (Figures 1J–L, 3B, 4). All species in this genus lack any apical structure. Coccoliths of these species are here referred to as furcatoliths. The presence or absence of the lower

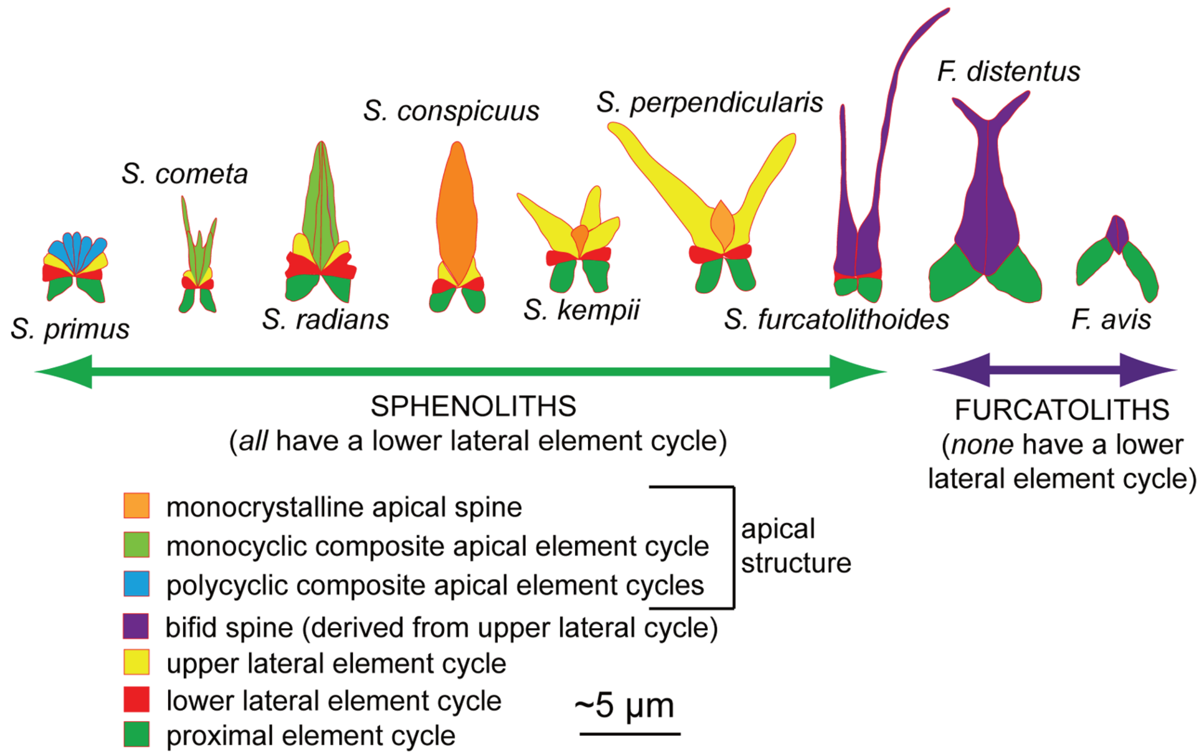

Figure 4: Schematic sketches of a range of sphenoliths and furcatoliths (based on holotype or paratype specimens) showing the major ultrastructural components. Only elements with the long axes parallel to the plane of the slide are shown

lateral cycle is the major structural difference between *Sphenolithus* and *Furcatolithus*, and is used here as the primary criterion for separating them (Figure 4). In some sphenoliths and all furcatoliths (except the last furcatolith species, *F. umbrellus,* which usually lacks any structure above the proximal cycle), the upper lateral element cycle is present, but is reduced to two elements, and is greatly enlarged vertically, forming a bifurcated distal spine. This spine is here termed the bifid spine (Figures 1H–K, 3B, 4). The structural components of sphenoliths and furcatoliths are discussed in detail below.

3.1 Element shape and arrangement

In electron microscope (EM) images of well-preserved specimens of many sphenolith species, it is evident that the individual elements are elongated, triradiate laths, with three blades extending at varying angles to the long axis of the elements, resulting in a 'Y' shape in cross-section (Figure 5). The intersection of the blades is here termed the blade axis. The three blades of each element share a single *c*-axis orientation, suggesting that the blades are all part of a single crystal of calcite. Individual elements showing this triradiate morphology were termed triades by Aubry (2014). The fact that early *Sphenolithus* species (e.g. specimens of *Sphenolithus primus* in Bybell & Self-Trail, 1997, pl. 5, fig. 8) and one of the last surviving species (e.g. specimens of *S. abies* in Figure 5, and in Perch-Nielsen, 1972, pl. 17, fig. 6) both possess similar-shaped triradiate elements demonstrates that this ultrastructure has been conserved throughout the history of the genus, particularly in species belonging to the long-ranging *S. primus* group, from which all other groups of sphenoliths are here interpreted to have evolved.

In well-preserved sphenoliths with triradiate elements, their blades can be seen to form a honeycomb structure (see the scanning electron microscope [SEM] images in Figures 2A, 5). The blades of each element are adjoined to the blades of either adjacent elements, or the blades of elements in the cycle above or below. Where the blades from adjacent or higher/lower elements adjoin each other, the suture where the blades meet is here termed a blade junction (Figure 5). With diagenetic calcite overgrowth, the space between the blades in each element is filled in, and the elements assume an overall lath shape. Not all elements in sphenoliths are triradiate. For example, the apical structure in *S. heteromorphus* is a monocrystalline,

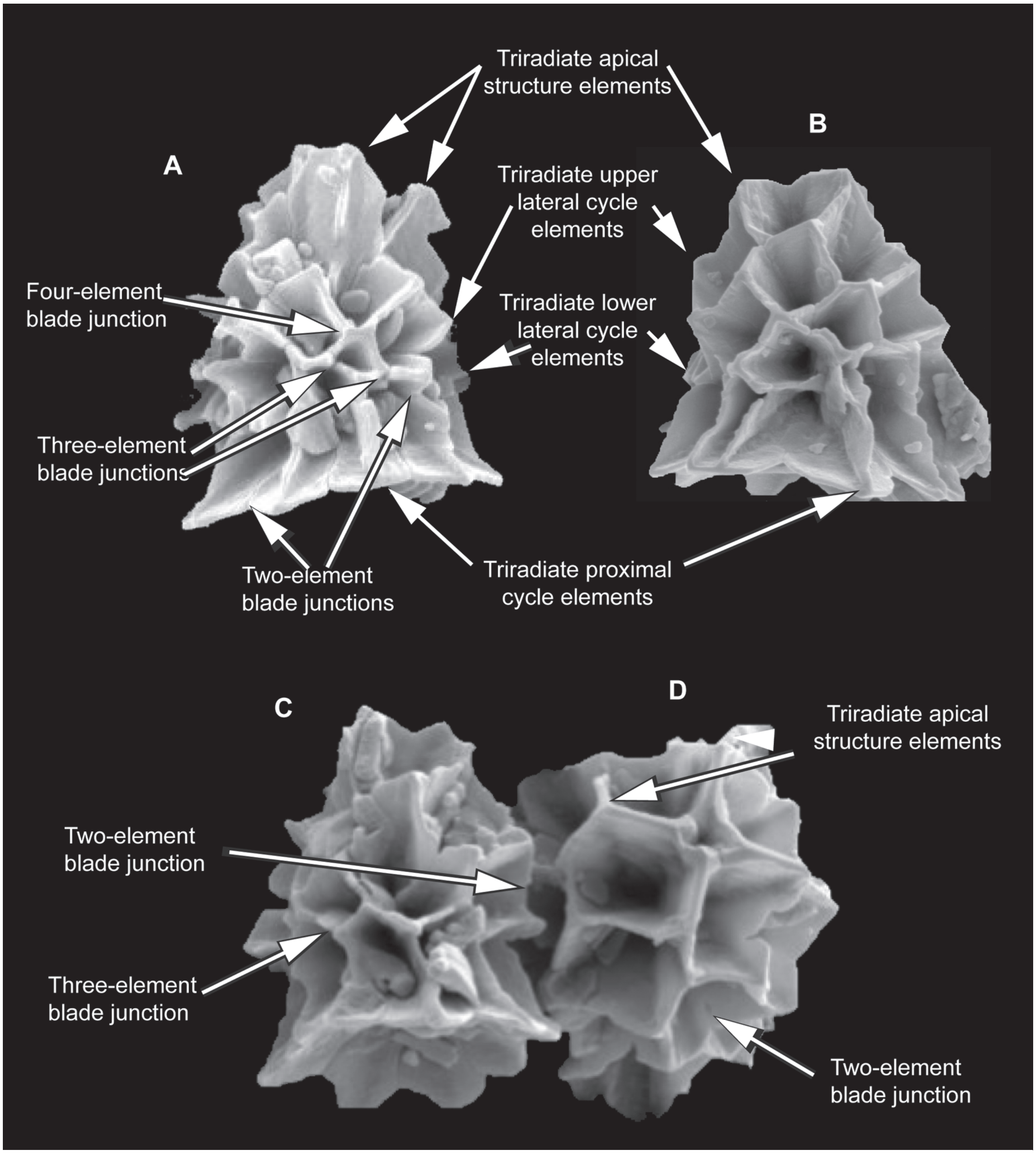

Figure 5: SEM photomicrographs of typical specimens of *S. abies* showing the triradiate-bladed shape of each element and the different types of junctions between adjacent blades. The distribution of two-, three- and four-element blade junctions imparts a pervasive asymmetry to these specimens

biconical spine (Figure 3A, Plate 3, figs 7, 8). There are no published photographs of furcatoliths with triradiate elements, which may indicate that they are more susceptible to diagenetic overgrowth than sphenoliths, or that bladed elements are not a primary feature of furcatoliths.

In all sphenoliths, there are a greater number of elements in the proximal cycle than in the uppermost distal cycle (i.e. the apical structure in most sphenoliths or the bifid spine in some sphenoliths). The lateral element cycles have intermediate numbers of elements. Where the element count between two adjacent cycles differs by an odd number, it is not possible for the blades in these cycles to be adjoined in a regular way, where two blades (one from the lower cycle and one from the upper cycle) meet to form a blade junction. The difference in the element count between adjacent cycles is accommodated by blade junctions where three, or even four (rather than the usual two), blades meet. The apparently irregular distribution of two-, three- and four-element blade junctions throughout these sphenoliths results in a pervasive asymmetry in the arrangement of elements in the sphenolith. Three- and four-element blade junctions have been observed in almost all SEM photomicrographs of well-preserved *S. abies* (Figure 5). It is assumed here that variable-element blade junctions, and the pervasive asymmetry that results from these, are a characteristic of most, if not all, *Sphenolithus* species.

3.2 Calcite *c*-axis orientation and birefringence patterns

In most sphenolithid species, the *c*-axis of the calcite crystal comprising each individual element is aligned with the long axis of the element. For elements in the horizontal plane (i.e. the plane of the microscope slide), the primary control on birefringence is the angle between the long axis of the element and the polarising axes. When the median axis of the sphenolithid is aligned with one of the polarising axes, the elements with long axes that are near vertical or horizontal will be dark under cross-polarised light. Elements with long axes that are near 45° to the polarising axes will be bright, and those with long axes between ~10 and 35° will be partially bright or dim.

In specimens where the blades of each element are well-preserved, the orientation of each individual blade affects the observed birefringence of the element. Blades that are at, or near, right angles to the plane of the microscope slide will have higher birefringence than the other two blades of the same element (when the element is brightest; i.e. when its long axis is at 45° to the polarising axes), as they present a greater thickness of calcite relative to the plane of the slide (i.e. the full width of the blade). This is best observed in large specimens that are very well preserved (e.g. the holotype of *S. acervus,* Bown, 2005a, pl. 43, fig. 15), and that may give the appearance of there being more elements than are actually present. In most specimens, where some overgrowth is present, this blade effect is minimal compared to the overall orientation of the element relative to the polarising axes and the plane of the slide.

In sphenolithids that possess a bifid spine (Figure 6), the *c*-axes of the elements in the bifid spine may not be closely aligned with the long axis of each element, instead being at an angle of ~10–45° to the median axis of the coccolith. For angles between ~30 and 45° between the *c*-axes of the bifid spine elements and the median axis, the spine elements will be bright when the median axis is parallel to one of the polarising axes, and dark when the median axis is at 45° to the polarising axes (see *S. shamrockiae* n. sp., Plate 2, figs 3, 4). For angles between 15 and 30°, the spine elements will be dim (i.e. partially bright) at both parallel, and at 45°, to the polarising axes (see *Furcatolithus akropodus* n. comb., Plate 4, figs 15, 16). For angles of less than 15°, the spine elements will be dark when parallel to one of the polarising axes, and bright at 45° to the polarising axes (see *F. ciperoensis* n. comb., Plate 4, figs 23, 24).

Many published light-microscope (LM) photomicrographs of sphenolithids are over-exposed, including the images of many holotypes (e.g. the images of the holotype of *S. belemnos* in Bramlette & Wilcoxon, 1967 and *S. capricornutus* in Bukry & Percival, 1971). Because the elements of the four structural components in *Sphenolithus* (proximal cycle, lower lateral element cycle, upper lateral cycle and apical structure) have *c*-axes that radiate from the core, each of the elements is dark when parallel to one of the polarising axes, bright when at, or near, 45°, and neither fully bright nor dark when oriented obliquely to the polarising axes. Recognition of the upper and lower lateral cycles is generally easy in the LM, but can be very difficult in over-exposed photographs, hindering the assignment of specimens in the LM to published species.

3.3 Proximal cycle

All sphenolithids share a proximal cycle (Young et al., 1997) of adpressed elements that are arranged radially in plan view (Figures 2, 3), often with slight imbrication and suture kinking (see pl. 2, fig. 4 in Wilcoxon, 1970). In lateral view, the proximal cycle elements are approximately trapezoidal in outline. In well-preserved material, the proximal cycle elements are bladed, with two sub-horizontal blades and one vertical blade extending laterally from each element (see Figure 5C).

The elements of the proximal cycle vary in height and lateral extension of the base of the element relative to the top (termed the degree of flare) between species. Some species have minimal lateral extension of the base of the proximal cycle relative to the top (low degree of flare),

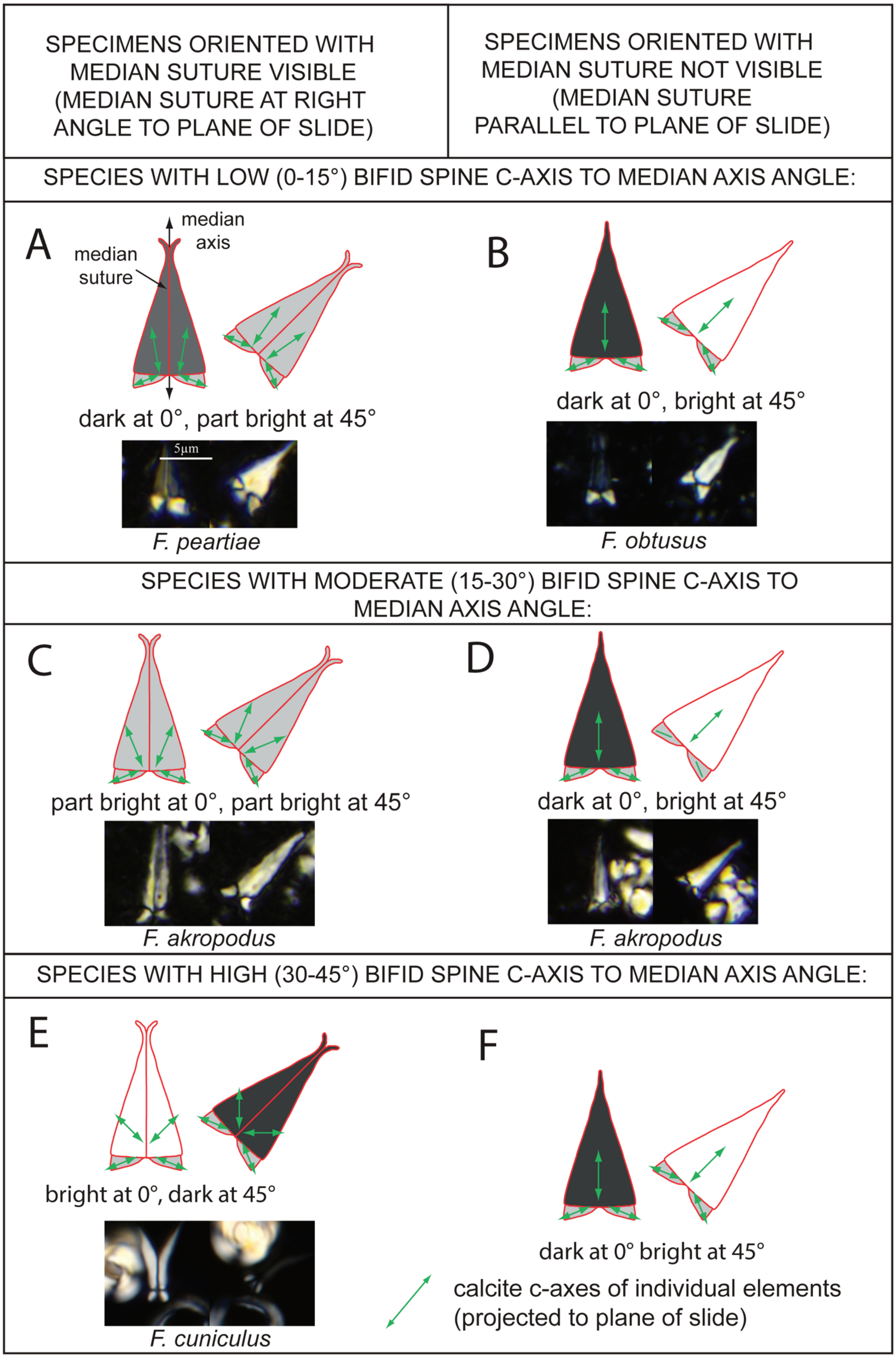
SPECIMENS ORIENTED WITH MEDIAN SUTURE VISIBLE (MEDIAN SUTURE AT RIGHT ANGLE TO PLANE OF SLIDE)
SPECIMENS ORIENTED WITH MEDIAN SUTURE NOT VISIBLE (MEDIAN SUTURE PARALLEL TO PLANE OF SLIDE)
SPECIES WITH LOW (0-15°) BIFID SPINE C-AXIS TO MEDIAN AXIS ANGLE:
A
median axis
median suture
dark at 0°, part bright at 45°
5µm
F. peartiae
B
dark at 0°, bright at 45°
F. obtusus
SPECIES WITH MODERATE (15-30°) BIFID SPINE C-AXIS TO MEDIAN AXIS ANGLE:
C
part bright at 0°, part bright at 45°
F. akropodus
D
dark at 0°, bright at 45°
F. akropodus
SPECIES WITH HIGH (30-45°) BIFID SPINE C-AXIS TO MEDIAN AXIS ANGLE:
E
bright at 0°, dark at 45°
F. cuniculus
F
dark at 0° bright at 45°
calcite c-axes of individual elements (projected to plane of slide)

resulting in an approximately cylindrical proximal cycle with a sub-vertical lateral periphery (e.g. *S. dissimilis,* Plate 2, figs 23, 24). Others have strong lateral extension of the base (high degree of flare), resulting in a proximal cycle with a lateral periphery that is at a low angle to the vertical (e.g. *S. delphix,* Plate 3, figs 19–22). In lateral view, the basal surface of each element can be linear or curved, resulting in the basal surface of the proximal cycle being concave to a greater or lesser degree. The general form of the proximal cycle is similar among all sphenolithid species, reflecting their common origin. The proximal cycle has been termed the proximal shield or column by Roth et al. (1971) and Perch-Nielsen (1985), the column by Romein (1979) and Aubry (2014), and the basal feet by Bown & Dunkley Jones (2012).

3.4 Lateral element cycles

All sphenoliths have two lateral element cycles (Young et al., 1997)—the lower and upper lateral element cycles—which lie above the proximal element cycle, and below the apical structure, if one is present (Figures 1A–I, 2A, B, 3A, 4). In well-preserved material, it can be seen that the elements in the lateral cycles are bladed, with the blades of each element joined at blade junctions to the blades in adjacent element cycles. In most species, the long axes of the lower lateral cycle elements are sub-horizontal in lateral view, and those of the upper lateral cycle elements lie at approximately 45° to the median axis. Elements in each of the lateral element cycles are arranged radially in plan view. Other, similar cycles may exist above the two lateral cycles (see the discussion on the apical structure, below), but in all sphenoliths, there are always two lateral element cycles. The lateral element cycles vary between species in their thickness, height and degree of lateral extension. The lateral element cycles have been termed the basal cycles by Romein (1979), the lower calyptra by Aubry (2014) and the lateral elements by Roth et al. (1971) and Perch-Nielsen (1985).

Much confusion exists in the literature regarding the upper and lower lateral cycles and their distinction from each other, and from the proximal cycle, in cross-polarised light. Many workers have referred to the four bright elements seen in the base of a typical sphenolith under cross-polarised light as the upper and lower basal quadrants or ‘basal quads’ (Young et al., 1997; Bergen et al., 2017). The lower quadrants are the birefringent elements of the proximal cycle, while the upper quadrants are the birefringent elements of the two lateral element cycles. Many species descriptions refer to the size ratios between the upper and lower quadrants.

This is problematic because, when a sphenolith is rotated relative to the polariser, the lower and upper lateral element cycles alternate their birefringence relative to each other. Effectively, the bright upper quadrants are reflecting the birefringence of different elements as the sphenolith is rotated (the upper lateral element cycle is bright when the median axis is parallel to one of the polarising axes, and the lower lateral element cycle is bright when the median axis is at 45° to the polarising axes), making size ratios between the upper and lower basal quadrants an unreliable criterion for distinguishing between species, unless one is clear on which lateral cycle is bright when the size ratio is being observed.

Figure 6 (left): Sketches showing the birefringence of taxa with a bifid spine, indicating that the angle between the calcite *c*-axes in the bifid spine elements and the median suture, *and* the orientation of the plane of the median suture of the bifid spine, relative to the plane of the slide, *both* strongly affect the birefringence observed in the bifid spine in the LM. Only elements with the long axes lying parallel to the plane of the slide are shown. (**A, B**) Species with the *c*-axis of the bifid spine elements lying between 0 and 15° to the median axis. (**A**) When the specimen is oriented with the plane of the median suture lying orthogonal to the slide, the bifid spine is dark (but not fully so) at 0° to the optical axes, and bright (but not fully so) at 45°. (**B**) When the same specimen is lying on the slide with the plane of the median suture lying parallel to the slide, the bifid spine is fully dark at 0° to the optical axes, and fully bright at 45°. (**C, D**) Species with the *c*-axis of the bifid spine elements lying between 15 and 30° to the median axis. (**C**) When the specimen is lying on the slide with the plane of the median suture lying orthogonal to the slide, the bifid spine is moderately bright at 0° to the optical axes, and also moderately bright at 45°. (**D**) When the same specimen is lying on the slide with the plane of the median suture lying parallel to the slide, the bifid spine is fully dark at 0° to the optical axes, and fully bright at 45°. (**E, F**) Species with the *c*-axis in the bifid spine elements lying between 30 and 45° to the median axis. (**E**) When the specimen is lying on the slide with the plane of the median suture lying orthogonal to the slide, the bifid spine is fully bright at 0° to the optical axes, and dark at 45°. (**F**) When the same specimen is lying on the slide with the plane of the median suture lying parallel to the slide, the bifid spine is fully dark at 0° to the optical axes, and fully bright at 45°

3.5 Apical structure

In most sphenolith species, there are one or more element cycles above the upper lateral element cycle. The elements in these cycles are arranged in lateral (i.e. horizontal) to distal (i.e. vertical) orientations, radiating from the core (Figures 1A–H, 2A, B, 3A, 4, 5). These form the apical structure. The apical structure can comprise either a single element, termed a monocrystalline apical structure (Figures 1E–G, 3A), or multiple elements, termed a composite apical structure (Figures 1A–D, 2A, B). A composite apical structure may have a single cycle of elements, termed a monocyclic composite apical structure (Figures 1A–D, 2B, 4), or multiple cycles of elements, termed a polycyclic composite apical structure (Figures 1A–C, 2A, 4). Where there is a polycyclic composite apical structure (other than their position above the lateral element cycles), the elements in the apical cycles are usually minimally differentiated from the elements of the lateral element cycles (e.g. in species of the *S. primus* group). For all composite apical structures, it can be seen in well-preserved material that the elements in the apical structure are bladed, with blades from each element joining at blade junctions to the blades in adjacent element cycles (Figure 5). The apical structure has been referred to as the apical spine by Roth et al. (1971), the cone or centro-distal spine by Romein (1979), the apical spine or apical elements by Perch-Nielsen (1985) and the upper calyptra by Aubry (2014).

The long-ranging *S. primus* group, from which all other sphenoliths are descended, has a polycyclic composite apical structure that is hemispherical in shape. The evolution of new species of *Sphenolithus* involves modification of this apical structure (and also changes in the shape of the proximal cycle). There seems to be a trend in which a lineage begins with a new species that evolves a monocyclic composite apical structure from a polycyclic ancestor in the *S. primus* group. Once a monocyclic composite apical structure has been established, the apical structure often becomes taller, turning into a monocrystalline apical structure in later species in the lineage. An example of this can be seen in the *S. radians* group, where *S. editus*, with a monocyclic composite apical structure, evolved from *S. moriformis* (Plate 1, figs 5, 6) or *S. apoxis* (Plate 1, figs 9, 10), with polycyclic composite apical structures. Later, *S. richteri*, with a monocrystalline apical structure, evolved from *S. spiniger* (Plate 1, figs 23, 24), with a monocyclic composite apical structure. Monocrystalline apical structures have evolved from monocyclic composite apical structures several times, so species with monocrystalline apical structures are clearly polyphyletic and cannot be grouped together.

Monocyclic composite apical structures with a conical shape can be distinguished from monocrystalline apical structures with a similar shape by their diffuse extinction when aligned with one of the major polarising axes (reflecting multiple elements radiating from the core, at slight angles to each other, e.g. *S. conicus,* Plate 2, figs 29, 30), in contrast to the total extinction of a monocrystalline apical structure (e.g. *S. heteromorphus,* Plate 3, figs 7, 8). In some species, there is a cycle of small, thin apical elements above the upper lateral element cycle, above which there is a tall monocrystalline apical structure (e.g. *S. pseudoheteromorphus,* Plate 3, figs 5, 6; also, see the holotype specimen in Fornaciari & Agnini, 2009, pl. 1, fig. 1).

3.6 Bifid spine

In later members of the *S. kempii* group, the apical structure is reduced in height. The upper lateral element cycle has grown vertically, and has a reduced element count, down to three or four elements in *S. kempii* (Figure 1G; Plate 1, figs 27, 28), and two in *S. shamrockiae* n. sp. (Figure 1H; Plate 2, figs 3–6), *S. furcatolithoides* (Plate 2, figs 1, 2) and *S. labradorensis* (Figure 1I; Plate 2, figs 7–10). With vertical growth of the upper lateral element cycle, the apical structure becomes relatively lower, eventually disappearing completely in *S. furcatolithoides* and *S. labradorensis*. Effectively, in *S. furcatolithoides* and *S. labradorensis,* with vertical growth of the upper lateral cycle, and reduction in the element count to two elements, the upper lateral cycle becomes the dominant apical element, at the expense of the apical structure, which has disappeared. This highly modified upper lateral element cycle is here termed the bifid spine and is a key characteristic of most species in the genus *Furcatolithus*, which is descended from the *S. kempii* group. The bifid spine becomes reduced in size in the *F. triangularis* group, becoming miniscule or disappearing completely in the transition between *F. avis* n. comb. (Plate 4, figs 27, 28) and *F. umbrellus* n. comb. (Figure 1L; Plate 4, figs 29, 30)—the last representative of the genus. The bifid spine has been referred to as a duocrystalline spine by Bown & Dunkley Jones (2012) and Bergen et al. (2017).

There is considerably more variation in the birefringence pattern in the bifid spine in the furcatoliths (and those sphenoliths in the *S. kempii* group that have a bifid spine) than there is variation in the birefringence of the apical structure among most sphenoliths. Morphologically similar species can have essentially opposite birefringence patterns in the bifid spine under cross-polarised light, based solely on differing *c*-axis orientations in the bifid spine (Figure 6). This is in contrast to most sphenoliths (i.e. those that lack a bifid spine), where the *c*-axis orientations are always parallel to the long axis of each individual element, so the birefringence of an element is based largely on its position in the sphenolith structure and its thickness.

Because the bifid spine has two elements, separated by a median plane, the orientation of the spine relative to the plane of the microscope slide is critically important in determining the observed birefringence of the spine under cross-polarised light. When the specimen is oriented so that the median plane of the spine is horizontal (i.e. parallel to the slide), the bifid spine appears as a single element in the LM (Figure 6b, d, f). When the median axis of the specimen is aligned with one of the polarising axes, the bifid spine is dark, and when the specimen is aligned at 45° to the polarising axes, it is bright. In this orientation (with the median plane of the bifid spine being horizontal), the angle between the *c*-axes of the bifid spine elements and the median axis of the coccolith (typically between 10° and 45°) has no effect on the birefringence, so different species, with different *c*-axis angles in the bifid spine, will display similar birefringence.

In contrast, when the median plane of the bifid spine is vertical (i.e. at right angles to the plane of the slide), the median plane appears as a sharp suture down the middle of the bifid spine (Figure 6a, c, e). The two elements of the spine are clearly visible, and their birefringence depends on the orientation of their *c*-axes in the horizontal plane. The *c*-axes in the bifid spine elements are typically between 10 and 45° to the median axis of the coccolith, so, depending on the *c*-axis orientation, the birefringence when the median axis is parallel to one of the polarising axes could be bright (for specimens with the *c*-axis between 35 and 45°: Figure 6e), dark (for specimens with the *c*-axis at an angle between 10 and 15°: Figure 6a) or dim (angles between 15 and 35°: Figure 6c).

The best example of this is *S. labradorensis* (Plate 2, figs 7–10; junior synonym *S. strigosus*), which was illustrated with a median suture clearly visible, and bifid spine elements that are brightly birefringent when parallel to the polarising axes and dark at 45° (Firth, 1989, pl. 2, figs 15, 16). The holotype of the otherwise similar *S. runus* (Bown & Dunkley Jones, 2006, pl. 8, figs 18–20), which is similar in size and has a similar range, has the median suture of the bifid spine oriented obliquely to the plane of the slide. The median suture is visible near the left and right edges of the spine, and the spine is mostly dark when parallel to the polarising axes and bright at 45°, opposite to the birefringence observed in the bifid spine of *S. labradorensis*. The holotype of *S. runus* is here interpreted as being a specimen of *S. labradorensis* where the median plane of the bifid spine is slightly oblique to the horizontal, rather than vertical. Accordingly, *S. runus* is considered here to be a junior synonym of *S. labradorensis*.

In photomicrographs of well-preserved specimens of sphenolithids with a bifid spine, many specimens show long, thin extensions of the two bifid spine elements that extend distally and laterally. These bifid spine extensions sometimes extend to several times the height of the specimen below the spine extensions (see pl. 11, figs 7, 9, 18, 19, 22, 23, 25–29, 40, 41 in Bown & Newsam, 2017 for excellent illustrations of numerous species with bifid spines that bear long extensions). In most specimens, these bifid spine extensions are missing, presumably because they have broken off or dissolved.

4. Systematic palaeontology

With a relatively simple ultrastructure that was mostly conserved during the history of the family, separating sphenolithid species into an approximation of phylogenetic lineages is difficult. Most of the variation among sphenolithid species is in the size and shape of components that are shared by most species. Previous studies that considered sphenolithid ultrastructure and taxonomy include Roth et al. (1971), Romein (1979), Perch-Nielsen (1985), Young et al. (1997), Aubry (2014) and Bergen et al. (2017). These studies classified sphenolithids into informal groups based on varying combinations of overall shape, ultrastructural units and optical features. None of these studies recognised the full range of sphenolithid ultrastructure, particularly that lateral element cycles are present in all sphenoliths, that the lower lateral element cycle is not present in any furcatoliths, and that the bifid spine present in some sphenolith species and most furcatoliths is derived from the upper lateral element cycle of sphenoliths.

Also unrecognised in previous studies is the importance of the number of cycles in the apical structure of sphenoliths (i.e. whether the composite apical structure is monocyclic or polycyclic). Without considering whether the apical structure is monocyclic or polycyclic, unrelated species with superficially similar gross morphologies have been placed in the same group. Examples of this are classification schemes that group the conical species *Sphenolithus abies* and *S. radians* together. These species are unrelated, but share a gross conical morphology. *Sphenolithus abies* has a polycyclic composite apical structure with a conical shape, and was derived from the polycyclic *S. primus* lineage during the Neogene, while *S. radians* has a monocyclic composite apical structure with a similar conical shape, and was derived from a similar, but lower, spine in *S. editus,* which in turn was derived from the polycyclic *S. primus* lineage during the Eocene. The entire *S. radians* lineage was extinct well before *S. abies* evolved from the *S. primus* group, so classifying *S. radians* and *S. abies* together because their disparate apical structures share a conical morphology obscures their differing phylogenies. Similar arguments apply to classification schemes that have grouped species with high proximal element cycles that have curved elements, as seen in *S. orphanknollensis, F. umbrellus* n. comb. and *S. milanetti*, a characteristic that evolved separately in these unrelated species.

The approach taken here was to group *Sphenolithus* species primarily by the nature of their apical structures, and secondarily by the shape of the proximal cycle (Figure 7). Although necessarily speculative, this results in lineages that are plausibly phylogenetic. Species in the ancestral and long-lived *S. primus* lineage have a polycyclic composite apical structure, which varies in height and shape. From this basal lineage, lineages with monocyclic apical structures diverged several times. In these lineages, an initial monocyclic composite apical structure often gave rise to monocrystalline apical structures before the lineage went extinct (e.g. *S. richteri*, with a monocrystalline apical structure evolving from *S. spiniger*, which has a monocyclic composite apical structure). Species within lineages tend to have proximal cycles that are similar in height and degree of flare.

For species of Furcatolithus, which have much less ultrastructural variability than Sphenolithus species, the approach taken here was to group the species based on the angle between the median suture and the top of the proximal element cycle (Figure 1J, K), and also the height of the proximal cycle as a proportion of the total height.

The size terms used here follow Young et al. (1997); that is, <3 μm—small, 3–5 μm—medium, 5–8 μm—large, >8 μm—very large. These are used here to describe the height of the coccolith, from the base of the proximal element cycle to the top of the apical structure, which for most sphenolithids is the largest dimension. For most furcatolith species, the height does not include the thin distal and lateral extensions of the bifid spine, which can be as long as 30 μm, but which are often missing due to breakage or dissolution. A representative subset of each of the informal groups of sphenolithid species discussed here is illustrated on Plates 1–4.

Order **DISCOASTERALES** Hay, 1977 emend. Bown, 2010

Family **SPHENOLITHACEAE** Deflandre, 1952 emend.

Emended diagnosis: Domed, conical, cylindrical or biconical coccoliths with a proximal element cycle of radially and proximally oriented elements. Above the proximal element cycle, there is usually one or more cycles of radially to distally arranged elements. The calcite *c*-axes in each element are usually oriented parallel to the long axis of the element. All of the elements radiate from a point on the median axis, just above the proximal cycle. **Included genera**: *Sphenolithus, Furcatolithus*. **Range**: Paleocene (Late Danian) to Pliocene (Zanclean). **Discussion**: The original description for the family by Deflandre (1952) is "Sphenoliths, or wedge-shaped bodies, with a distinctive 'spherolithic' structure, producing a black cross in cross polarised light, when positioned longitudinally" (translation from Aubry, 2014). This was understood here to mean that when sphenolithid specimens are viewed laterally, with the long axis of the specimen aligned with one of the polarising axes, that a black cross is visible on the specimen, with the axes of the cross being aligned with the polarising axes. While such a birefringence pattern is shown by many sphenolithid species, it is not shown by any furcatolith species, or by any sphenolith species that have a bifid spine (e.g. *S. furcatolithoides*). Accordingly, the family is emended here.

Genus ***Sphenolithus*** Deflandre, 1952 emend.

Emended diagnosis: Domed, conical, cylindrical or bi-

Figure 7 (right): Range chart showing the stratigraphical distributions of the species groupings used in this study. Ranges based on Bergen et al. (2017), Bown & Dunkley-Jones (2012) and Aubry (2014). All measurements are based on the author's measurements of the holotype or paratype images. All sketches were traced from the holotype or paratype images

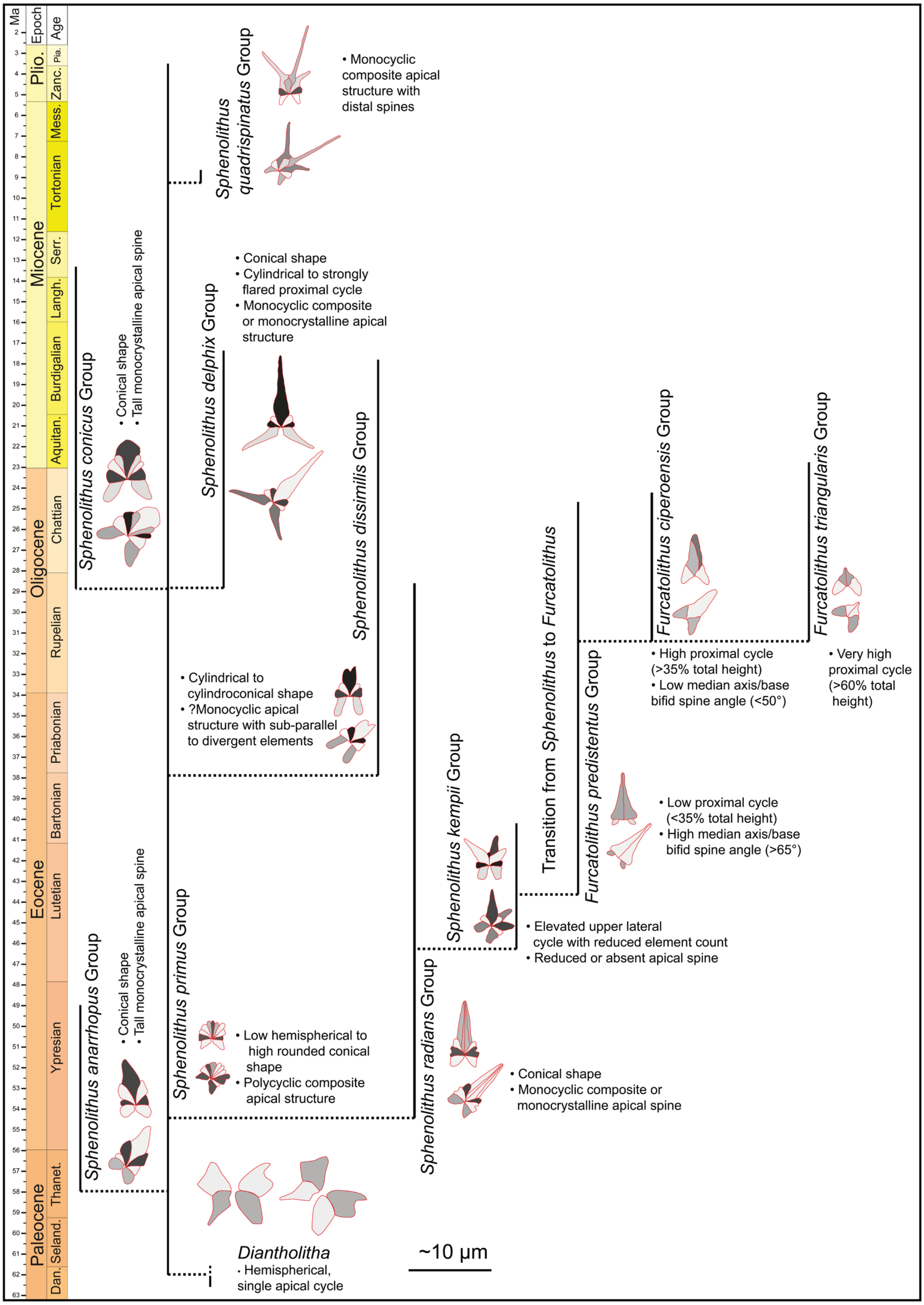

Ma
Epoch
Age
Plio.
Miocene
Oligocene
Eocene
Paleocene
Pia.
Zanc.
Mess.
Tortonian
Serr.
Langh.
Burdigalian
Aquitan.
Chattian
Rupelian
Priabonian
Bartonian
Lutetian
Ypresian
Thanet.
Seland.
Dan.
Sphenolithus quadrispinatus Group
• Monocyclic composite apical structure with distal spines
Sphenolithus conicus Group
• Conical shape
• Tall monocrystalline apical spine
Sphenolithus delphix Group
• Conical shape
• Cylindrical to strongly flared proximal cycle
• Monocyclic composite or monocrystalline apical structure
Sphenolithus dissimilis Group
• Cylindrical to cylindroconical shape
• ?Monocyclic apical structure with sub-parallel to divergent elements
Furcatolithus ciperoensis Group
• High proximal cycle (>35% total height)
• Low median axis/base bifid spine angle (<50°)
Furcatolithus triangularis Group
• Very high proximal cycle (>60% total height)
Transition from Sphenolithus to Furcatolithus
Furcatolithus predistentus Group
• Low proximal cycle (<35% total height)
• High median axis/base bifid spine angle (>65°)
Sphenolithus kempii Group
• Elevated upper lateral cycle with reduced element count
• Reduced or absent apical spine
Sphenolithus anarrhopus Group
• Conical shape
• Tall monocrystalline apical spine
Sphenolithus primus Group
• Low hemispherical to high rounded conical shape
• Polycyclic composite apical structure
Sphenolithus radians Group
• Conical shape
• Monocyclic composite or monocrystalline apical spine
Diantholitha
• Hemispherical, single apical cycle
~10 μm

conical coccoliths with a proximal element cycle situated below two radially oriented, vertically superimposed element cycles—the lower and upper lateral element cycles. Above the upper lateral element cycle, an apical structure is usually present. The apical structure may comprise single or multiple cycles of vertically stacked, radially and distally oriented elements, or a single vertical to sub-vertical element, or may be entirely absent. **Type species**: *Sphenolithus radians* Deflandre, 1952. **Synonyms**: *Nannoturbella* Brönnimann & Stradner, 1960, the generotype of which is *Nannoturbella moriformis* Brönnimann & Stradner, 1960, a species that clearly belongs in *Sphenolithus*. *Sphenaster* Wilcoxon, 1970, the generotype of which, *Sphenaster metula* Wilcoxon, 1970, is an isolated proximal element cycle of a sphenolith, probably from the *S. primus* group. **Discussion**: In the sphenolith lineage (the *S. kempii* group) that give rise to the genus *Furcatolithus*, the upper lateral element cycle increases in size vertically, with the number of elements reducing to two and becoming the bifid spine present in most species of *Furcatolithus*. The apical structure is completely absent in the last members of this lineage—*S. furcatolithoides* and *S. labradorensis*.

The origin of *S. primus* (and hence the genus *Sphenolithus* and the family Sphenolithaceae) is likely related to the genus *Diantholitha* (as noted by Aubry, 2014), which has a very similar proximal cycle to *S. primus*. Above the proximal cycle, *Diantholitha* species have a single radial cycle of upward- and outward-extending apical elements. As in *S. primus,* the calcite *c*-axes of the elements lie parallel to their long axes. The addition of extra cycles of elements distally to form both the lateral and apical element cycles of *Sphenolithus* seems a plausible mechanism for the evolution of *Sphenolithus* from *Diantholitha*. The generotype of *Diantholitha*, *D. mariposa* Rodriguez & Aubry *in* Aubry et al., 2011 is illustrated on Plate 1, figs 1, 2 for comparison.

The holotype of *S. elongatus* Perch-Nielsen, 1980 (pl. 2, figs 5, 6) does not appear to have an ultrastructure that belongs to either *Sphenolithus* or *Furcatolithus*. What superficially appears to be a proximal element cycle has elements that do not resemble those of any other sphenolithid. No lateral cycle elements appear to be present, and no median suture appears in the spine. Accordingly, this species was not considered to be a true sphenolithid and is not considered further.

The genus *Ilselithina* Stradner *in* Stradner & Adamiker, 1966 has small to medium biconical coccoliths that have been considered by Aubry (2014) and Bergen et al. (2017) to be possibly related to *Sphenolithus*, based largely on the similarity between their proximal element cycles. Young *in* Young et al. (2018) noted that the elements considered by previous studies to belong to separate proximal and distal cycles, are actually one piece, with the elements that appear to belong to the distal cycle actually being distal extensions of the proximal cycle elements. This construction is quite unlike any sphenolithid, so *Ilselithina* was not considered to be a member of the Sphenolithaceae, and is not considered here.

Forty-eight species in the genus *Sphenolithus* were recognised as valid in this study. These species have been divided into eight informal groups of species, based on shared morphology and likely phylogeny. These groups are listed in Table 1 and detailed below, with both groups and species approximately ordered by first stratigraphic appearance. A selection of species from each group is illustrated on Plates 1–3.

Sphenolithus primus Group

The species in this group all have simple domed morphologies and a polycyclic composite apical structure with multiple apical element cycles, which are minimally differentiated from the lower and upper lateral element cycles. This group is long-ranging, with representatives present throughout the history of the genus, forming a plexus of closely related species of varying sizes, and with varying apical structure heights. All other groups of sphenolithids evolved from this group.

The species in this group are discussed below in approximate order of first stratigraphic appearance: *S. primus, S. acervus, S. moriformis, S. apoxis, S. puniceus, S. neoabies, S. abies, S. verensis* and *S. grandis*. Range charts for this group are presented in Figures 8–10.

Sphenolithus primus Perch-Nielsen, 1971a
Pl. 1, figs 3, 4

1971a *Sphenolithus primus* Perch-Nielsen: p. 357, pl. 11,

Figure 8 (right): Range chart for the *S. primus, S. conicus* and *S. quadrispinatus* groups. Ranges based on Bergen et al. (2017), Bown & Dunkley-Jones (2012) and Aubry (2014). All measurements are based on the author's measurements of the holotype or paratype images. All of the sketches were traced from the holotype (HT) or paratype (PT) images, either LM or EM

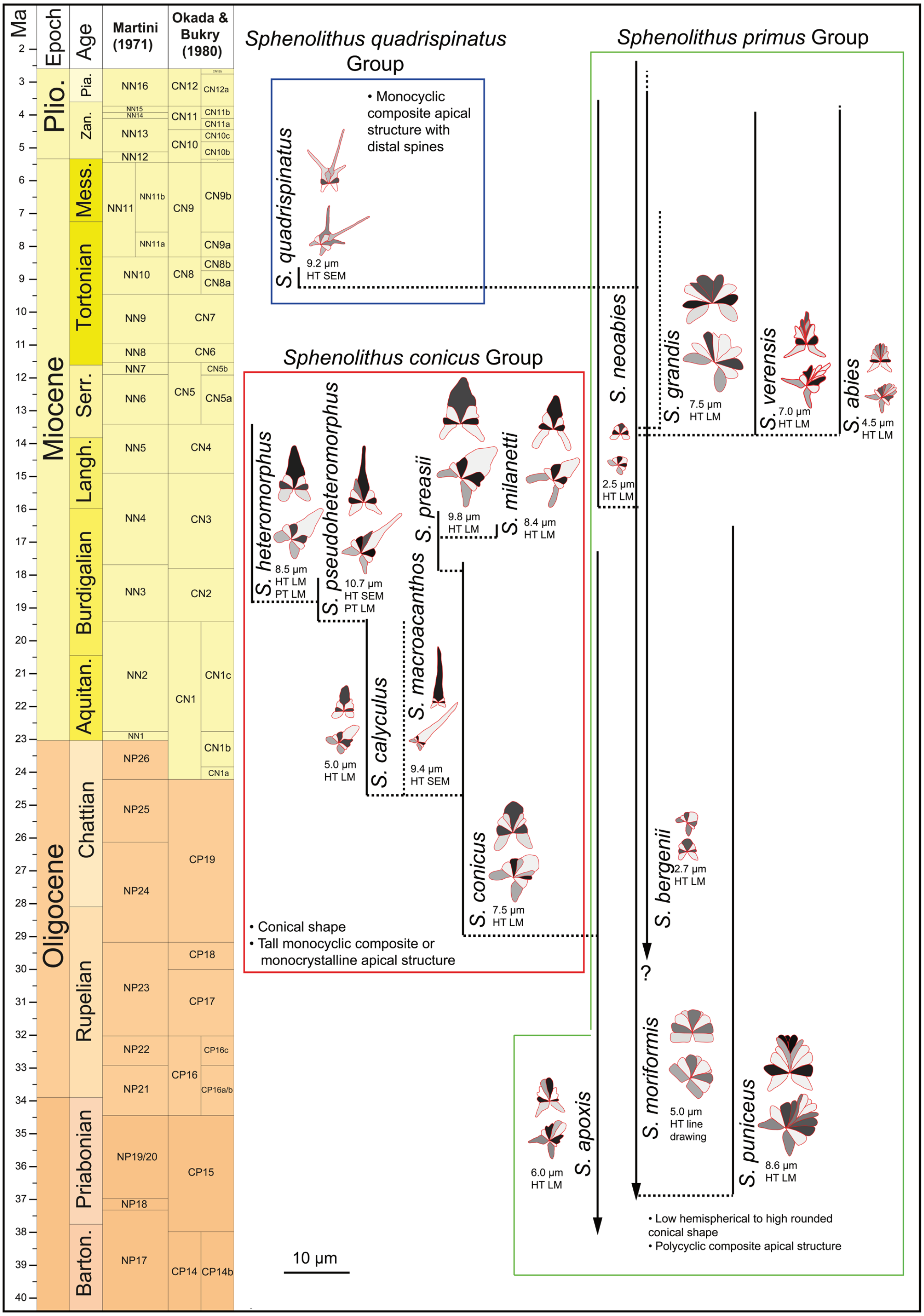

Ma
Epoch
Age
Martini (1971)
Okada & Bukry (1980)
Plio.
Miocene
Oligocene
Pia.
Zan.
Mess.
Tortonian
Serr.
Langh.
Burdigalian
Aquitan.
Chattian
Rupelian
Priabonian
Barton.
NN16
NN15
NN14
NN13
NN12
NN11
NN11b
NN11a
NN10
NN9
NN8
NN7
NN6
NN5
NN4
NN3
NN2
NN1
NP26
NP25
NP24
NP23
NP22
NP21
NP19/20
NP18
NP17
CN12
CN12a
CN11
CN11b
CN11a
CN10
CN10c
CN10b
CN9
CN9b
CN9a
CN8
CN8b
CN8a
CN7
CN6
CN5
CN5b
CN5a
CN4
CN3
CN2
CN1
CN1c
CN1b
CN1a
CP19
CP18
CP17
CP16
CP16c
CP16a/b
CP15
CP14
CP14b
Sphenolithus quadrispinatus Group
• Monocyclic composite apical structure with distal spines
S. quadrispinatus
9.2 µm HT SEM
Sphenolithus conicus Group
S. heteromorphus
8.5 µm HT LM PT LM
S. pseudoheteromorphus
10.7 µm HT SEM PT LM
S. preasii
9.8 µm HT LM
S. milanetti
8.4 µm HT LM
S. calyculus
5.0 µm HT LM
S. macroacanthos
9.4 µm HT SEM
S. conicus
7.5 µm HT LM
• Conical shape
• Tall monocyclic composite or monocrystalline apical structure
Sphenolithus primus Group
S. neoabies
2.5 µm HT LM
S. grandis
7.5 µm HT LM
S. verensis
7.0 µm HT LM
S. abies
4.5 µm HT LM
S. bergenii
2.7 µm HT LM
?
S. apoxis
6.0 µm HT LM
S. moriformis
5.0 µm HT line drawing
S. puniceus
8.6 µm HT LM
• Low hemispherical to high rounded conical shape
• Polycyclic composite apical structure
10 µm

Table 1: Species of *Sphenolithus* grouped into informal morphological groups, in approximate order of first stratigraphic appearance (see Figure 7)

GROUP	MORPHOLOGICAL CRITERION	RANGE	SPECIES
S. primus	Simple domed shape Polycyclic composite apical structure	Early Paleocene–Early Pliocene (Danian–Zanclean)	*S. primus* *S. acervus* *S. moriformis* *S. bergenii* *S. apoxis* *S. puniceus* *S. neoabies* *S. abies* *S. verensis* *S. grandis*
S. anarrhopus	Conical shape High, sharply pointed monocrystalline apical structure	Late Paleocene–Early Eocene (Thanetian–Ypresian)	*S. anarrhopus* *S. villae* *S. conspicuus*
S. radians	Conical shape Monocyclic composite or monocrystalline apical structure	Early Eocene–Early Oligocene (Ypresian–Rupelian)	*S. editus* *S. arthurii* *S. radians* *S. orphanknollensis* *S. spiniger* *S. richteri* *S. pseudoradians*
S. kempii	Divergent upper lateral element cycle Trend of increasing upper lateral element length, with reduction in element count	Middle Eocene (Lutetian–Bartonian)	*S. stellatus* *S. kempii* *S. perpendicularis* *S. shamrockiae* *S. furcatolithoides* *S. labradorensis*
S. dissimilis	Polycyclic composite apical structure with subparallel to divergent elements	Late Eocene–Early Miocene (Priabonian–Burdigalian)	*S. truaxii* *S. procerus* *S. capricornutus* *S. compactus* *S. disbelemnos* *S. multispinatus* *S. dissimilis* *S. cometa*
S. conicus	Conical shape Medium to high, sharply pointed to rounded monocyclic or monocrystalline apical structure	Early Oligocene–Middle Miocene (Rupelian–Serravallian)	*S. conicus* *S. calyculus* *S. macroacanthos* *S. pseudoheteromorphus* *S. heteromorphus* *S. preasii* *S. milanetti*
S. delphix	Strongly flared proximal element cycle Monocyclic or monocrystalline apical structure	Early Oligocene–Early Miocene (Rupelian–Burdigalian)	*S. bipedis* *S. spinula* *S. microdelphix* *S. delphix* *S. tintinnabulum* *S. belemnos*
S. quadrispinatus	Monocyclic apical structure with divergent elements with thin lateral and distal extensions	Late Miocene (Tortonian)	*S. quadrispinatus*

fig. 4; pl. 12, figs 4, 5, 7–12, pl. 14, figs 22–24.

1997 *Sphenolithus primus* Perch-Nielsen, 1971a – Bybell & Self-Trail: pl. 5, fig. 8.

2008 *Sphenolithus primus* Perch-Nielsen, 1971a – Steurbaut & Sztrákos: pl. II, figs 5, 6.

2014 *Sphenolithus primus* Perch-Nielsen, 1971a – Khalil & Al Sawy: pl. 8, figs 17, 18.

Diagnosis: A small sphenolith with a medium-height, slightly conical proximal element cycle, thin lower and upper lateral element cycles, and polycyclic composite apical element cycles forming a low apical dome. **Remarks**: This was the first sphenolithid species to evolve. Given that *Diantholitha* evolved in NP4 in the Danian, and was likely the ancestor of *S. primus*, it is clear that the first *S. primus* evolved in NP4. However, *Diantholitha* was not described (Aubry *in* Aubry et al., 2011) until well after *S. primus* had been described (Perch-Nielsen, 1971a) and, given the strong similarity between the side views of *Diantholitha* and *S. primus*, it is possible that some records in the literature of the earliest *S. primus* are actually records of *Diantholitha*. The simple morphology of *S. primus* is long-lived, persisting to the end of the Zanclean in *S. moriformis,* a larger, but otherwise similar, species.

Sphenolithus acervus **Bown, 2005a**

2005a *Sphenolithus acervus* Bown: pl. 43, figs 13–19.

Diagnosis: A large sphenolith with a medium-height, slightly conical proximal element cycle, thick lower and upper lateral element cycles, and polycyclic composite apical element cycles forming a medium-height apical dome. **Remarks**: Individual elements in this species appear very strongly triradiate, resulting in a relatively open structure in three dimensions. This explains why this large species only has moderate birefringence, rather than the high birefringence exhibited by similarly large species in this group, such as *S. puniceus,* which has coarser elements and high birefringence, with first-order red and blue colours under cross-polarised light.

Sphenolithus moriformis (Brönnimann & Stradner, 1960) Bramlette & Wilcoxon, 1967
Pl. 1, figs 5, 6

1960 *Nannoturbella moriformis* Brönnimann & Stradner: p. 368, figs 11–13, 16, *non* figs 14, 15.
1965 *Sphenolithus pacificus* Martini: p. 407, pl. 36, figs 7–10.
1967 *Sphenolithus moriformis* (Brönnimann & Stradner, 1960) Bramlette & Wilcoxon: p. 124, pl. 3, figs 1–4, *non* figs 5, 6.
2012 *Sphenolithus moriformis* (Brönnimann & Stradner, 1960) Bramlette & Wilcoxon, 1967 – Bown & Dunkley Jones: pl. 13, fig. 37.

Diagnosis: A medium-sized sphenolith with a low to medium-height proximal element cycle, thin lower and upper lateral element cycles, and polycyclic composite apical cycles forming a low apical dome. **Remarks**: Brönnimann & Stradner (1960) illustrated *Nannoturbella moriformis* with a series of line-drawings featuring two different morphotypes—a low-domed form (their figs 11–13, 16), which they clearly designated as the holotype, and a higher-domed form (their figs 14, 15), which was later described as *S. apoxis* by Bergen & de Kaenel *in* Bergen et al. (2017). The transition from *S. primus* to *S. moriformis* is unclear, as there is little difference between the two species, other than size (the holotype of *S. primus* is ~3.5 μm high, that of *S. moriformis* is ~5 μm high). Most authors, somewhat arbitrarily, have placed this transition around the base of the Eocene. *Sphenolithus moriformis* has the longest range of all sphenolithid species, from the basal Eocene to the mid-Pliocene.

Sphenolithus bergenii n. sp.
Pl. 1, figs 7, 8

non 1980 *Sphenolithus compactus* Backman: p. 59, pl. 3, fig. 20.

Derivation of name: Named in honour of Dr Jim Bergen, retired Amoco and BP nannofossil biostratigrapher and mentor. **Diagnosis**: A very small to small sphenolith with a low, moderately flared proximal element cycle, thin lower and upper lateral element cycles, and a low-domed apical structure. **Remarks**: Small sphenoliths with a low-domed apical structure have been placed in *S. compactus* by most workers, largely following Perch-Nielsen (1985, pp. 522, 523, fig. 71, based on sketches in Aubry, 1989). Perch-Nielsen (1985, fig. 71) provided three sketches of *S. compactus*—two showing its appearance in the LM, and one an interpretation of what the species would look like in the EM. The two sketches showing the appearance of *S. compactus* in the LM show a form with a low proximal cycle, while the figure illustrating its appearance in the EM shows a tall, cylindrical proximal cycle, much like the holotype of *S. compactus* and unlike the other two sketches. **Holotype**: Pl. 1, figs 7, 8. **Holotype height**: 2.7 μm. **Type locality**: DSDP Leg 12, Hole 116, Rockall Plateau, Atlantic Ocean. **Type level**: DSDP-12-116, 12-1, 80–81 cm; NN3 (of Martini, 1971), Burdigalian. **Occurrence**: The range of this species has not been fully established due to the taxonomic confusion with *S. compactus*. In the distribution data for a composite section through most of the Oligocene and Neogene in ODP Leg 154 holes, Bergen et al. (2019b) recorded this species as *S. compactus* (which they distinguished from *S. paratintinnabulum*, which, as discussed in this paper, is a junior synonym of *S. compactus*) throughout, from the base of their dataset at ~30.7 Ma, up to 3.607 Ma, just below the extinction of the genus.

Sphenolithus apoxis Bergen & de Kaenel *in* Bergen et al., 2017
Pl. 1, figs 9, 10

1960 *Nannoturbella moriformis* Brönnimann & Stradner: p. 368, figs 14, 15, *non* figs 11–13, 16.
1967 *Sphenolithus moriformis* (Brönnimann & Stradner, 1960) Bramlette & Wilcoxon: p. 124, pl. 3, figs 5, 6, *non* figs 1–4.

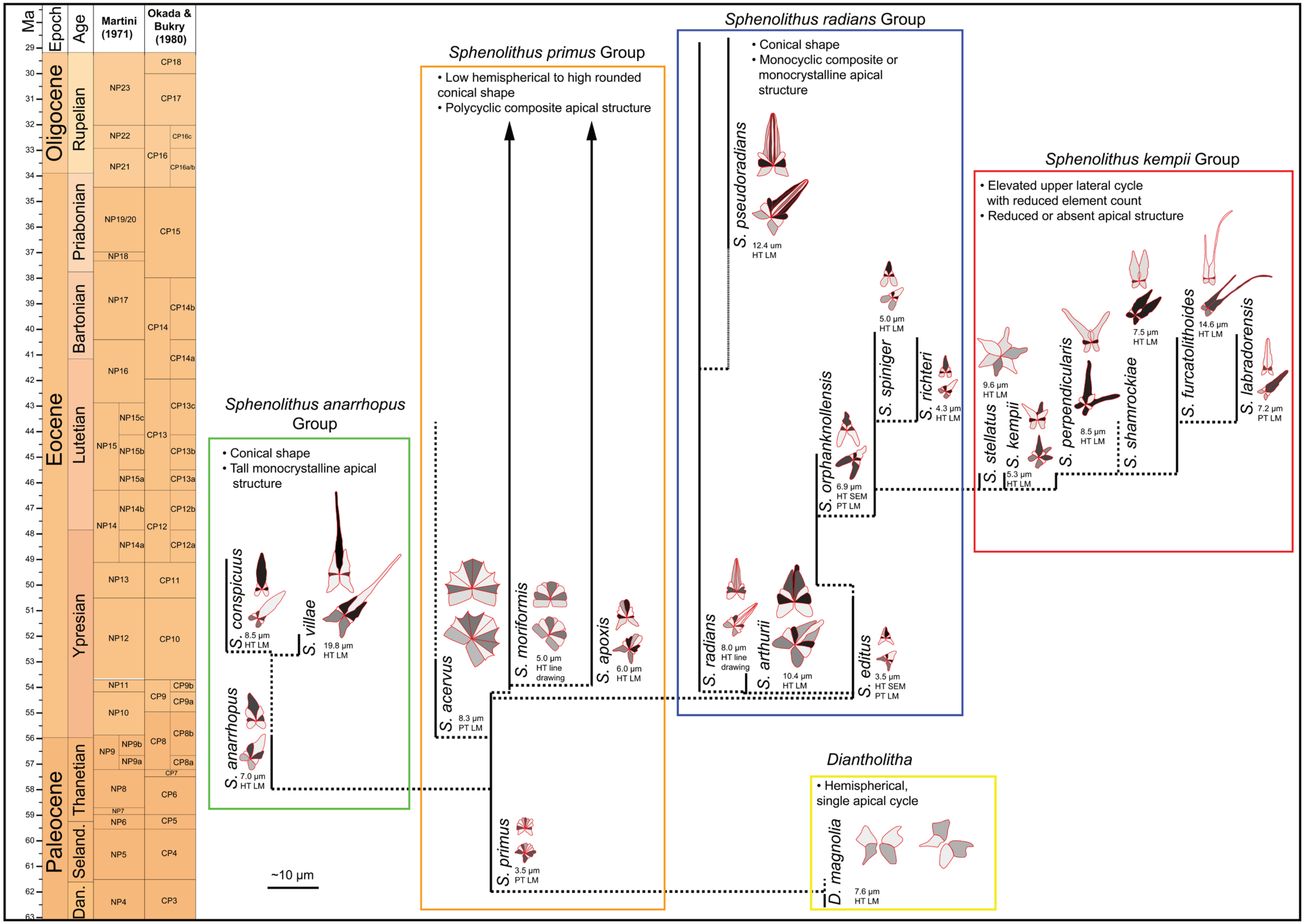

Figure 9: Range chart for the *S. primus*, *S. anarrhopus*, *S. radians* and *S. kempii* groups. Ranges based on Bergen et al. (2017), Bown & Dunkley-Jones (2012) and Aubry (2014). All measurements are based on the author's measurements of the holotype or paratype images. All sketches were traced from the holotype or paratype images, either LM or EM

2017 *Sphenolithus apoxis* Bergen & de Kaenel *in* Bergen et al.: pl. 2, figs 11–20.

Diagnosis: A medium-sized sphenolith with a medium-height, slightly flared proximal element cycle, thin lower and upper lateral element cycles, and a polycyclic composite apical structure forming a high apical dome. **Remarks**: This species is essentially a high-domed, rather than low-domed, form of *S. moriformis*. It forms a plexus with *S. moriformis* for its entire range, from the Ypresian to the Burdigalian.

Sphenolithus puniceus Bergen & de Kaenel *in* Bergen et al., 2017
Pl. 1, figs 11, 12

2017 *Sphenolithus puniceus* Bergen & de Kaenel *in* Bergen et al.: pl. 1, figs 19–26.

Diagnosis: A large sphenolith with a medium-height proximal element cycle, thick lower and upper lateral element cycles, and polycyclic composite apical element cycles forming a medium-height apical dome. All of the elements appear coarsely constructed, although this is probably a function of the large size of the sphenolith. **Remarks**: The large size and coarse elements of this species result in high birefringence relative to most other sphenolithids, with first-order orange, red and blue colours under cross-polarised light.

Sphenolithus neoabies Bukry & Bramlette, 1969
Pl. 1, figs 13, 14

1969 *Sphenolithus neoabies* Bukry & Bramlette: pl. 3, figs 9–11.
2017 *Sphenolithus neoabies* Bukry & Bramlette, 1969 – Bergen et al.: pl. 1, figs 1–4.

Diagnosis: A small sphenolith with a low, strongly flared proximal element cycle, thin lower and upper lateral element cycles, and polycyclic composite apical element cycles forming a very low, pointed apical dome. **Remarks**: The strongly flared proximal cycle and small pointed apical structure of this species give it a distinctive triangular lateral outline.

Sphenolithus abies Deflandre *in* Deflandre & Fert, 1954
Pl. 1, figs 15, 16

1953 *Sphenolithus abies* Deflandre: p. 1786.
1954 *Sphenolithus abies* Deflandre *in* Deflandre & Fert: p. 50, pl. X, figs 1–4.
2017 *Sphenolithus abies* Deflandre *in* Deflandre & Fert, 1954 – Bergen et al.: pl. 2, figs 5–10.

Diagnosis: A medium to large sphenolith with a medium-height, moderately flared proximal element cycle. The lower and upper lateral element cycles are thin. The apical structure is composite and polycyclic, and has the form of a high, rounded cone. **Remarks**: Along with *S. moriformis*, this species is consistently common throughout the late Middle Miocene to Early Pliocene interval.

Sphenolithus verensis Backman, 1978
Pl. 1, figs 17, 18

1978 *Sphenolithus verensis* Backman: p. 111, pl. 2, figs 4–6, 11, 12.
2017 *Sphenolithus verensis* Backman, 1978 – Bergen et al.: pl. 2, figs 1–4.

Diagnosis: A large sphenolith with a medium-height, strongly flared proximal element cycle. The lower and upper lateral element cycles are thin. The apical structure is composite and polycyclic, and has the form of a high, rounded cone. **Remarks**: The strongly flared proximal element cycle is the only significant difference between this species and *S. abies*.

Sphenolithus grandis Haq & Berggren, 1978

1978 *Sphenolithus grandis* Haq & Berggren: figs 17, 18.
2017 *Sphenolithus grandis* Haq & Berggren, 1978 – Bergen et al.: pl. 1, figs 27–30.

Diagnosis: A large sphenolith with a medium-height proximal element cycle, thick lower and upper lateral element cycles, and polycyclic composite apical element cycles forming a medium-height apical dome. **Remarks**: This large species is essentially a large form of *S. moriformis*. The birefringence of this species reaches first-order yellow and orange—higher than *S. moriformis,* as its elements are

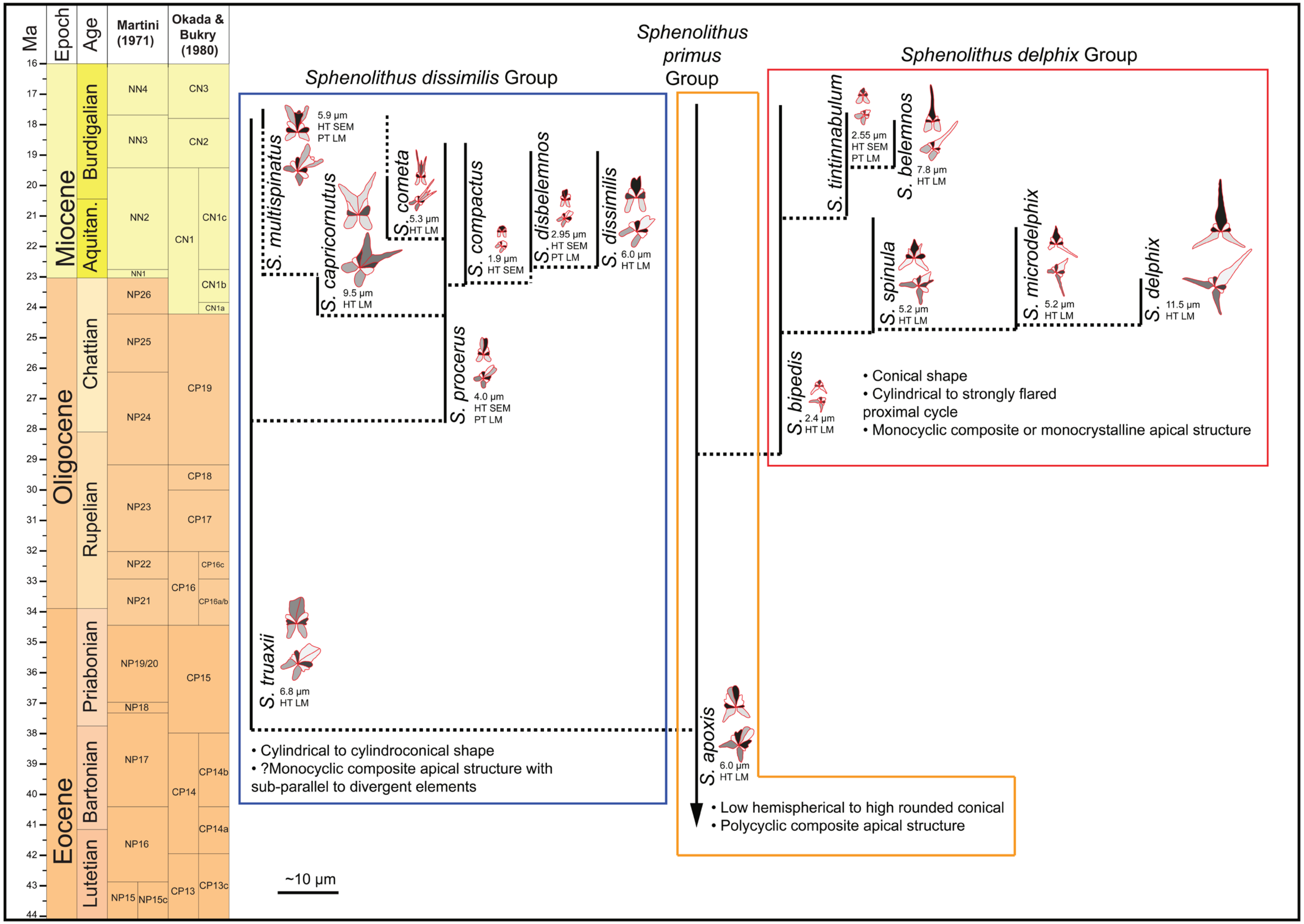

Figure 10: Range chart for the *S. primus*, *S. dissimilis* and *S. delphix* groups. Ranges based on Bergen et al. (2017), Bown & Dunkley-Jones (2012) and Aubry (2014). All measurements are based on the author's measurements of the holotype or paratype images. All sketches were traced from the holotype or paratype images, either LM or EM

larger and thicker, but lower than the first-order red and blue birefringence exhibited by *S. puniceus*.

Sphenolithus anarrhopus Group

The species in this group are all conical, with a high, sharply pointed, monocrystalline or monocyclic composite apical structure. In most specimens, the apical structure is monocrystalline, but occasionally (e.g. *S. villae* in Bown, 2005a, pl. P9, figs 23, 24, 35, 36) it can be seen that the apical structure is composite and monocyclic, comprising several elements, but with one larger element dominating the spine. This is the first group of sphenolithids to diverge from the simple-domed morphologies of the *S. primus* group. The species in this group are discussed below in approximate order of first stratigraphic appearance: *S. anarrhopus, S. villae* and *S. conspicuus*. A range chart for this group is presented in Figure 9.

Sphenolithus anarrhopus Bukry & Bramlette, 1969
Pl. 1, figs 19, 20

1969 *Sphenolithus anarrhopus* Bukry & Bramlette: pl. 3, figs 5–8.
2005a *Sphenolithus anarrhopus* Bukry & Bramlette, 1969 – Bown: pl. 44, figs 2–5.
2008 *Sphenolithus rioi* Agnini et al.: pl. 2, figs 3–8.

Diagnosis: A large, conical sphenolith with a medium-height proximal element cycle, a thin lower lateral element cycle, a thick upper lateral element cycle, and a tall, sharply pointed, conical monocrystalline apical structure. The apical structure is usually slightly asymmetric with respect to the median axis of the sphenolith. **Remarks**: *Sphenolithus rioi* was described as having a straight spine that is generally longer than the spine of *S. anarrhopus*. The holotypes of the two species are very similar in size (6.8 μm for *S. rioi* and 7.0 μm for *S. anarrhopus*), with similarly sized spines. Whilst most specimens of *S. anarrhopus* have slightly asymmetric apical structures, it seems clear that even with an asymmetric spine, if the spine is pointing downwards or upwards relative to the plane of the slide, it would appear to be symmetrical in plan view. For these reasons, *S. rioi* is considered to be a junior synonym of *S. anarrhopus*.

Sphenolithus villae Bown, 2005a

2005a *Sphenolithus villae* Bown: pl. 44, figs 11–24.
2005b *Sphenolithus villae* Bown, 2005a – Bown: pl. P9, figs 28–30.

Diagnosis: A very large, conical sphenolith with a high, slightly flaring proximal element cycle, a thin lower lateral element cycle, a thick upper lateral element cycle, and a very tall, pointed, conical monocyclic composite or monocrystalline apical structure. **Remarks**: Distinguished from the otherwise similar *S. anarrhopus* and *S. conspicuus* by its symmetrical apical structure and larger size.

Sphenolithus conspicuus Martini, 1976

1976 *Sphenolithus conspicuus* Martini: pl. 13, figs 1–3.
2012 *Sphenolithus conspicuus* Martini, 1976 – Bown & Dunkley Jones: pl. 10, figs 16–18.

Diagnosis: A large conical sphenolith with a medium-height cylindrical proximal element cycle, a thin lower lateral element cycle, a slightly thickened upper lateral element cycle, and a tall conical apical structure. **Remarks**: *Sphenolithus conspicuus* has a symmetrical apical structure and is taller and narrower than *S. anarrhopus*, but is otherwise similar.

Sphenolithus radians Group

Species in this group all have a conical shape and a monocyclic composite or monocrystalline apical structure. They are clearly differentiated from species of the *S. primus* group, which all have polycyclic apical structures. The species in this group are discussed below in approximate order of first stratigraphic appearance: *S. editus, S. arthurii, S. radians, S. orphanknollensis, S. spiniger, S. richteri* and *S. pseudoradians*. A range chart for this group is presented in Figure 9.

Sphenolithus editus Perch-Nielsen *in* Perch-Nielsen et al., 1978

1978 *Sphenolithus editus* Perch-Nielsen *in* Perch-Nielsen et al.: p. 352, pl. 8, figs 22–27; pl. 20, figs 5–19.
1997 *Sphenolithus editus* Perch-Nielsen *in* Perch-Nielsen et al. (1978) – Bybell & Self-Trail: pl. 5, figs 9, 12.

2012 *Sphenolithus editus* Perch-Nielsen *in* Perch-Nielsen et al. (1978) – Bown & Dunkley Jones: pl. 10, figs 3, 4.

Diagnosis: A small, conical sphenolith with a medium-height, moderately flared proximal element cycle, thin lower and upper lateral element cycles, and a medium-height, pointed, conical monocyclic composite apical structure. **Remarks**: SEM photomicrographs of this small species by Bybell & Self-Trail (1997, pl. 5, figs 9, 12) clearly show that the apical structure is composite and monocyclic, with vertically oriented, blade-shaped elements. The apical structure is very similar in appearance to that of *S. radians* (see the SEM photomicrograph of Perch-Nielsen, 1977, pl. 31, fig. 8).

Sphenolithus arthurii Bown, 2005b

2005b *Sphenolithus arthurii* Bown: p. 9, pl. 9, figs 1–7.

Diagnosis: A large to very large, stoutly constructed, conical sphenolith, with a medium-height, slightly flaring proximal element cycle, thick lower and upper lateral element cycles, and a medium-height, pointed, conical monocyclic composite apical structure. **Remarks**: This species appears to be restricted to the Early Eocene. It is essentially a heavily constructed form of *S. radians*, but with a lower apical structure.

Sphenolithus radians Deflandre, 1952

1952 *Sphenolithus radians* Deflandre: p. 466, figs 363A–G.
2015 *Sphenolithus radians* Deflandre, 1952 – Fioroni et al.: pl. 2, figs 11, 12.

Diagnosis: A medium to large, conical sphenolith, with a medium-height, slightly flared proximal element cycle, slightly thick lateral element cycles, and a high, conical, sharply pointed, monocyclic composite apical structure with vertically oriented, blade-shaped elements. **Remarks**: This long-ranging species is the generotype of *Sphenolithus*, and was the first *Sphenolithus* species described.

Sphenolithus orphanknollensis Perch-Nielsen, 1971b
Pl. 1, figs 21, 22

1971b *Sphenolithus orphanknolli* Perch-Nielsen: p. 56, pl. 3, figs 1–3; *non* pl. 7, figs 30–32.
1972 *Sphenolithus orphanknolli* Perch-Nielsen, 1971b – Perch-Nielsen: pl. 17, fig. 2.
1978 *Sphenolithus orphanknolli* Perch-Nielsen, 1971b – Proto Decima et al.: pl. 12, figs 4a–c, 5a–d.
non 2012 *Sphenolithus orphanknollensis* Perch-Nielsen, 1971b – Bown & Dunkley Jones: pl. 10, figs 19–24.

Diagnosis: A medium-sized, conical sphenolith, with a high, moderately flaring proximal element cycle. In lateral view, the elements in the proximal element cycle are slightly curved, with the concave side facing down. The lower and upper lateral element cycles are thin, and there is a low, slightly rounded, conical monocyclic composite apical structure. **Remarks**: The holotype of this species is a high-quality SEM image (Perch-Nielsen, 1971b, pl. 3, fig. 2) that clearly shows a high proximal cycle with curved elements, thin lateral element cycles, and a low monocyclic composite apical structure (the apical structure is much lower, but otherwise strongly resembles that of *S. radians* Deflandre, 1952). The LM images (pl. 7, figs 30–32) in Perch-Nielsen (1971b) and Bown & Dunkley Jones (2012, pl. 10, figs 19–24) show other specimens that do not have a high, arcuate proximal cycle, and these are not considered here to belong to *S. orphanknollensis*.

Sphenolithus spiniger Bukry, 1971a
Pl. 1, figs 23, 24

1971a *Sphenolithus spiniger* Bukry: p. 322, pl. 6, figs 10–12.
2012 *Sphenolithus spiniger* Bukry, 1971a – Bown & Dunkley Jones: pl. 10, figs 5, 6.

Diagnosis: A small to medium, conical sphenolith, with a high and moderately flaring proximal element cycle, a thin lower lateral element cycle, a thick upper lateral element cycle, and a conical, pointed monocyclic composite apical structure. **Remarks**: This small species is easily distinguished from *S. editus* by its higher proximal cycle and lower apical structure.

Sphenolithus richteri Bown & Dunkley Jones, 2012

2012 *Sphenolithus richteri* Bown & Dunkley Jones: p. 33, pl. 11, figs 7–12.

Diagnosis: A small, conical sphenolith, with a medium-height, cylindrical proximal element cycle, thin lower lateral cycle elements, thick upper lateral cycle elements, and a narrow, sharply pointed, monocrystalline apical structure. **Remarks**: This species has a monocrystalline apical structure, and is clearly descended from *S. spiniger,* which has a monocyclic composite apical structure. No other *Sphenolithus* species with a monocrystalline apical structure exist when *S. richteri* first occurs in the mid-Eocene. This indicates that *S. richteri* is not descended from the earlier *S. anarrhopus* lineage of sphenoliths with monocrystalline apical structures, thus demonstrating that monocrystalline apical structures are polyphyletic.

Sphenolithus pseudoradians Bramlette & Wilcoxon, 1967
Pl. 1, figs 25, 26

1967 *Sphenolithus pseudoradians* Bramlette & Wilcoxon: p. 126, pl. 2, figs 12–14.
2005b *Sphenolithus pseudoradians* Bramlette & Wilcoxon, 1967 – Bown: pl. P9, figs 19, 20.

Diagnosis: A very large, conical sphenolith, with a low to medium-height, slightly flared proximal element cycle, thick lateral element cycles, and a high, conical, sharply pointed monocyclic composite apical structure. **Remarks**: This species is essentially a larger and more robustly constructed variety of *S. radians*.

Sphenolithus kempii **Group**

The species in this group all have low to medium-height proximal element cycles and a thin lower lateral element cycle. The apical structure is monocyclic and reduced in size, disappearing completely in *S. furcatolithoides* and younger species. With a reduction in element count in the upper lateral element cycle through time, ultimately to two elements in *S. perpendicularis*, the upper lateral cycle elements increase in length laterally and vertically through time, to become the bifid spine of *S. shamrockiae* n. sp. and younger species.

The species in this group are discussed below in approximate order from first stratigraphic appearance: *S. stellatus*, *S. kempii*, *S. perpendicularis*, *S. shamrockiae* n. sp., *S. furcatolithoides* and *S. labradorensis*. A range chart for this group is presented in Figure 9.

Sphenolithus stellatus Gartner, 1971

1971 *Sphenolithus stellatus* Gartner: p. 114, pl. 5, fig. 3a, b.
1995 *Sphenolithus stellatus* Gartner, 1971 – Bralower & Mutterlose: pl. 7, figs 27, 28.
2006 *Sphenolithus stellatus* Gartner, 1971 – Lupi & Wise: pl. 2, figs 23, 24.

Diagnosis: The type illustrations in Gartner (1971, pl. 5, fig. 3a, b) are black and white photomicrographs of a single specimen in a single orientation (plan view), so the exact ultrastructure of this species is unclear. It appears to have an upper lateral element cycle comprising at least four, and probably six, elements. Other elements are present between these four elements, but these are slightly out of focus, suggesting they may be lower lateral cycle elements. Without images of lateral views of this species, it is difficult to fully characterise the proximal and lower lateral element cycles, or the apical structure. The type specimen is ~9.4 μm wide. **Remarks**: This species is interpreted here as an intermediate form between *S. spiniger* and *S. kempii*, or perhaps between *S. kempii* and *S. perpendicularis*. With at least four large, distally and laterally divergent spines in the upper lateral element cycle, this species is far less likely than most other sphenolith species to lie on its side on the microscope slide, being more likely to lie top-up or top-down, so it has only been figured in plan view and not lateral view. If there are only four divergent spines, it is possible that this species is a senior synonym of *S. kempii*. Until this species has been figured in side view, and its exact relationship to *S. kempii* and/or *S. perpendicularis* has been made clear, it was decided here to retain it as a separate species.

In his original description, Gartner (1971, p. 114) described the type level of *S. stellatus* (and separately in the figure caption for the holotype) as being a sample at 251 ft in JOIDES Core J-6B, offshore Florida. The summary range chart for the JOIDES cores studied by Gartner (1971, fig. 2) showed the sample from 251 ft in Core J-6B as belonging to his *Isthmolithus recurvus* Zone of Late Eocene age, but the nannofossil distribution chart for Core J-6B (Gartner, 1971, fig. 5) does not show any occurrence of *S. stellatus*. Gartner (1971, p. 114) described the occurrence of *S. stellatus* as "the middle Eocene interval of the JOIDES Blake Plateau Core J-3", with no further information given. The nannofossil distribution chart for Core J-3 (Gartner, 1971, fig. 4) showed *S. stellatus* occurring as rare to few in samples from 516–536 ft, an interval belonging to his *Chiphragmalithus quadratus* and *Reticulofenestra umbilica* Zones, which he regarded as being of latest Early and Middle Eocene age. These two zones are shown as being equivalent to planktonic foraminiferal zones P10 and P11 (using the planktonic foraminiferal zonation of Blow, 1979), which are Middle Eocene in age (Wade et al., 2011).

The best guide we have to the actual age of this taxon, which has rarely been recorded since being described (suggesting it has a very short range), is the distribution data of Bralower & Mutterlose (1995), who record *S. stellatus* from ODP Holes 865B and 865C in the mid-Pacific. They recorded its occurrence from Section 8H-6 in Hole 865B and 9H-3 in Hole 865C, at the base of CP13a (of Okada & Bukry, 1980)/within NP15 (of Martini, 1971), to Section 7H-6 in Hole 865B and 8H-3 in Hole 865C, low in CP13b/within NP15. This species has also been recorded by Lupi & Wise (2006) from ODP Hole 1260A on the Demerara Rise. They recorded occurrences of *S. stellatus* from Section 21R-2, in the uppermost part of CP12a/NP14 to Section 18R-6 at the base of CP13b/within NP15. From these records, it seems that the range is essentially within CP13a/NP15, which closely matches the range from JOIDES Blake Plateau Core J-3 (Gartner, 1971, fig. 4), and also the range of *S. kempii* (Bown & Dunkley Jones, 2012, p. 33). It seems clear that *S. stellatus* is closely related to *S. kempii*, and has a similarly short range.

Sphenolithus kempii **Bown & Dunkley Jones, 2012**
Pl. 1, figs 27, 28

1990 *Sphenolithus* sp. 1 Okada: p. 154, pl. 2, figs 9–12.
2012 *Sphenolithus kempii* Bown & Dunkley Jones: p. 33, pl. 10, figs 25–30, 32–35.
2012 *Sphenolithus* cf. *S. kempii* Bown & Dunkley Jones: p. 33, pl. 10, figs 36, 37.
2015 *Sphenolithus kempii* Bown & Dunkley Jones, 2012 – Fioroni et al.: pl. 1, figs 19–24.

Diagnosis: Medium-sized sphenolith with a medium-height, cylindrical proximal element cycle and a thin lower lateral element cycle. The upper lateral element cycle has a reduced element count, with three or four elements that are elongated vertically and laterally, forming distally divergent spines. The calcite *c*-axes in the upper lateral cycle elements are at an angle of ~45° to the median axis, so when the long axis of an element is parallel to the plane of the slide, and the median axis of the sphenolith is parallel to one of the polarising axes, the element is bright, and when the median axis is at 45°, it is dark. A small apical structure may be present, which appears to be monocyclic and monocrystalline. **Remarks**: This species, which appears to be descended from *S. spiniger*, marks the beginning of a lineage in which the upper lateral element cycle grows vertically and laterally, ultimately becoming the bifid spine that characterises most *Furcatolithus* species. It is possible that *S. stellatus* (Gartner, 1971, p. 114, pl. 5, fig. 3a, b) is a plan view of *S. kempii*, in which case, *S. kempii* would be a junior synonym of *S. stellatus*. Until this can be shown conclusively, the name *S. kempii* is retained here.

Sphenolithus perpendicularis **Shamrock, 2010**
Pl. 1, figs 29, 30

1995 *Sphenolithus* "*spinatus*" Bralower & Mutterlose: p. 59, pl. 7, figs 29, 30.
2010 *Sphenolithus perpendicularis* Shamrock: p. 8, pl. 1, figs 1-1, 1-2, 2-1, 2-2, 3-1, 3-2, 4-1, 4-2, 5-1, 5-2.
2012 *Sphenolithus perpendicularis* Shamrock, 2010 – Bown & Dunkley Jones: pl. 10, fig. 41.
2017 *Sphenolithus perpendicularis* Shamrock, 2010 – Bown & Newsam: pl. 11, figs 7–10, 13, *non* figs 11, 12.

Diagnosis: A large to very large sphenolith with a low to moderate-height, cylindrical proximal element cycle. The lower lateral cycle elements are thin. The upper lateral cycle elements are reduced in number to two, and are enlarged vertically and laterally to form two distally divergent spines, with an angle of ~90° between the spines. The calcite *c*-axes in the upper lateral cycle elements are at an angle of ~45° to the median axis, so they are brightly birefringent in lateral view when the median axis is parallel to one of the polarising axes, and dark when the median axis is at 45°. A small apical structure is present, which appears to be monocyclic and monocrystalline. The top of the apical structure is level with the base of the interspine area between the two upper lateral element spines, or projects slightly above it. **Remarks**: This is a very distinctive species with a very short range (within NP15, Middle Eocene), making it an excellent biostratigraphic marker. This is also the first species where the element count in the upper lateral element cycle is reduced to two elements—a critical step in the formation of the bifid spine characteristic of most species of *Furcatolithus*.

Sphenolithus shamrockiae n. sp.
Pl. 2, figs 1–4

2010 *Sphenolithus furcatolithoides* Locker, 1967 – Shamrock: pl. 1, figs 7-1, 7-2, 8-1, 8-2.
2014 *Sphenolithus furcatolithoides* Locker, 1967 morphotype A – Agnini et al.: pl. 3, figs 2, 3.

Derivation of name: In honour of Dr Jamie Shamrock, who figured the holotype of this species as *S. furcatolithoides* in Shamrock (2010). **Diagnosis**: A sphenolith with a low proximal element cycle, a thin lower lateral element cycle, and a high to very high, bifurcated upper lateral element cycle with two elements that form a bifid spine. A small, monocyclic apical structure is present, which does not extend above the base of the bifurcation of the bifid spine. **Remarks**: The presence of an apical structure (clearly visible when the specimen is oriented at 45° to the polarising axes as a small birefringent element above the birefringent elements of the lower lateral element cycle; see Shamrock, 2010, pl. 1, fig. 7-2) distinguishes this species from the otherwise similar *S. furcatolithoides,* the holotype of which completely lacks an apical structure. The apical structure is small, so it is unclear whether it is monocrystalline or a monocyclic composite. This is the first sphenolithid species known to have a bifid spine. **Holotype**: Shamrock (2010, pl. 1, figs 7-1, 7-2). **Holotype height**: 7.5 μm. **Paratype**: Shamrock (2010, pl. 1, figs 8-1, 8-2). Sample ODP-122-762C-15-2, 125–126 cm. **Type locality**: ODP Leg 122, Hole 762C, Exmouth Plateau, offshore western Australia, southeastern Indian Ocean. **Type level**: ODP-122-762C-15X-1, 48–49 cm; NP15b (of Martini, 1971)/CP13b (of Okada & Bukry, 1980), Middle Eocene (Lutetian), according to Shamrock (2010). **Occurrence**: The range of this species has not been fully established because most previous studies have not distinguished it from the similar, and closely related, *S. furcatolithoides*. Agnini et al. (2014) separated *S. shamrockiae* (as *S. furcatolithoides* morphotype A) from *S. furcatolithoides* (as *S. furcatolithoides* morphotype B), finding it restricted to their zone CNE10 (= middle NP15).

Sphenolithus furcatolithoides Locker, 1967 emend.
Pl. 2, figs 5, 6

1967 *Sphenolithus furcatolithoides* Locker: p. 363, pl. 1, figs 14–16, text-figs 7, 8.
2005a *Sphenolithus furcatolithoides* Locker, 1967 – Bown: pl. 45, figs 1–3.
2014 *Sphenolithus furcatolithoides* Locker, 1967 morphotype B – Agnini et al.: pl. 3, figs 11, 12.

Emended diagnosis: A sphenolith with a low proximal element cycle, a thin lower lateral element cycle, and a high to very high upper lateral element cycle. The upper lateral element cycle has two vertically adjoined elements, which bifurcate distally, forming a bifid spine. The point at which the bifid spine bifurcates is approximately one-third from the base of the spine. Thin distal and lateral extensions of the two vertical elements of the bifid spine may or may not be present, but if present, can vary greatly in length. No apical structure is present. **Remarks**: The photomicrographs of the holotype (Locker, 1967, figs 14, 15) of *S. furcatolithoides* are over-exposed, making it difficult to determine whether a lower lateral element cycle is present, although Locker's sketches of the holotype (figs 7, 8) strongly suggest that it is. Most subsequent illustrations of this species clearly show the presence of a lower lateral element cycle (e.g. Bown, 2005a, pl. 45, figs 1, 2). The holotype clearly lacks any apical structure. The high, bifurcated upper lateral element cycle in *S. furcatolithoides* and the closely related *S. shamrockiae* n. sp., formed from the high upper lateral element cycle of *S. perpendicularis,* and mark the evolution of the bifid spine, which is a key structural component of subsequent species in the genus *Furcatolithus*.

Sphenolithus labradorensis Firth, 1989 stat. nov.
Pl. 2, figs 7–10

1989 *Sphenolithus furcatolithoides* Locker, 1967 subsp. *labradorensis* Firth: p. 277, pl. 2, figs 15, 16; pl. 3, figs 1–4.

2006 *Sphenolithus strigosus* Bown & Dunkley Jones: p. 23, pl. 8, figs 6–15.

2006 *Sphenolithus runus* Bown & Dunkley Jones: p. 23, pl. 8, figs 16–24.

2012 *Sphenolithus strigosus* Bown & Dunkley Jones, 2006 – Bown & Dunkley Jones: pl. 10, figs 44, 45.

2014 *Sphenolithus labradorensis* (Firth, 1989) Aubry: pp. 150, 282 (invalid, see remarks below).

2017 *Sphenolithus runus* Bown & Dunkley Jones, 2006 – Bown & Newsam: pl. 11, figs 30–35.

2017 *Sphenolithus strigosus* Bown & Dunkley Jones, 2006 – Bown & Newsam: pl. 11, figs 27–29.

Basionym: *Sphenolithus furcatolithoides* Locker, 1967 subsp. *labradorensis* Firth, 1989, p. 277, pl. 2, figs 15, 16; pl. 3, figs 1–4. Firth, J.V. 1989. Eocene and Oligocene calcareous nannofossils from the Labrador Sea, ODP Leg 105. *Proceedings of the ODP, Scientific Results,* **105**: 263–286. **Diagnosis**: A sphenolith with a low proximal element cycle, a thin lower lateral element cycle, and a high upper lateral element cycle. The upper lateral element cycle is reduced to two vertical elements, which bifurcate distally. Thin distal extensions of these vertical elements may or may not be present. No apical structure is present. **Remarks**: The change in status by Aubry (2014) is invalid under ICN Art. 41.6 because, whilst the basionym was cited, as required under Art. 41.5, the page and figure numbers of the description of *S. furcatolithoides* subsp. *labradorensis* by Firth were entirely omitted, which is not permitted under ICN Art. 41.6. This species is likely the immediate ancestor to *Furcatolithus cuniculus* n. comb., with the main difference being the presence of a lower lateral element cycle in *S. labradorensis*, which is lost in the transition to *F. cuniculus*. The presence or absence of a lower lateral element cycle is the key structural difference between the two species and the two genera.

The holotype of *S. strigosus* is very similar to that of *S. labradorensis*, with both specimens clearly showing the presence of a lower lateral element cycle and a bifid spine, so *S. strigosus* is considered here to be a junior synonym of *S. labradorensis*. The holotype of *S. runus* is similar in size and overall appearance to the holotypes of both *S. labradorensis* and *S. strigosus,* with a clearly visible lower lateral element cycle, but no visible apical structure. The bifid spine of the holotype (Bown & Dunkley Jones, 2006, pl. 8, figs 18–20) is dark at 0° and bright at 45°, which is opposite to the extinction pattern for the bifid spine of the holotype specimen of *S. labradorensis*. A suture can be seen surrounding the periphery of the spine, which here is interpreted as the median suture of the bifid spine, at a low oblique angle to the plane of the slide. The other specimens of *S. runus* figured in Bown & Dunkley Jones (2006, pl. 8, figs 16, 17, 21–24) show a similar pattern, as do the specimens of *S. runus* figured by Bown & Newsam (2017, pl. 11, figs 30, 31, 34, 35). The specimen figured as *S. runus* by Bown & Newsam (2017, pl. 11, figs 32, 33) has a bifid spine that is partially bright in both the 0° and 45° orientations to the polarising axes, and has a clearly visible median suture (their pl. 11, fig. 32), where the specimen is oriented at 0° to the polariser, so this specimen is considered to be specimen of *S. labradorensis,* even by their criteria.

For these reasons, the holotype of *S. runus* is interpreted here as being a specimen of *S. labradorensis* oriented with the median suture of the bifid spine lying parallel, or slightly oblique, to the plane of the slide, rather than orthogonal to the plane of the slide, as in the holotype image of *S. labradorensis,* and in which orientation the median suture of the bifid spine is visible. Accordingly, *S. runus* is interpreted to be a junior synonym of *S. labradorensis*.

Sphenolithus dissimilis Group

The species in this group all have medium-high to high, cylindrical to slightly flaring proximal element cycles, thin lateral element cycles, and monocyclic composite apical structures with subparallel to divergent elements, resulting in a cylindrical or biconical overall shape in some species. In some species, the elements in the apical structure are all similar in height, giving the apical structure a cylindrical appearance with a flat distal surface, which is not seen in any other group of sphenoliths. The species in this group are discussed below in approximate order of first stratigraphic appearance: *S. truaxii*, *S. procerus*, *S. capricornutus*, *S. compactus*, *S. disbelemnos*, *S. multispinatus*, *S. dissimilis* and *S. cometa*. A range chart for this group is presented in Figure 10.

Sphenolithus truaxii Bergen & de Kaenel *in* Bergen et al., 2017
Pl. 2, figs 11, 12

2017 *Sphenolithus truaxii* Bergen & de Kaenel *in* Bergen et al.: p. 87, pl. 2, figs 21–26.

Diagnosis: A large sphenolith with a medium to tall cylindrical proximal element cycle. The elements of the lower and upper lateral cycles are thick and extend laterally slightly beyond the top of the proximal cycle, giving the lateral profile a slightly stepped appearance. The composite apical structure is monocyclic and cylindrical with a gently convex to flat distal surface. The apical structure is tall. **Remarks**: Under the LM, some specimens of this species present an unusual appearance where the proximal element cycle and the apical structure are approximately equal in size and shape. In specimens like this, the proximal cycle and the apical structure can be difficult to distinguish.

Sphenolithus procerus Maiorano & Monechi, 1997
Pl. 2, figs 13, 14

1997 *Sphenolithus procerus* Maiorano & Monechi: p. 103, pl. 1, figs 1–3.

Diagnosis: A medium-sized sphenolith with a medium-high, slightly flared proximal element cycle. The lower and upper lateral element cycles are slightly thickened. The composite apical structure is monocyclic and cylindrical, with a relatively flat distal surface. **Remarks**: This species resembles *S. truaxii* but differs in having a lower proximal element cycle.

Sphenolithus capricornutus Bukry & Percival, 1971
Pl. 2, figs 15, 16

1971 *Sphenolithus capricornutus* Bukry & Percival: p. 140, pl. 6, figs 4–6.
2007 *Sphenolithus capricornutus* Bukry & Percival, 1971 – Denne: pl. 1, fig. 14.

Diagnosis: A large to very large sphenolith with a medium-high to high, slightly to moderately flared proximal element cycle. The lower lateral cycle elements are thin, and the upper lateral cycle elements are thick. The high apical structure is monocyclic and composite, and comprises two prominent apical elements that diverge distally and laterally. **Remarks**: Such a pair of divergent apical elements is not found in any other post-Eocene sphenolith. Differentiation of the upper lateral cycle elements from the two apical elements is difficult in this species because the apical elements are at an angle of ~45° to the median axis, so the *c*-axis orientations of the elements in the spines are similar to the *c*-axis orientations of the elements in the upper lateral element cycle, and hence their birefringence is similar. Close examination of most published images of specimens where the median axis is parallel to one of the polarising axes (e.g. Denne, 2007, pl. 1, fig. 14; Bergen et al., 2017, pl. 7, figs 26, 28, 30; Gennari et al., 2017, fig. 9a) shows that the upper lateral cycle elements are slightly brighter than the two apical elements, and can be recognised as ultrastructurally distinct. **Differentiation**: This species is superficially similar to the Eocene *S. perpendicularis*, although it is phylogenetically and ultrastructurally unrelated, as the divergent spines in *S. perpendicularis* are elongated upper lateral cycle elements, and not elongated apical structure elements, as seen in *S. capricornutus*.

Sphenolithus compactus Backman, 1980
Pl. 2, figs 17, 18

1980 *Sphenolithus compactus* Backman: p. 59, pl. 3, fig. 20.
2017 *Sphenolithus paratintinnabulum* Bergen & de Kaenel *in* Bergen et al.: p. 88, pl. 3, figs 29, 30; pl. 4, figs 1–6.

Diagnosis: A very small to small sphenolith with a high, cylindrical proximal element cycle. The lateral element cycles are thin. The composite apical structure is domed and low. It is unclear whether the apical structure is mono- or polycyclic. **Remarks**: The holotype of *S. compactus* was described by Backman (1980) from NN3, in the Early Miocene, and falls within the range described by Bergen et al. (2017) for *S. paratintinnabulum*, the holotype of which was described from NN2, but which ranges up to the middle of NN3, to 18.612Ma (Bergen et al., 2017, 2019a). The holotypes of the two species are very similar, with relatively tall, cylindrical proximal element cycles and low apical structures, so *S. paratintinnabulum* is regarded here as a junior synonym of *S. compactus*. This species has been regarded by many workers as a small variety of *S. primus* or *S. moriformis* (e.g. Perch-Nielsen, 1985, pp. 522, 523), but its tall, cylindrical proximal cycle is quite unlike the much lower and slightly flaring proximal cycle of *S. moriformis*.

Sphenolithus disbelemnos Fornaciari & Rio, 1996
Pl. 2, figs 19, 20

1996 *Sphenolithus disbelemnos* Fornaciari & Rio: pl. 2, figs 7–10; pl. 3, figs 19, 20; pl. 4, fig. 2.
1996 *Sphenolithus aubryae* de Kaenel & Villa: p. 128, pl. 11, figs 16–18.
2017 *Sphenolithus disbelemnos* Fornaciari & Rio, 1996 – Bergen et al.: pl. 3, figs 11–28.

Diagnosis: A small sphenolith with a tall, cylindrical proximal element cycle. The elements of the lower and upper lateral cycles are thick, and extend laterally slightly beyond the top of the proximal cycle, giving the lateral profile a slightly stepped appearance. The composite apical structure is monocyclic and cylindrical, with a relatively flat distal surface. The apical structure is low in height. **Remarks**: The holotype of *S. aubryae* is very similar to that of *S. disbelemnos,* other than being slightly larger (the holotype of *S. disbelemnos* is 2.95 μm high, that of *S. aubryae* 4.1 μm high), so *S. aubryae* is considered to be a junior synonym of *S. disbelemnos*.

Sphenolithus multispinatus Maiorano & Monechi, 1997
Pl. 2, figs 21, 22

1997 *Sphenolithus multispinatus* Maiorano & Monechi: pl. 1, figs 14–16.
2017 *Sphenolithus multispinatus* Maiorano & Monechi, 1997 – Bergen et al.: pl. 7, figs 14–17.

Diagnosis: A large sphenolith with a low, moderately flaring proximal element cycle, and relatively thick lateral element cycles. The apical structure is composite and monocyclic, with distally and laterally diverging elements, resulting in an overall biconical shape. The elements in the apical structure are variable in length, so in lateral view, the distal surface of the apical structure appears uneven. **Remarks**: The degree of divergence of the elements in the apical structure is greater in *S. multispinatus* than in *S. cometa*, and the elements are coarser.

Sphenolithus dissimilis Bukry & Percival, 1971
Pl. 2, figs 23–26

1971 *Sphenolithus dissimilis* Bukry & Percival, pl. 6, figs 7, 9, *non* fig. 8.
2017 *Sphenolithus dissimilis* Bukry & Percival, 1971 – Bergen et al.: pl. 3, figs 7–10.

Diagnosis: A large sphenolith with a tall, cylindrical proximal element cycle, slightly thickened lower and upper lateral element cycles, and a moderately tall, monocyclic composite apical structure that is cylindrical in shape. The distal surface of the apical structure appears flat in lateral view. **Remarks**: This species has a similar range to *S. disbelemnos*, with which it appears to form a plexus in which the height of the apical structure is variable—low in *S. disbelemnos,* moderately high in *S. dissimilis*.

Sphenolithus cometa de Kaenel & Villa, 1996
Pl. 2, figs 27, 28

1996 *Sphenolithus cometa* de Kaenel & Villa: pl. 11, figs 22–24.
2017 *Sphenolithus cometa* de Kaenel & Villa, 1996 – Bergen et al.: pl. 7, figs 18–25.

Diagnosis: A medium-sized sphenolith with a tall, slightly flaring to cylindrical proximal element cycle. The lower and upper lateral element cycles are thin. The apical structure is monocyclic, tall, and has distally diverging elements that give this species an overall biconical shape. The distal surface of the apical structure appears flat in lateral view. **Remarks**: The divergent apical structure of this species is clearly different to the cylindrical apical structure of the otherwise similar *S. dissimilis*.

Sphenolithus conicus Group

The species in this group are all medium-high to high, conical, with a medium-high to high, sharply pointed to rounded, monocyclic apical structure. As with the *S. anarrhopus* group, the apical structures in most specimens of species in this group are monocrystalline, but occasionally (particularly in *S. conicus*), it can be seen that the apical structure is monocyclic and composite, comprising several elements, but with one or two larger elements dominating the spine. The species in this group are discussed below in approximate order of first stratigraphic appearance: *S. conicus*, *S. calyculus*, *S. macroacanthos*, *S. pseudoheteromorphus*, *S. heteromorphus*, *S. preasii* and *S. milanetti*. A range chart for this group is presented in Figure 8.

Sphenolithus conicus Bukry, 1971a
Pl. 2, figs 29, 30

1971a *Sphenolithus conicus* Bukry: p. 320, pl. 5, figs 10–12.
2012 *Sphenolithus conicus* Bukry, 1971a – Bown & Dunkley Jones: pl. 13, figs 13–18.
2017 *Sphenolithus conicus* Bukry, 1971a – Bergen et al.: pl. 5, figs 7–18.

Diagnosis: A large sphenolith with a medium-high, moderately flaring proximal element cycle, thin lower and upper lateral element cycles, and a medium-high, rounded, conical, monocyclic composite apical structure, usually dominated by one or two large, sub-vertical elements. Some specimens have a fully monocrystalline apical structure. **Remarks**: The transition from a monocyclic composite spine to a monocrystalline spine occurs in this species. These two morphotypes could be split into different species. This is considered impractical here because it can be very difficult to distinguish between a composite apical structure with a few coarse elements and a monocrystalline apical structure. All subsequent species in this lineage have monocrystalline apical structures, although *S. pseudoheteromorphus* can have a cycle of small, thin apical elements at the base of the large monocrystalline spine, resulting in a composite apical structure.

Sphenolithus calyculus Bukry, 1985
Pl. 3, figs 1, 2

1985 *Sphenolithus calyculus* Bukry: p. 600, pl. 1, figs 13–19.
2017 *Sphenolithus calyculus* Bukry, 1985 – Bergen et al.: pl. 5, figs 1–4, *non* figs 5, 6.

Diagnosis: A medium-sized sphenolith with a medium-high proximal cycle, thin lower and upper lateral element cycles, and a tall, narrow, conical monocrystalline apical structure. **Remarks**: This species is transitional between *S. conicus* and *S. pseudoheteromorphus*. It is distinguished from both of these species by its taller and thinner apical structure, which is symmetrical, in contrast to the spine in *S. pseudoheteromorphus*.

Sphenolithus macroacanthos Aubry, 2014
Pl. 3, figs 3, 4

non 1980 *Sphenolithus elongatus* Perch-Nielsen: p. 2, pl. 1, figs 14, 15; pl. 2, figs 5–11 (not considered here to be a true sphenolithid).
1986 *Sphenolithus elongatus* Martini: p. 753, pl. 2, figs 7, 8 (homonym of *S. elongatus* Perch-Nielsen, 1980).
2014 *Sphenolithus macroacanthos* Aubry: pp. 150, 346, *nom. nov. pro Sphenolithus elongatus* Martini, 1986.
2017 *Sphenolithus calyculus* Bukry, 1985 – Bergen et al.: pl. 5, figs 5, 6, *non* figs 1–4.

Diagnosis: A large to very large sphenolith with a medium-high proximal cycle, thin lower and upper lateral element cycles, and a tall, narrow monocrystalline apical structure. **Remarks**: *Sphenolithus elongatus* Martini, 1986 is a homonym of *S. elongatus* Perch-Nielsen, 1980. Aubry (2014) erected the name *S. macroacanthos* as a *nomen novum* for *S. elongatus* Martini, 1986. *Sphenolithus elongatus* Perch-Nielsen, 1980 is not considered to be a true sphenolithid, as the holotype does not appear to have a sphenolithid proximal cycle, and hence does not belong to the family Sphenolithaceae. The holotype of *S. elongatus* Martini, 1986 is 9.6 μm high, while that of *S. calyculus* is 5.0 μm. Otherwise the two species are very similar.

Sphenolithus pseudoheteromorphus Fornaciari & Agnini, 2009
Pl. 3, figs 5, 6

2009 *Sphenolithus pseudoheteromorphus* Fornaciari & Agnini: p. 97, pl. 1, figs 1–16; pl. 2, figs 1–5, 9, 13.
2017 *Sphenolithus pseudoheteromorphus* Fornaciari & Agnini, 2009 – Bergen et al.: pl. 7, figs 1–5.

Diagnosis: A very large sphenolith with a low, moderately flared proximal element cycle, thin lower and upper lateral element cycles, and a tall, pointed-conical monocrystalline apical structure that is usually at a slight angle to the median axis of the sphenolith. A cycle of small apical elements may be present around the base of the apical structure. **Remarks**: This species is generally taller and thinner overall than the closely related *S. heteromorphus*. The two species can be separated by the inclination of the apical structure in *S. pseudoheteromorphus*.

Sphenolithus heteromorphus Deflandre, 1953
Pl. 3, figs 7, 8

1953 *Sphenolithus heteromorphus* Deflandre: p. 1786, pl. 1, figs 1–2.
2017 *Sphenolithus heteromorphus* Deflandre, 1953 – Bergen et al.: pl. 7, figs 6–11.

Diagnosis: A large to very large sphenolith with a low, moderately flared proximal element cycle, slightly thickened lower and upper lateral element cycles, and a tall, pointed monocrystalline apical structure. **Remarks**: *Sphenolithus heteromorphus* can be very common in CN3 (of Okada &Bukry, 1980)/NN4 (of Martini, 1971) in the Burdigalian, where it is an excellent marker species.

Sphenolithus preasii Bergen & de Kaenel *in* Bergen et al., 2017
Pl. 3, figs 9, 10

2017 *Sphenolithus preasii* Bergen & de Kaenel *in* Bergen et al.: p. 90, pl. 5, figs 19–30.

Diagnosis: A very large sphenolith with a medium-high, moderately flared proximal element cycle, thickened lower and upper lateral element cycles, and a medium-high, pointed apical structure. In lateral view, the elements of the proximal cycle are slightly curved. **Remarks**: As noted by Bergen et al. (2017), *S. preasii* is transitional between *S. conicus* and *S. milanetti*, with the elements in the proximal cycle being slightly curved in lateral view, rather than strongly curved, as in *S. milanetti*. The holotype of *S. preasii* has a monocrystalline apical structure, in contrast to the monocyclic composite apical structure of *S. conicus,* which is usually dominated by one or two large subvertical elements.

Sphenolithus milanetti Maiorano & Monechi, 1998
Pl. 3, figs 11, 12

1989 *Sphenolithus* sp. 1 Olafsson: p. 19, pl. 1, fig. 6.
1990 *Sphenolithus milanetti* Fornaciari & Rio *in* Fornaciari et al. (*nomen nudum*): pl. 3, figs 6A–D.
1998 *Sphenolithus milanetti* Maiorano & Monechi: pl. II, figs 30, 31.
2016 *Sphenolithus pospichalii* Jiang et al.: p. 61, pl. 1, figs 1–8.
2017 *Sphenolithus milanetti* Maiorano & Monechi, 1998 – Bergen et al.: pl. 8, figs 1–9.

Diagnosis: A large to very large sphenolith with a high proximal element cycle. In lateral view, the elements of the proximal cycle are distinctly curved, resulting in a strongly concave proximal surface. The lower and upper lateral element cycles are slightly thickened, and the apical structure is monocrystalline and moderate in height. **Remarks**: This species is superficially similar to the Eocene *S. orphanknollensis*, as both species have high proximal element cycles, with elements that are strongly curved in lateral view. *Sphenolithus pospichalii* was described as having a taller apical structure than *S. milanetti*; however, the difference in the height of the apical structure between the two holotypes is minimal. As noted by Bergen et al. (2017), the two holotypes are both 8 μm in height, and both species were described from NN4, so they are here considered synonymous.

***Sphenolithus delphix* Group**

The species in this group all have a flared proximal element cycle. The apical structure is monocyclic, composite in *S. bipedis* and monocrystalline in *S. spinula*, *S. microdelphix, S. delphix*, *S. tintinnabulum* and *S. belemnos*. Species in this group are discussed below in approximate order of first stratigraphic appearance: *S. bipedis, S. spinula, S. microdelphix, S. delphix, S. tintinnabulum* and *S. belemnos*. A range chart for this group is presented in Figure 10.

Sphenolithus bipedis Bergen & de Kaenel *in* Bergen et al., 2017
Pl. 3, figs 13, 14

2017 *Sphenolithus bipedis* Bergen & de Kaenel *in* Bergen et al.: p. 83, pl. 1, figs 5–12.

Diagnosis: A small sphenolith with a medium-high, strongly flared proximal element cycle. The lateral element cycles are thin, and there is a low, conical monocyclic composite apical structure. **Remarks**: This species resembles *S. neoabies* in having a strongly flared proximal element cycle and a low apical structure, but is older, and has a disjunct range (Bergen et al., 2017).

Sphenolithus spinula Bergen & de Kaenel *in* Bergen et al., 2017
Pl. 3, figs 15, 16

2017 *Sphenolithus spinula* Bergen & de Kaenel *in* Bergen et al.: p. 91, pl. 6, figs 1–8.

Diagnosis: A medium-sized sphenolith with a tall, strongly flared proximal element cycle. The lower and upper lateral element cycles are thin, and the monocrystalline apical structure is medium-high. **Remarks**: *Sphenolithus spinula* is distinguished from the otherwise similar *S. microdelphix* in having a taller, but equally strongly flared proximal element cycle.

Sphenolithus microdelphix Bergen & de Kaenel *in* Bergen et al., 2017
Pl. 3, figs 17, 18

2017 *Sphenolithus microdelphix* Bergen & de Kaenel *in* Bergen et al.: p. 91, pl. 6, figs 21–25.
2017 *Sphenolithus delphix* Bukry, 1973 – Gennari et al.: figs 9m, n, *non* figs 9i–l.

Diagnosis: A medium-sized sphenolith with a medium-high, strongly flared proximal element cycle, a thin lower lateral element cycle, a slightly thickened upper lateral element cycle, and a tall, conical apical structure. In well-preserved specimens, two horizontally opposite elements in the proximal cycle are proximally and laterally extended, with lengths similar to the height of the apical structure. **Remarks**: The holotype of *S. microdelphix* clearly shows an extended element in the proximal cycle (Bergen et al., 2017, pl. 6, figs 11, 12, on the right-hand side of the specimen). See remarks for *S. delphix*.

Sphenolithus delphix Bukry, 1973
Pl. 3, figs 19–22

1973 *Sphenolithus delphix* Bukry: pl. 3, figs 19–22.
1974 *Sphenolithus* sp. 1 Müller, pl. 4, figs 3–6.
1974 *Sphenolithus* sp. 2 Müller, pl. 4, figs 7, 8.
1986 *Sphenolithus delphix* Bukry, 1973 – Knüttel: pl. 4, figs 1–5, 8.
1989 *Sphenolithus delphix* Bukry, 1973 – Firth: pl. 4, figs 7, 8.
2017 *Sphenolithus delphix* Bukry, 1973 – Bergen et al.: pl. 6, figs 21–25.
2017 *Sphenolithus delphix* Bukry, 1973 – Gennari et al.: figs 9i–n.

Diagnosis: A large sphenolith with a medium-high, strongly flared proximal element cycle, a thin lower lateral element cycle, a slightly thickened upper lateral element cycle, and a tall, conical, monocrystalline apical structure. In well-preserved specimens, two horizontally opposite elements in the proximal cycle are proximally and laterally extended, to a variable degree. **Remarks**: Most descriptions of *S. delphix* emphasise the strongly flared proximal element cycle as characteristic of this species. Published images of this species show a wide range of variation in the degree of flare of the proximal cycle, with some images showing the length of the elements in the proximal cycle being approximately equal to the length of the apical structure. The type description by Bukry (1973) clearly mentioned that "The apical spine and two of the basal spines are slender and elongate, resulting in a triradiate outline", and in the remarks, Bukry commented that "The structure of some specimens suggests that the two long basal spines are secondary elongations. Because of the regular position of these spines and the low abundance of *S. delphix* in populations of fossil coccoliths, however, these structures are probably biologic in origin".

Close examination of the LM images of the holotype (Bukry, 1973, pl. 3, figs 19, 21, 22) show a difference in the lengths of the proximal cycle elements between his fig. 19 (a transmitted light image) and fig. 20 (a cross-polarised-light image), which is interpreted here as evidence that the holotype specimen bears extended elements in the proximal cycle, which are about half the height of the apical structure in length. The specimen figured here in Plate 3, figs 21 and 22, shows an extended proximal cycle element on the right-hand side of the proximal cycle, which is similar in length to the apical structure. This extension of some of the proximal cycle elements is a structural innovation not shown by any sphenolithid other than the closely related *S. microdelphix,* which is smaller, with a proportionally shorter apical structure, but is otherwise very similar.

It is clear from the SEM images of Müller (1974, pl. 4, figs 7, 8) and Knüttel (1986, pl. 4, figs 1, 2), and the LM images of Firth (1989, pl. 4, figs 7, 8) that these horizontally opposed proximal cycle elements can be extended in length, elongating into long spines, similar in length to the apical structure. This form was described, but not figured, as a “long triradiated” *S. delphix* by de Kaenel & Villa (1996, p. 99), who mentioned that “Moreover, a very short, characteristic interval contains abundant forms of large *S. delphix*. This ‘triradiated’ form possesses a very long apical spine and two extremely elongated proximal elements, and it occurs near the top of the range of *S. delphix*, together with frequent *T. carinatus*”.

Sphenolithus tintinnabulum Maiorano & Monechi, 1997
Pl. 3, figs 23, 24

1997 *Sphenolithus tintinnabulum* Maiorano & Monechi: p. 104, pl. 1, figs 4–6.
2017 *Sphenolithus tintinnabulum* Bergen et al.: pl. 4, figs 7–18.

Diagnosis: A small sphenolith with a moderately high, moderately flared proximal element cycle, thin lower and upper lateral element cycles, and a low monocrystalline apical structure that is conical in shape. **Remarks**: See remarks for *S. belemnos*.

Sphenolithus belemnos Bramlette & Wilcoxon, 1967
Pl. 3, figs 25–28

1967 *Sphenolithus belemnos* Bramlette & Wilcoxon: p. 118, pl. 2, figs 1–3.
2017 *Sphenolithus belemnos* Bramlette & Wilcoxon, 1967 – Bergen et al.: pl. 4, figs 19–30.

Diagnosis: A large sphenolith with a moderately tall, slightly flaring proximal element cycle. Both the lower and upper lateral element cycles are thin. The monocrystalline apical structure is tall and conical. **Remarks**: The proximal element cycle of *S. belemnos* is taller than that of *S. tintinnabulum*, but is not as flared. It is similar in height to that of *S. disbelemnos*, but is more flared. The apical structure of *S. belemnos* is monocrystalline, like that of *S. tintinnabulum* (and unlike the monocyclic composite apical structure of *S. disbelemnos*), so, overall, *S. belemnos* is considered here to be likely descended from *S. tintinnabulum*, although it could also be descended from *S. disbelemnos*.

***Sphenolithus quadrispinatus* Group**

The single species in this group has a low to medium-high, cylindrical proximal element cycle. The apical structure is monocyclic, with usually four elements bearing thin extensions that extend laterally and vertically. A range chart for the single species in this group is presented in Figure 8.

Sphenolithus quadrispinatus Perch-Nielsen, 1980

1980 *Sphenolithus quadrispinatus* Perch-Nielsen: p. 3, pl. 1, figs 11, 13; pl. 2, figs 1–4.

Diagnosis: A large to very large sphenolith with a low to medium-high, cylindrical proximal element cycle, thin lateral element cycles, and a monocyclic apical structure with usually four elements bearing thin extensions that extend laterally and vertically. **Remarks**: This species is a partial homeomorph of species in the *S. dissimilis* group—particularly *S. capricornutus* and *S. multispinatus*—with which it shares an apical structure with distally and laterally diverging elements. The EM images of this species in Perch-Nielsen (1980, pl. 2, figs 1–4) are of high quality and show multiple well-preserved specimens. It seems clear from these images that this species is distinct from species of the *S. dissimilis* group.

Sphenolithus quadrispinatus has a short range in the Tortonian, and has very rarely been recorded. The only record in the International Ocean Discovery Program SEDIS database of DSDP, ODP and IODP data is that of Quinterno (1994) who recorded it from CN8 (of Okada & Bukry, 1980) in ODP Hole 841B, from the Tonga Trench in the Pacific Ocean, but did not present any images.

Genus *Furcatolithus* Martini, 1965 emend.

Emended diagnosis: Conical coccoliths with a proximal element cycle of radially arranged elements. Above the proximal element cycle, there is usually a vertically split bifid spine, composed of two vertical elements. The two elements of the bifid spine often bear thin extensions that extend distally and laterally. No lower lateral element cycle, or apical structure (apical cycle or spine), as seen in species of the genus *Sphenolithus*, is ever present. **Type species**: *Furcatolithus distentus* Martini, 1965. **Synonym**: *Pseudozygrhablithus* Haq, 1971. **Discussion**: Martini (1965) described *F. distentus* as the generotype of *Furcatolithus*. The holotype (Martini, 1965, figs 8, 9) is an isolated bifid spine, with thin distal extensions. No proximal cycle is present; it is interpreted here as having broken off. The holotype was interpreted by Martini (1965) to be of Miocene age (*Catapsydrax dissimilis* planktonic foraminiferal zone). As *F. distentus* has been reported in subsequent works by many authors (e.g. Perch-Nielsen, 1985; Bown & Dunkley Jones, 2012) to be of mid-Oligocene age, the age interpretation of Martini (1965) is considered erroneous. Bramlette & Wilcoxon (1967) examined material from the same core that Martini (1965) described *F. distentus* from, and figured specimens (Bramlette & Wilcoxon, 1967, pl. 1, fig. 5; pl. 2, figs 4, 5) that clearly show the presence of a proximal element cycle (which they termed 'short basal spines'), the absence of a lower lateral element cycle, and the absence of an apical element cycle or spine. They commented that "The apical spine is easily separated from the short basal spines, particularly in the poorly preserved specimens of some samples", which seems to be a reference to the fact that Martini's (1965) holotype has a missing proximal element cycle. They considered the core examined by Martini (1965) to belong to the upper *Globigerina ampliapertura* or lower *Globorotalia opima opima* planktonic foraminiferal zones, supporting a mid-Oligocene range for *F. distentus*.

Bramlette & Wilcoxon (1967) recombined *F. distentus* into the genus *Sphenolithus* Deflandre, 1952, presumably because of the overall similarity of the forms (i.e. conical gross morphology) between the generotype of *Sphenolithus* (*S. radians* Deflandre, 1952) and *F. distentus*. Curiously, Bramlette & Wilcoxon (1967) did not attempt to justify or discuss their recombination at all, instead confining their discussion to the ultrastructure of *F. distentus,* and its geographical and stratigraphical distribution. Their recombination has been followed by almost all nannofossil workers, having the effect of completely suppressing the genus *Furcatolithus*. This recombination is rejected here, due to the major structural differences between the generotypes of the two genera—the presence of a bifid spine and the absence of a lower lateral element cycle and any apical structure in *F. distentus,* and the presence of lower and upper lateral element cycles and an apical structure in *S. radians,* which lacks a bifid spine.

Furcatolithus is interpreted to have evolved from the *S. kempii* group during the Middle Eocene. The lineage from *S. kempii* to *S. perpendicularis* to *S. shamrockiae* to *S. furcatolithoides* to *S. labradorensis* shows a trend of increasing height and decreasing element count in the upper lateral element cycle—which became the two-part bifid spine in *Furcatolithus* species—along with a reduction in height of the apical structure. The eventual complete loss of the apical structure occurred in the transition from *S. furcatolithoides* to *S. labradorensis*, and was followed by loss of the lower lateral element cycle in the transition from *S. labradorensis* to *F. cuniculus*—the oldest species of *Furcatolithus*. The bifid spine is reduced in size in the *F. triangularis* group, and is ultimately lost completely in the last representative of the genus—*F. umbrellus*.

Seventeen *Furcatolithus* species are recognised as valid here. These species have been divided into three informal groups of species, based on shared morphology. These groups are listed in Table 2 and are detailed below, with both groups and species in approximate order of first stratigraphical appearance.

Furcatolithus predistentus Group

The species in this group all have high (>~65°) median-axis/base bifid spine angles. Most species (e.g. *F. predistentus*) have low proximal cycles (~10–15% of the total height, excluding distal bifurcations), although some species (*F. obtusus, F. peartiae* and *F. tawfikii*) have higher proximal cycles. The species in this group are discussed below in approximate order of first stratigraphical appearance: *F. cuniculus*, *F. predistentus*, *F. obtusus*, *F. celsus*, *F. intercalaris*, *F. akropodus*, *F. tribulosus*, *F. peartiae* and *F. tawfikii*. A range chart for this group is presented in Figure 11. A selection of species from each group in the genus is presented on Plate 4.

Furcatolithus cuniculus (Bown, 2005a) n. comb.
Pl. 4, figs 1–4

2005a *Sphenolithus cuniculus* Bown: p. 46, pl. 45, figs 6–10.

Basionym: *Sphenolithus cuniculus* Bown, 2005a, p. 46, pl. 45, figs 6–10. Bown, P.R. 2005a. Palaeogene calcareous nannofossils from the Kilwa and Lindi areas of coastal Tanzania (Tanzania Drilling Project 2003–4). *Journal of Nannoplankton Research*, **27**(1): 21–95. **Diagnosis**: A medium to large furcatolith with a high, blocky bifid spine, and a low proximal element cycle. The tips of the bifid spine bifurcate 30% of the way down the spine. The angle between the median axis and the top of the proximal element cycle is approximately 90°. The base of the proximal element cycle is concave. **Remarks**: Bown (2005a) described this species as being similar to (and possibly a preservational variant of) *S. furcatolithoides*, but with shorter lower quadrants (i.e. a lower proximal element cycle) and broader upper quadrants (i.e. a broader bifid spine). Unlike *S. furcatolithoides*, which has a lower lateral element cycle (a key characteristic of *Sphenolithus*, as emended here), *F. cuniculus* completely lacks a lower lateral element cycle, and so belongs to *Furcatolithus*. *Furcatolithus cuniculus* has an unusually blocky bifid spine, with thick vertical bifurcations, so measurement of the total height is taken to the top of the bifurcations. For the holotype, this results in the proximal cycle being 15% of the total height. *F. cuniculus* is the first species of the genus to have evolved.

Furcatolithus predistentus (Bramlette & Wilcoxon, 1967) n. comb.
Pl. 4, figs 5, 6

1967 *Sphenolithus predistentus* Bramlette & Wilcoxon: p. 126, pl. 1, fig. 6; pl. 2, figs 10, 11.
2012 *Sphenolithus predistentus* Bramlette & Wilcoxon, 1967 – Bown & Dunkley Jones: pl. 11, figs 17–22.
2017 *Sphenolithus predistentus* Bramlette & Wilcoxon, 1967 – Bergen et al.: pl. 11, figs 15, 17–20.

Basionym: *Sphenolithus predistentus* Bramlette & Wilcoxon, 1967, p. 126, pl. 1, fig. 6; pl. 2, figs 10, 11. Bramlette M.N. & Wilcoxon J.A. 1967. Middle Tertiary calcareous nannoplankton of the Cipero section, Trinidad, W.I. *Tulane Studies in Geology,* **5**(3): 93–131. **Diagnosis**: A large furcatolith with a very low proximal element cycle that is ~10% of the total height. The angle between the median axis and the top of the proximal element cycle is ~80–90°. The base of the proximal element cycle is concave. Thin distal extensions of the bifid spine may or may not be present, and if present, can vary greatly in length. **Remarks**: See remarks for *F. celsus* below.

Furcatolithus obtusus (Bukry, 1971a) n. comb.
Pl. 4, figs 7–12

1971a *Sphenolithus obtusus* Bukry: p. 321, pl. 6, figs 1–9.
2005a *Sphenolithus obtusus* Bukry, 1971a – Bown, pl. 45, figs 11–20.

Basionym: *Sphenolithus obtusus* Bukry, 1971a, p. 321, pl. 6, figs 1–9. Bukry, D. 1971a. Cenozoic Calcareous Nannofossils from the Pacific Ocean. *Transactions of the San Diego Society of Natural History,* **16**(14): 303–327. **Diagnosis**: A large furcatolith with a bifid spine, and a proximal element cycle that is ~25% of the total height. The angle between the median axis and the top of the proximal element cycle is ~50–60°. The base of the proximal element cycle is concave. Thin distal extensions of the bifid spine may or may not be present, and if present, can vary greatly in length. **Remarks**: The precise relationships between the earliest forms of *Furcatolithus* are unclear. Either *F. cuniculus* or *F. predistentus* could be the ancestor of *F. obtusus*.

Furcatolithus celsus (Haq, 1971) n. comb.

1971 *Sphenolithus celsus* Haq: p. 121, pl. 1, figs 1–5; pl. 5, fig. 4.
2012 *Sphenolithus celsus* Haq, 1971 – Bown & Dunkley Jones: pl. 11, figs 24–26.
2017 *Sphenolithus celsus* Haq, 1971 – Bergen et al.: pl. 11, figs 25–30.

Basionym: *Sphenolithus celsus* Haq, 1971, p. 121, pl. 1, figs 1–5; pl. 5, fig. 4. Haq, B.U. 1971. Paleogene calcareous nannoflora. Parts I–IV. *Stockholm Contributions in Geology,* **25**: 1–158. **Diagnosis**: A very large furcatolith with a bifid spine and a very low proximal element cycle that is ~10% of the total height. The total height is >9 μm. The bifid spine narrows to become thin and parallel-sided at about one-third of the total height of the spine. The angle between the median axis and the top of the proximal element cycle is ~80–90°. The base of the proximal element cycle is concave. Thin distal extensions of the bifid spine may or may not be present, and if present, can vary greatly in length. **Remarks**: The proximal element cycle and the lower part of the bifid spine are very similar to those of *F. predistentus*, but the upper part of the bifid spine, where it narrows to become parallel-sided (clearly visible in the holotype specimen in Haq, 1971, pl. 5, fig. 4), is different, and provides a criterion for separating the two species.

Furcatolithus intercalaris (Martini, 1976) n. comb.
Pl. 4, figs 13, 14

1976 *Sphenolithus intercalaris* Martini: p. 395, pl. 6, fig. 9; pl. 13, figs 25, 26.
2012 *Sphenolithus intercalaris* Martini, 1976 – Bown & Dunkley Jones: pl. 11, fig. 13.
2015 *Sphenolithus intercalaris* Martini, 1976 – Fioroni et al.: pl. 2, figs 15, 16.

Basionym: *Sphenolithus intercalaris* Martini, 1976, p. 395, pl. 6, fig. 9; pl. 13, figs 25, 26. Martini, E. 1976. Cretaceous to Recent calcareous nannoplankton from the Central Pacific Ocean (DSDP Leg 33). *Initial Reports of the Deep Sea Drilling Project*, **33**: 383–423. **Diagnosis**: A medium-sized furcatolith with a bifid spine and a proximal element cycle that is less than 5% of the total height. The proximal cycle is often missing. The angle between the median axis and the top of the proximal cycle is ~90°. The lateral profile of the bifid spine is outwardly convex. Thin distal extensions of the bifid spine may or may not be present, and if present, can vary greatly in length. **Remarks**: The holotype of *S. intercalaris* Martini, 1976 is an isolated bifid spine with the proximal cycle missing (much like the holotype of *F. distentus* Martini, 1965), which is interpreted here as being a broken specimen. The LM photograph by Fioroni et al. (2015, pl. 2, fig. 16) of *F. intercalaris* clearly shows very small proximal cycle elements below the bifid spine. This species seems to be very closely related to *S. predistentus*, as both species share a very low proximal element cycle with small elements, but clearly differs in the lateral profile of the bifid spine, which is strongly convex in *S. intercalaris,* and sub-linear in *S. predistentus*.

Furcatolithus akropodus (de Kaenel & Villa, 1996) n. comb.
Pl. 4, figs 15, 16

1990 *Sphenolithus* sp. 1 Fornaciari & Rio *in* Fornaciari et al.: p. 238, pl. 2, figs 1–3.
1996 *Sphenolithus akropodus* de Kaenel & Villa: p. 127, pl. 11, figs 1, 2, 4–11.
2012 *Sphenolithus akropodus* de Kaenel & Villa (1996) – Bown & Dunkley Jones: pl. 11, figs 29–38.
2017 *Sphenolithus akropodus* de Kaenel & Villa (1996) – Bergen et al.: pl. 10, figs 25–30; pl. 11, figs 1–4.

Basionym: *Sphenolithus obtusus* de Kaenel & Villa, 1996, p. 127, pl. 11, figs 1, 2, 4–11. de Kaenel, E. & Villa, G. 1996. Oligocene-Miocene calcareous nannofossil biostratigraphy and paleoecology from the Iberia Abyssal Plain. *Proceedings of the Ocean Drilling Program, Scientific Results*, **149**: 79–145. **Diagnosis**: A large to very large furcatolith with a tall bifid spine and a proximal element cycle that is ~15% of the total height. The angle between the median axis and the top of the proximal element cycle is >70°. The base of the proximal element cycle is concave. The tops of the elements in the proximal cycle are distally convex. The lateral end of the proximal cycle elements can extend slightly beyond the base of the bifid spine. Thin distal extensions of the bifid spine may or may not be present, and if present, can vary greatly in length. **Remarks**: The tall, linear-sided bifid spine of this species is diagnostic. The likely ancestor is *F. predistentus* or *F. celsus*.

Furcatolithus tribulosus (Roth, 1970) n. comb.
Pl. 4, figs 17, 18

1970 *Sphenolithus tribulosus* Roth: p. 870, pl. 14, figs 5, 7, 8.
2006 *Sphenolithus tribulosus* Roth, 1970 – Bown & Dunkley Jones: pl. 8, figs 1–5.

Basionym: *Sphenolithus tribulosus* Roth, 1970, p. 870, pl. 14, figs 5, 7, 8. Roth P.H. 1970. Oligocene calcareous nannoplankton biostratigraphy. *Eclogae Geologicae Helvetiae,* **63**(3): 799–881. **Diagnosis**: A large furcatolith with a bifid spine and a very low proximal element cycle that is <15% of the total height. The angle between the median axis and the top of the proximal element cycle is >80°. The base of the proximal element cycle is concave. Thin distal extensions of the bifid spine may or may not be present, and if present, can vary greatly in length. The base of the bifid spine is wider than in similar species (e.g. *S. predis-*

tentus), such that the lateral profile of the spine is concave. The bifid spine bears small serrate ridges, which are not often visible under the LM. **Remarks**: This species was very well illustrated by Bown & Dunkley Jones (2006, pl. 8, figs 1–5). It seems to be closely related to both *S. intercalaris* and *S. predistentus*, but differs from them in the concave lateral profile of the bifid spine.

Furcatolithus peartiae (Bown & Dunkley Jones, 2012 emend. Bergen & de Kaenel in Bergen et al., 2017) n. comb.
Pl. 4, figs 19, 20

2012 *Sphenolithus peartiae* Bown & Dunkley Jones: p. 34, pl. 11, figs 39–44.
2017 *Sphenolithus peartiae* Bown & Dunkley Jones, 2012 emend. Bergen & de Kaenel *in* Bergen et al.: p. 98, pl. 11, figs 5–14.

Basionym: *Sphenolithus peartiae* Bown & Dunkley Jones, 2012, p. 34, pl. 11, figs 39–44. Bown, P.R. & Dunkley Jones, T. 2012. Calcareous nannofossils from the Paleogene equatorial Pacific (IODP Expedition 320 Sites U1331–1334). *Journal of Nannoplankton Research,* **32**(2): 3–51. **Diagnosis**: A large furcatolith with a bifid spine and a proximal element cycle that is ~20–25% of the total height. The angle between the median axis and the top of the proximal element cycle is ~70°. The base of the proximal element cycle is concave. Thin distal extensions of the bifid spine may or may not be present, and if present, can vary greatly in length. The height of the bifid spine is lower than in similar species (e.g. *S. akropodus*). **Remarks**: This species is most similar to, and likely descended from, *F. akropodus*, but has a lower bifid spine.

Furcatolithus tawfikii (Bergen & de Kaenel *in* Bergen et al., 2017) n. comb.

2017 *Sphenolithus tawfikii* Bergen & de Kaenel *in* Bergen et al.: p. 95, pl. 9, figs 17–20.

Basionym: *Sphenolithus tawfikii* Bergen & de Kaenel *in* Bergen et al., 2017, p. 95, pl. 9, figs 17–20. Bergen, J., de Kaenel, E., Blair, S., Boesiger, T. & Browning, E. 2017. Oligocene–Pliocene taxonomy and stratigraphy of the genus *Sphenolithus* in the circum North Atlantic Basin: Gulf of Mexico and ODP Leg 154. *Journal of Nannoplankton Research*, **37**(2–3): 77–112. **Diagnosis**: A large furcatolith with a bifid spine and a proximal element cycle that is ~35–40% of the total height. The angle between the median axis and the top of the proximal element cycle is ~80°. The base of the proximal element cycle is linear at the periphery and steeply concave in the centre. Thin distal extensions of the bifid spine may or may not be present, and if present, can vary greatly in length. **Remarks**: This species has a taller proximal element cycle than any other species in the *F. predistentus* group, but, like the other members of the group, it has a high angle between the median axis and the top of the proximal cycle.

Furcatolithus ciperoensis Group

Species in this group all have low (<~50°) median axis/base bifid spine angles. The proximal cycles are high, ~30–45% of the total height, excluding the distal bifurca-

Table 2: Species of *Furcatolithus* grouped into informal morphological groups, by approximate order of first stratigraphical appearance

GROUP	MORPHOLOGICAL CRITERION	RANGE	SPECIES	PROXIMAL CYCLE % OF TOTAL HEIGHT	BIFID SPINE HEIGHT	MEDIAN AXIS/TOP OF PROXIMAL CYCLE ANGLE
F. predistentus	High (>~65°) median axis/base bifid spine angle	Middle Eocene–Late Oligocene (Lutetian–Chattian)	*F. cuniculus*	20–25%	high	90–100°
			F. predistentus	10%	high	80–90°
			F. obtusus	20–25%	high	60–65°
			F. celsus	10%	high	80–90°
			F. intercalaris	<10%	high	90°
			F. akropodus	15%	high	65–70°
			F. tribulosus	<15%	high	90–100°
			F. peartiae	20–25%	medium	65–70°
			F. tawfikii	35–40%	medium	80°
F. ciperoensis	Low (<~50°) median axis/base bifid spine angle High proximal cycle, ~30-45% of total height, excluding distal bifurcations	Oligocene (Rupelian–Chattian)	*F. bulbulus*	35%	medium	45–50°
			F. distentus	30–35%	medium	45°
			F. ciperoensis	40%	medium	40°
			F. patifunditis	40–45%	medium	30°
			F. directus	30–35%	medium	30–35°
F. triangularis	Very high proximal cycle, >60% of total height, excluding distal bifurcations	Early Oligocene–Early Miocene (Rupelian–Aquitanian)	*F. triangularis*	60%	low	40–50°
			F. avis	>65%	very low	40°
			F. umbrellus	>90%	very low to absent	n/a

tions. Species in this group are discussed below in approximate order of first stratigraphic appearance: *F. bulbulus*, *F. distentus*, *F. ciperoensis*, *F. patifunditis* and *F. directus*. A range chart for this group is presented in Figure 11.

Furcatolithus bulbulus (Bergen & de Kaenel *in* Bergen et al., 2017) n. comb.

2017 *Sphenolithus bulbulus* Bergen & de Kaenel *in* Bergen et al.: p. 96, pl. 9, figs 25–30; pl. 10, figs 1–6.

Basionym: *Sphenolithus bulbulus* Bergen & de Kaenel *in* Bergen et al., 2017, p. 96, pl. 9, figs 25–30; pl. 10, figs 1–6. Bergen, J., de Kaenel, E., Blair, S., Boesiger, T. & Browning, E. 2017. Oligocene–Pliocene taxonomy and stratigraphy of the genus *Sphenolithus* in the circum North Atlantic Basin: Gulf of Mexico and ODP Leg 154. *Journal of Nannoplankton Research*, **37**(2–3): 77–112. **Diagnosis**: A large furcatolith with a proximal element cycle that is ~35% of the total height. The angle between the median axis and the top of the proximal element cycle is ~45°. The base of the proximal element cycle is concave. The lateral periphery of the proximal cycle elements is convex. Thin distal extensions of the bifid spine may or may not be present, and if present, can vary greatly in length. **Remarks**: The indented lateral profile of the entire furcatolith, and the convex lateral periphery of the proximal cycle elements, distinguishes this species from the otherwise similar *F. ciperoensis* and *F. patifunditis*.

Furcatolithus distentus Martini, 1965
Pl. 4, figs 21, 22

1965 *Furcatolithus distentus* Martini: p. 407, pl. 35, figs 7–9.
1967 *Sphenolithus distentus* (Martini, 1965) Bramlette & Wilcoxon: pl. 1, fig. 5; pl. 2, figs 4, 5.
2017 *Sphenolithus distentus* (Martini, 1965) Bramlette & Wilcoxon – Bergen et al.: pl. 10, fig. 10.

Diagnosis: A large to very large furcatolith with a moderately high bifid spine, and a proximal element cycle that is ~25–30% of the total height. The angle between the median axis and the top of the proximal element cycle is approximately 45°. The base of the proximal element cycle is concave. Thin distal extensions of the bifid spine may or may not be present, and if present, can vary greatly in length. **Remarks**: See discussion for the genus.

Furcatolithus ciperoensis (Bramlette & Wilcoxon, 1967) n. comb.
Pl. 4, figs 23, 24

1967 *Sphenolithus ciperoensis* Bramlette & Wilcoxon: p. 120, pl. 2, figs 15–20.
2017 *Sphenolithus ciperoensis* Bramlette & Wilcoxon, 1967 – Bergen et al.: pl. 9, figs 5–10.

Basionym: *Sphenolithus ciperoensis* Bramlette & Wilcoxon, 1967, p. 120, pl. 2, figs 15–20. Bramlette, M.N. & Wilcoxon, J.A. 1967. Middle Tertiary calcareous nannoplankton of the Cipero section, Trinidad, W. I. *Tulane Studies in Geology,* **5**(3): 93–131. **Diagnosis**: A large furcatolith with a proximal element cycle that is ~40% of the total height and a moderately high bifid spine. The angle between the median axis and the top of the proximal element cycle is approximately 35–40°. The base of the proximal element cycle is concave. The lateral periphery is linear. Thin distal extensions of the bifid spine may or may not be present, and if present, can vary greatly in length. **Remarks**: This species is the most common furcatolith in Upper Oligocene assemblages. *Furcatolithus bulbulus, F. patifunditis* and *F. directus* are all similar to *F. ciperoensis*, and all have comparable ranges.

Furcatolithus patifunditus (Bergen & de Kaenel *in* Bergen et al., 2017) n. comb.

2017 *Sphenolithus patifunditus* Bergen & de Kaenel *in* Bergen et al.: pl. 9, figs 9–16.

Basionym: *Sphenolithus patifunditus* Bergen & de Kaenel *in* Bergen et al., 2017, p. 95, pl. 9, figs 9–16. Bergen, J., de Kaenel, E., Blair, S., Boesiger, T. & Browning, E. 2017. Oligocene–Pliocene taxonomy and stratigraphy of the genus *Sphenolithus* in the circum North Atlantic Basin: Gulf of Mexico and ODP Leg 154. *Journal of Nannoplankton Research*, **37**(2–3): 77–112. **Diagnosis**: A medium-sized furcatolith with a proximal element cycle that is ~40–45% of the total height, and a medium-height bifid spine. The angle between the median axis and the top of the proximal element cycle is approximately 30°. The base of the proxi-

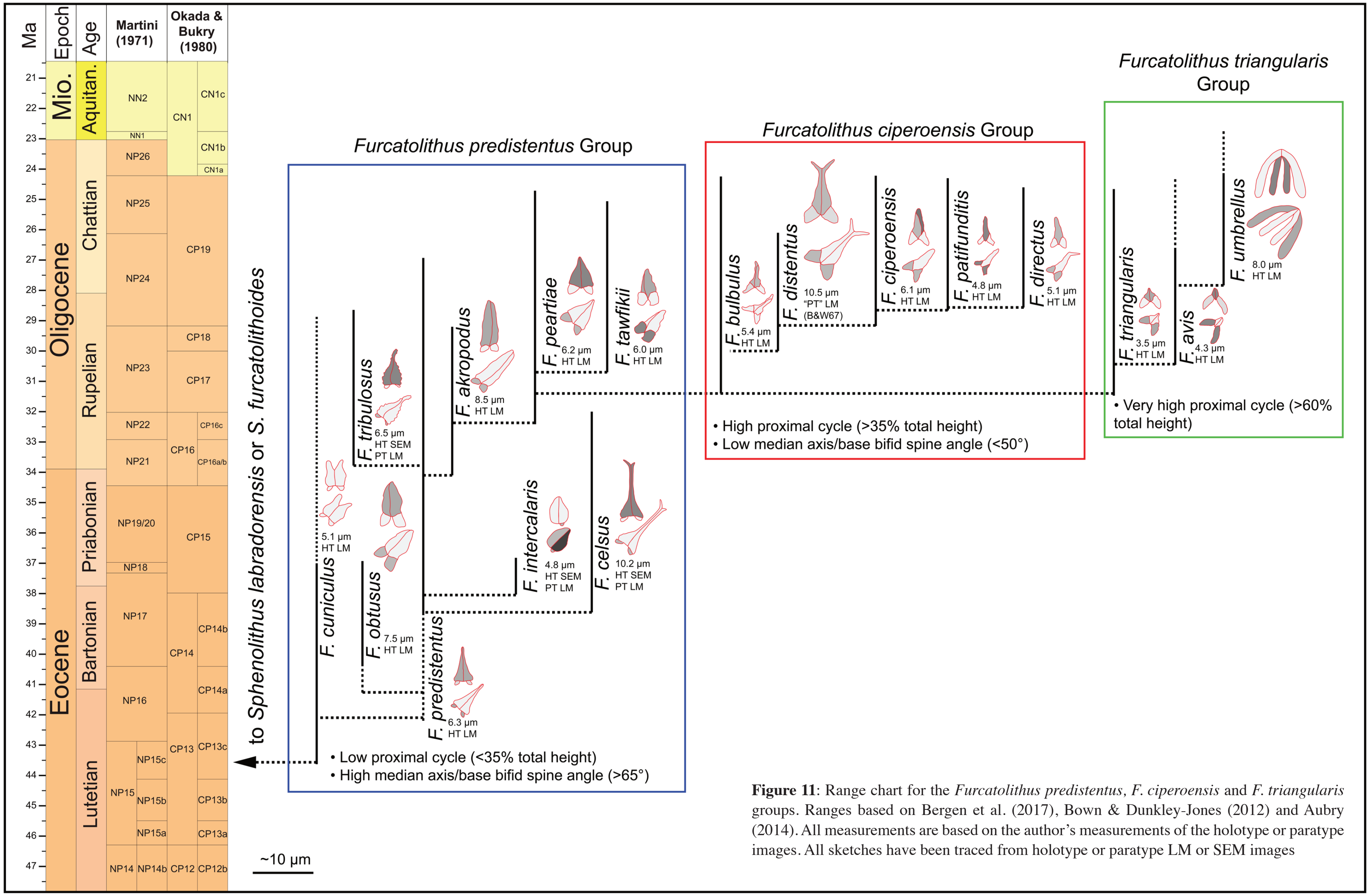

Figure 11: Range chart for the *Furcatolithus predistentus*, *F. ciperoensis* and *F. triangularis* groups. Ranges based on Bergen et al. (2017), Bown & Dunkley-Jones (2012) and Aubry (2014). All measurements are based on the author's measurements of the holotype or paratype images. All sketches have been traced from holotype or paratype LM or SEM images

mal element cycle is concave. Thin distal extensions of the bifid spine may or may not be present, and if present, can vary greatly in length. The lateral periphery is concave. **Remarks**: This species is very similar to *F. bulbulus*, in that both species have concave lateral peripheries, but *F. patifunditis* lacks the convex lateral periphery of the elements in the proximal cycle of that species.

Furcatolithus directus (Bergen & de Kaenel *in* Bergen et al., 2017) n. comb.

2017 *Sphenolithus directus* Bergen & de Kaenel *in* Bergen et al.: pl. 9, figs 21–24.

Basionym: *Sphenolithus directus* Bergen & de Kaenel *in* Bergen et al., 2017, p. 96, pl. 9, figs 21–24. Bergen, J., de Kaenel, E., Blair, S., Boesiger, T. & Browning, E. 2017. Oligocene–Pliocene taxonomy and stratigraphy of the genus *Sphenolithus* in the circum North Atlantic Basin: Gulf of Mexico and ODP Leg 154. *Journal of Nannoplankton Research*, **37**(2–3): 77–112. **Diagnosis**: A medium-sized furcatolith with a proximal element cycle that is ~35% of the total height, and a medium-height bifid spine. The angle between the median axis and the top of the proximal element cycle is 30–35°. Thin distal extensions of the bifid spine may or may not be present, and if present, can vary greatly in length. The lateral periphery is slightly concave. The proximal element cycle is less flared than similar species. **Remarks**: The main difference between this species and *F. ciperoensis* is that the proximal element cycle is less flared.

Furcatolithus triangularis **Group**

Species in this group all have very high proximal cycles, >60% of the total height, excluding the distal bifurcations. Species in this group are discussed below in approximate order of first stratigraphic appearance: *F. triangularis, F. avis* and *F. umbrellus*. A range chart for this group is presented in Figure 11.

Furcatolithus triangularis (Bergen & de Kaenel *in* Bergen et al., 2017) n. comb.
Pl. 4, figs 25, 26

1971 *Sphenolithus ciperoensis* Bramlette & Wilcoxon, 1967 – Roth et al.: pl. 3, figs 4, 9.

1990 *Sphenolithus* cf. *S. ciperoensis* Bramlette & Wilcoxon, 1967 – Okada, pl. 2, figs 3, 4.

2014 *Sphenolithus* sp. H Aubry: pp. 328, 329, 334.

2017 *Sphenolithus triangularis* Bergen & de Kaenel *in* Bergen et al.: p. 97, pl. 10, figs 15–24.

Basionym: *Sphenolithus triangularis* Bergen & de Kaenel *in* Bergen et al., 2017, p. 97, pl. 10, figs 15–24. Bergen, J., de Kaenel, E., Blair, S., Boesiger, T. & Browning, E. 2017. Oligocene–Pliocene taxonomy and stratigraphy of the genus *Sphenolithus* in the circum North Atlantic Basin: Gulf of Mexico and ODP Leg 154. *Journal of Nannoplankton Research,* **37**(2–3): 77–112. **Diagnosis**: A small furcatolith with a low bifid spine, and a proximal element cycle that is ~60% of the total height. The angle between the median axis and the top of the proximal element cycle is approximately 45°. The base of the proximal element cycle is strongly concave. Thin distal extensions of the bifid spine may or may not be present, and if present, can vary greatly in length. The total height and the basal width of the proximal cycle are approximately equal, such that the peripheral outline approximates an equilateral triangle. **Remarks**: This small species was probably overlooked in many earlier studies, where it may have been considered a small, low form of *S. ciperoensis*.

Furcatolithus avis (Aljahdali et al., 2015) n. comb.
Pl. 4, figs 27, 28

2015 *Sphenolithus avis* Aljahdali et al.: p. 193, pl. 1, figs 1–5.

Basionym: *Sphenolithus avis* Aljahdali et al., 2015, p. 193, pl. 1, figs 1a–d, 2a–d, 3a–d, 4a–f, 5a, b. Aljahdali, M., Wise, S.W. Jr., Bergen, J. & Pospichal, J.J. 2015. A new biostratigraphically significant Late Oligocene *Sphenolithus* species from the equatorial region. *Micropaleontology*, **61**(3): 193–197. **Diagnosis**: A small to medium-sized furcatolith with a very low bifid spine, and a proximal element cycle that is ~70% of the total height. The elements of the proximal cycle are curved in lateral view, such that the base of the proximal cycle is strongly concave. The angle between the median axis and the top of the proximal element cycle is approximately 40°. Thin distal extensions of the bifid spine may or may not be present, and if present, can vary greatly in length. The total height and basal width

Plate 1

1, 2: *Diantholitha*; 3–18: *S. primus* Group; 19, 20: *S. anarrhopus* Group; 21–26: *S.radians* Group; 27–30: *S. kempii* Group

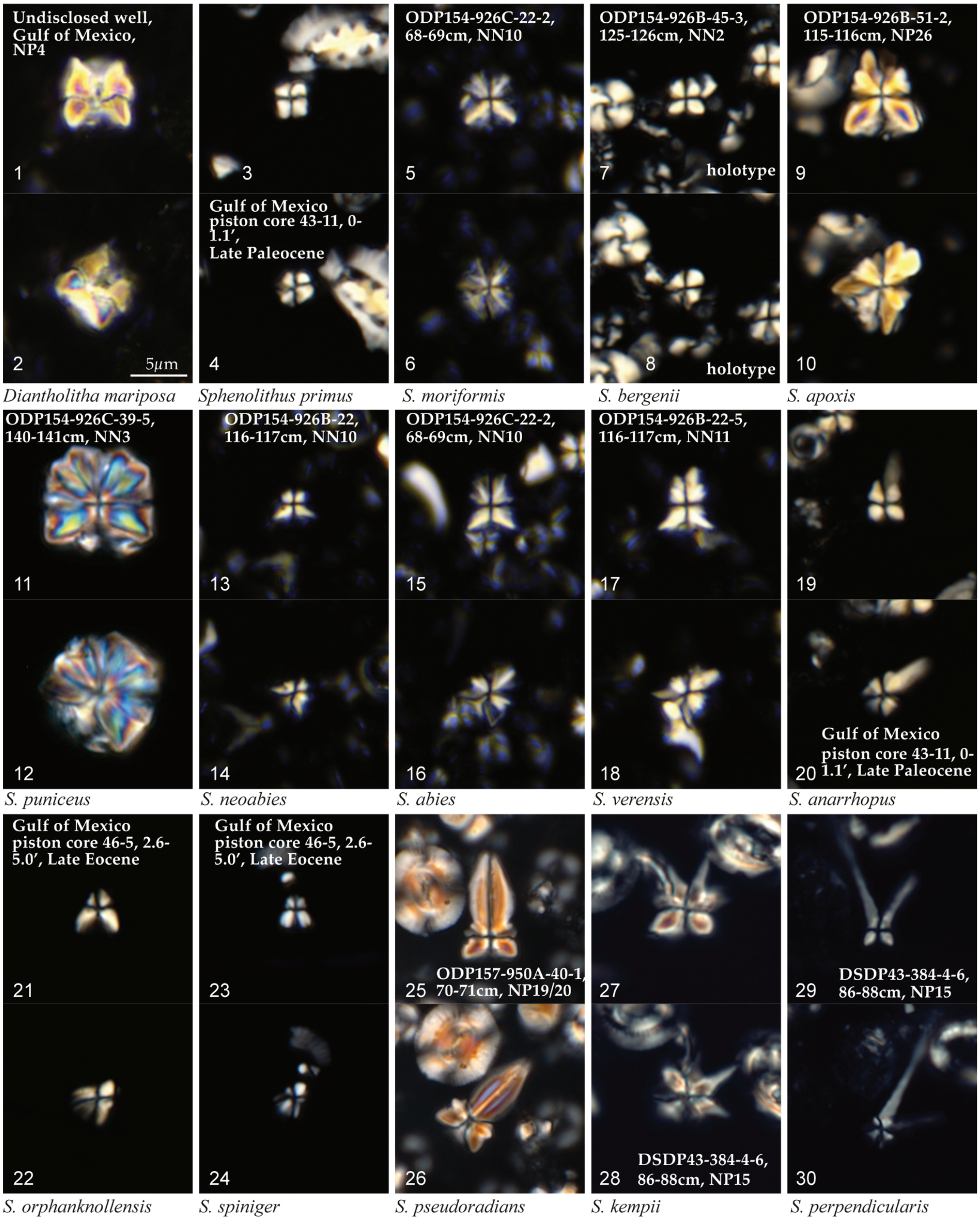

Plate 2

1–10: *S. kempii* Group; 11–28: *S. dissimilis* Group; 29, 30: *S. conicus* Group

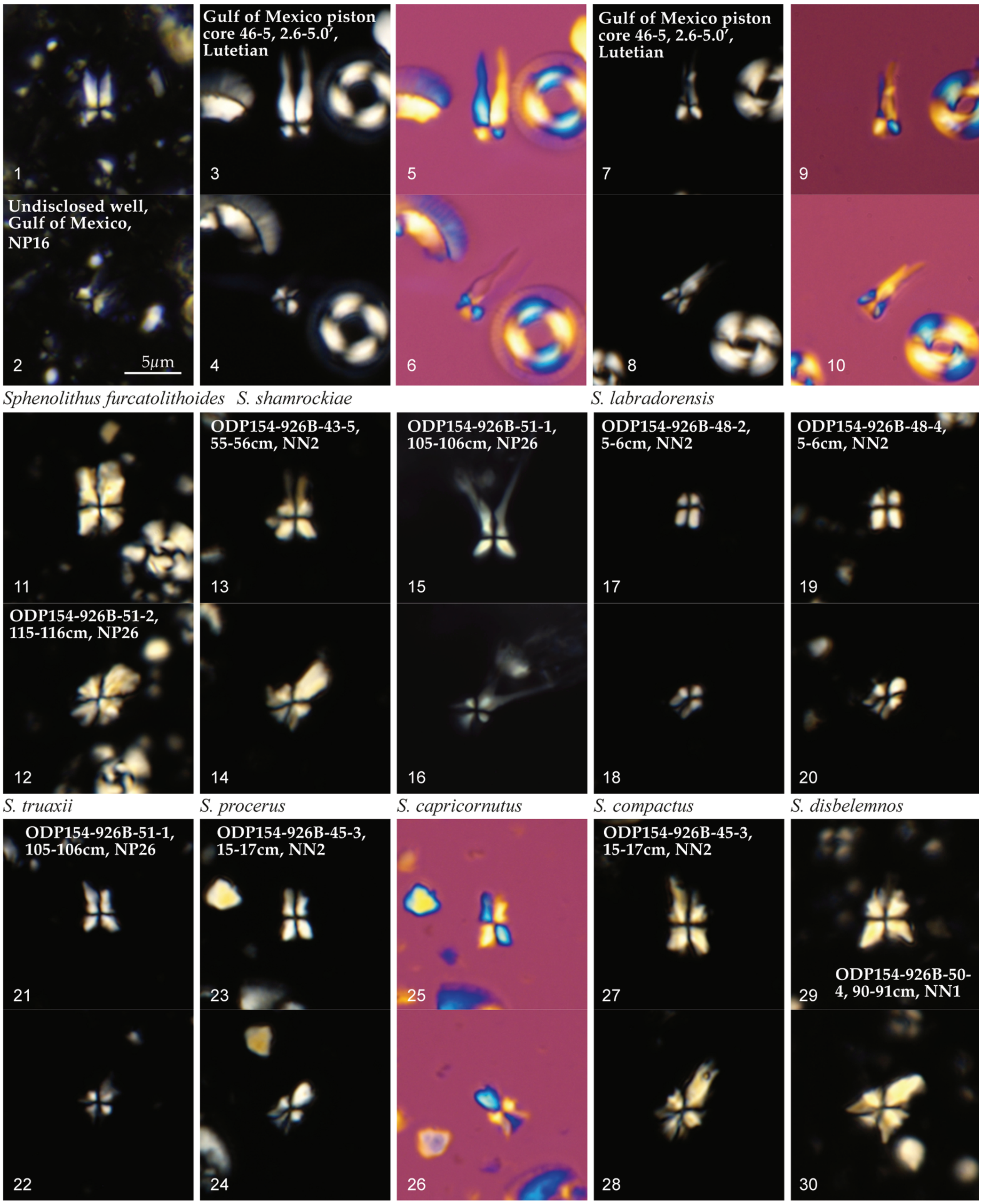

Sphenolithus furcatolithoides *S. shamrockiae* *S. labradorensis*

S. truaxii *S. procerus* *S. capricornutus* *S. compactus* *S. disbelemnos*

S. multispinatus *S. dissimilis* *S. cometa* *S. conicus*

Plate 3

1–12: *S. conicus* Group; 13–28: *S. delphix* Group

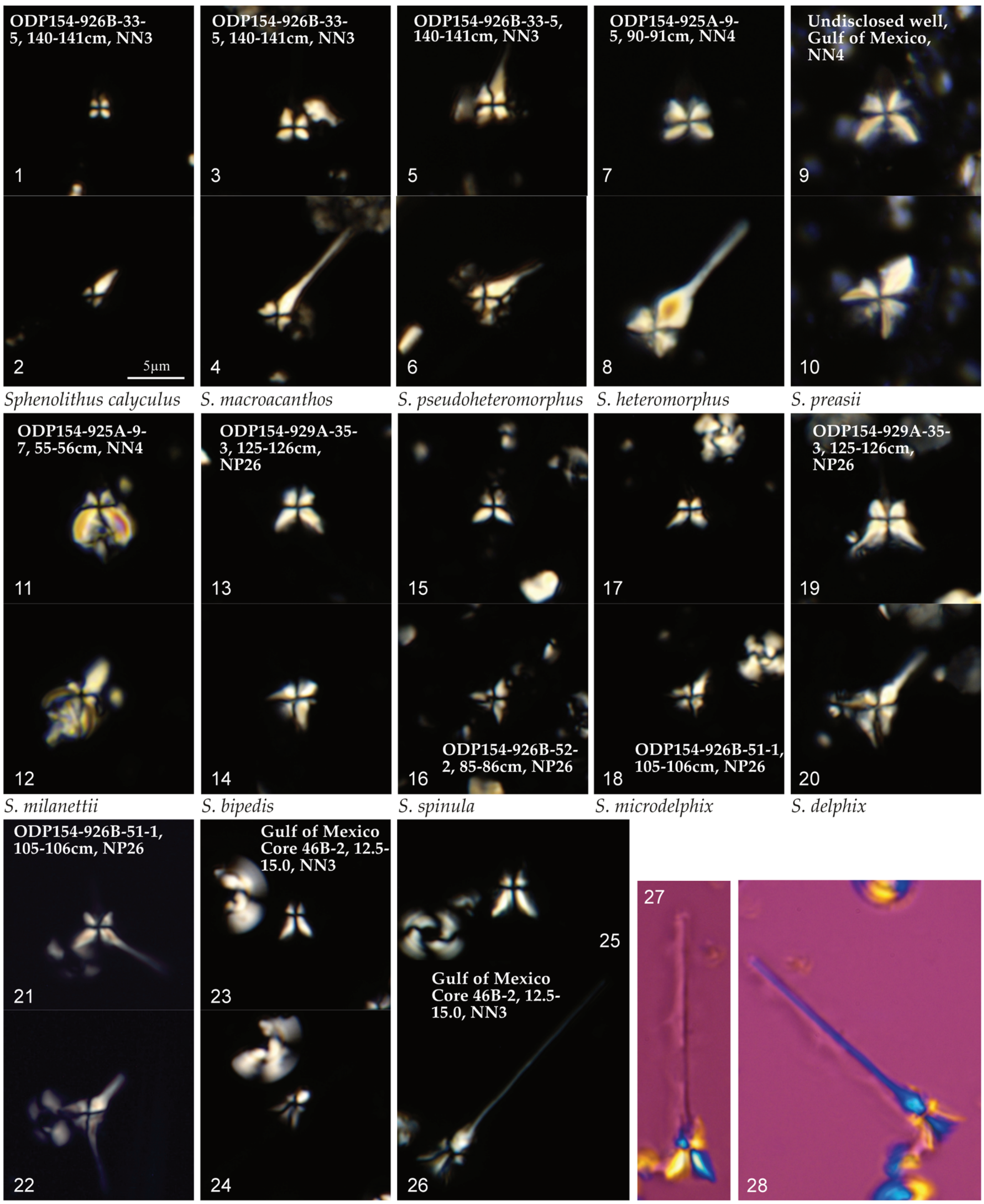

Sphenolithus calyculus | *S. macroacanthos* | *S. pseudoheteromorphus* | *S. heteromorphus* | *S. preasii*

S. milanettii | *S. bipedis* | *S. spinula* | *S. microdelphix* | *S. delphix*

S. delphix | *S. tintinnabulum* | *S. belemnos*

Plate 4

1–20: *F. predistentus* Group; 21–24: *F. ciperoensis* Group; 25–30: *F. triangularis* Group

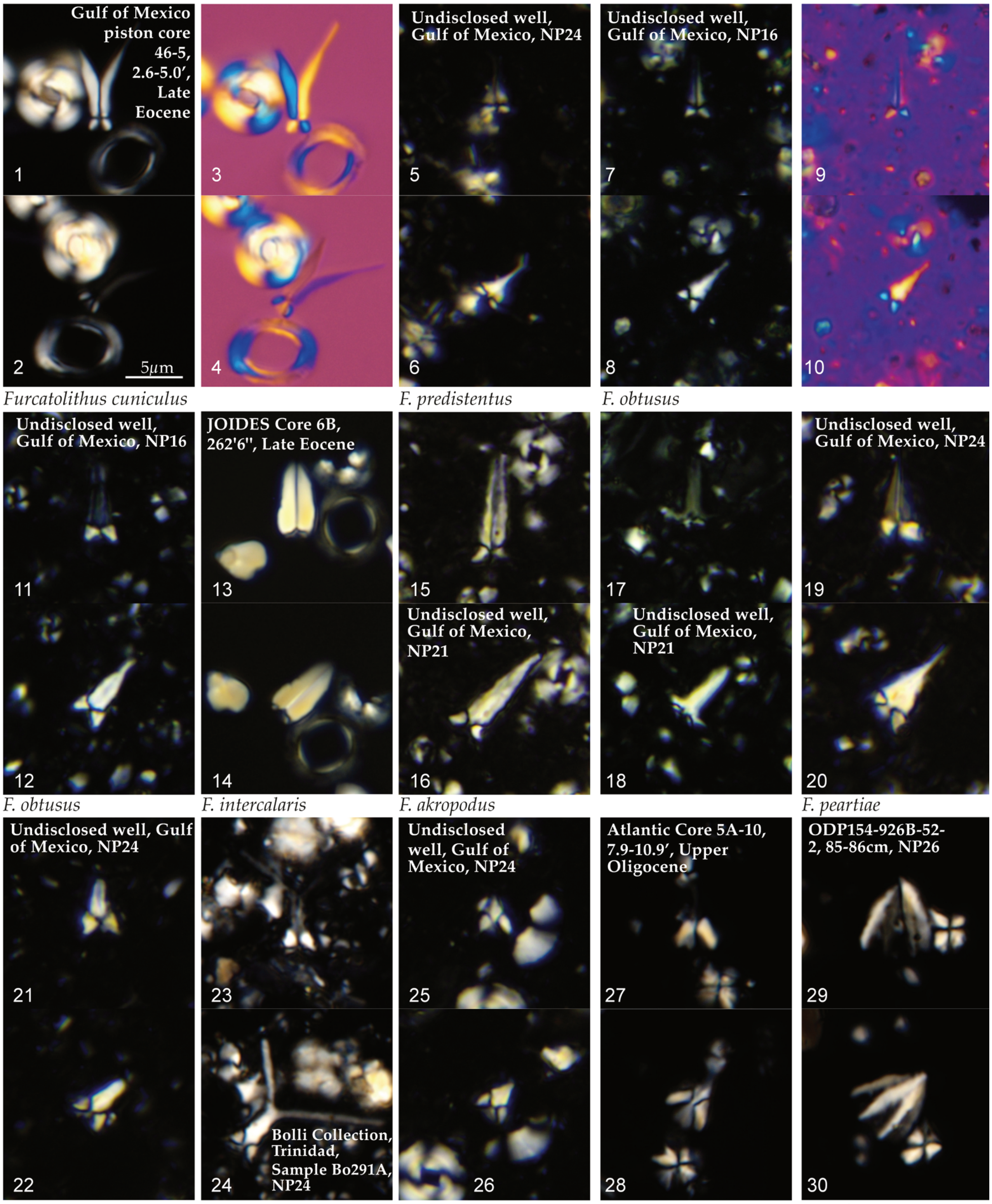

Furcatolithus cuniculus (1–4); *F. predistentus* (5–6); *F. obtusus* (7–8)

F. obtusus (11–12); *F. intercalaris* (13–14); *F. akropodus* (15–16); *F. peartiae* (19–20)

F. distentus (21–22); *F. ciperoensis* (23–24); *F. triangularis* (25–26); *F. avis* (27–28); *F. umbrellus* (29–30) of the proximal cycle are approximately equal, such that the peripheral outline approximates an equilateral triangle. **Remarks**: This species is clearly intermediate between *F. triangularis* and *F. umbrellus,* having the small bifid spine of *F. triangularis*, and a high proximal cycle with curved elements, similar to that of *F. umbrellus*.

Furcatolithus umbrellus (Bukry, 1971b) n. comb.
Pl. 4, figs 29, 30

1971b *Catinaster*? *umbrellus* Bukry: p. 50, pl. 3, figs 10–13.
1986 *Sphenolithus umbrellus* (Bukry, 1971b) Aubry & Knüttel *in* Knüttel: p. 279, pl. 5, figs 1, 2, 5–10.

Basionym: *Catinaster*? *umbrellus* Bukry, 1971b, p. 50, pl. 3, figs 10–13. Bukry, D. 1971b. *Discoaster* evolutionary trends. *Micropaleontology*, **17**(1): 43–52. **Diagnosis**: A large to very large furcatolith with a greatly reduced vestigial bifid spine, or no bifid spine. The proximal element cycle is >95% of the total height. The proximal cycle elements are curved, so that the base of the proximal element cycle is strongly concave. **Remarks**: This species is the last representative of the genus before its extinction in the Early Miocene. The SEM photographs of Knüttel (1986, pl. 5, figs 1, 2) show some specimens of *F. umbrellus* with tiny elements just above the top of the proximal cycle, which may be the vestigial elements of a bifid spine.

5. Conclusions

From their origin at ~62 Ma, the Sphenolithaceae flourished alongside other heterococcolith groups before becoming extinct at ~3.5 Ma, providing an ~59.5 Myr record of their evolution. Their ultrastructure has been shown here to be relatively simple, the major components being shared by most species, and with variability between species mostly accommodated by varying proportions of these major components. Characterisation of the proximal element cycle, the lower and upper lateral element cycles and the apical structure is necessary to reliably identify *Sphenolithus* species, while characterisation of the proximal element cycle and bifid spine is necessary to recognise *Furcatolithus* species. The upward growth of the upper lateral element cycle and its transition into a bifid spine, as well as recognition that the lower lateral element cycle is absent in some species, has been shown to be key to understanding the evolution of *Furcatolithus* from *Sphenolithus*. When examining species with a bifid spine under cross-polarised light, particular attention must be paid to the orientation of the median suture of the spine relative to the microscope slide because the birefringence of the spine changes greatly between orientations where the median suture is parallel or orthogonal to the slide.

Acknowledgements

Many thanks to Dr Jeremy Young, who encouraged me to follow up on my initial observations on the lateral element cycles of *Sphenolithus*. His advice and insights throughout the writing of this paper were invaluable, although any errors are mine alone. Jeremy astutely made the observation that *S. compactus* is a senior synonym of *S. paratintinnabulum*. My colleague Dr Dave Bord was very helpful in discussing and refining the concepts in this paper. I am very grateful to Drs Jean Self-Trail and Jim Bergen, who provided invaluable advice on the manuscript before submission. The reviews of Drs Denise Kulhanek and Tom Dunkley Jones were much appreciated and improved the manuscript substantially. Thanks also to Dr Daniel Peyrot of the School of Earth and Environment at the University of Western Australia for providing me with access to the research facilities and equipment.

References

Agnini, C., Fornaciari, E. & Raffi, I. 2008. Three new species of calcareous nannofossil from Late Palaeocene and Early Eocene assemblages (Ocean Drilling Program Site 1262, Walvis Ridge, SE Atlantic Ocean). *Journal of Nannoplankton Research*, **30**: 51–56.

Agnini, C., Fornaciari, E., Raffi, I., Catanzariti, R., Pälike, H., Backman, J. & Rio, D. 2014. Biozonation and biochronology of Paleogene calcareous nannofossils from low and middle latitudes. *Newsletters on Stratigraphy*, **47**(2): 131–181.

Aljahdali, M., Wise, S.W. Jr., Bergen, J. & Pospichal, J.J. 2015. A new biostratigraphically significant Late Oligocene *Sphenolithus* species from the equatorial region. *Micropaleontology*, **61**(3): 193–197.

Aubry, M-P. 1989. *Handbook of Cenozoic calcareous nannoplankton, Book 3: Ortholithae (Pentaliths and others), Heliolithae (Fasciculiths, Sphenoliths and others).* Micropaleontology Press, New York.

Aubry, M-P. 2014. *Cenozoic coccolithophores: Discoasterales (CC-B).* Atlas of Micropaleontology Series. Micropaleontology Press, New York: 431 pp.

Aubry, M-P., Bord, D. & Rodriguez, O. 2011. New taxa of the Order Discoasterales Hay, 1977. *Micropaleontology,* **57**(3): 269–287.

Backman, J. 1978. Late Miocene–Early Pliocene nannofossil biochronology and biogeography in the Vera Basin, SE Spain. *Stockholm Contributions in Geology,* **32**(2): 93–114.

Backman, J. 1980. Miocene–Pliocene nannofossils and sedimentation rates in the Hatton–Rockall Basin, NE Atlantic Ocean. *Stockholm Contributions in Geology,* **36**: 1–91.

Bergen, J.A., de Kaenel, E., Blair, S., Boesiger, T. & Browning, E. 2017. Oligocene–Pliocene taxonomy and stratigraphy of the genus *Sphenolithus* in the circum North Atlantic Basin: Gulf of Mexico and ODP Leg 154. *Journal of Nannoplankton Research,* **37**(2–3): 77–112.

Bergen, J.A., Truax, S., de Kaenel, E., Blair, S., Browning, E., Lundquist, J., Boesiger, T., Bolivar, M. & Clark, K. 2019a. BP Gulf of Mexico Neogene astronomically tuned time scale (BP GNATTS). *Geological Society of America Bulletin,* **131**(11–12): 1871–1888. https://doi.org/10.1130/B35062.1

Bergen, J.A., Truax S., de Kaenel, E., Blair, S., Browning, E., Lundquist, J., Boesiger, T., Bolivar, M. & Clark, K. 2019b. Gulf of Mexico Neogene astronomically-tuned time scale. https://doi.org/10.1594/PANGAEA.897069. Supplement to Bergen et al., 2019a.

Blow, W.H. 1979. *The Cainozoic Globigerinida*. E.J. Brill, Leiden.

Bown, P.R. 2005a. Palaeogene calcareous nannofossils from the Kilwa and Lindi areas of coastal Tanzania (Tanzania Drilling Project 2003–4). *Journal of Nannoplankton Research*, **27**(1): 21–95.

Bown, P.R. 2005b. Cenozoic calcareous nannofossil biostratigraphy, ODP Leg 198 Site 1208 (Shatsky Rise, northwest Pacific Ocean). *Proceedings of the ODP, Scientific Results*, **198**: 1–44.

Bown, P.R. 2010. Calcareous nannofossils from the Paleocene/Eocene Thermal Maximum interval of southern Tanzania (TDP Site 14). *Journal of Nannoplankton Research*, **31**(1): 11–38.

Bown, P.R. & Dunkley Jones, T. 2006. New Palaeogene calcareous nannofossil taxa from coastal Tanzania: Tanzania Drilling Project Sites 11 to 14. *Journal of Nannoplankton Research*, **28**(1): 17–34.

Bown, P.R. & Dunkley Jones, T. 2012. Calcareous nannofossils from the Paleogene equatorial Pacific (IODP Expedition 320 Sites U1331–1334). *Journal of Nannoplankton Research*, **32**(2): 3–51.

Bown, P.R. & Newsam, C. 2017. Calcareous nannofossils from the Eocene North Atlantic Ocean (IODP Expedition 342 Sites U1403–1411). *Journal of Nannoplankton Research*, **37**(1): 25–60.

Bramlette, M.N. & Wilcoxon, J.A. 1967. Middle Tertiary calcareous nannoplankton of the Cipero Section, Trinidad, W. I. *Tulane Studies in Geology*, **5**: 93–131.

Brönnimann, P. & Stradner, H. 1960. Die Foraminiferen- und Discoasteridenzonen von Kuba und ihre interkontinentale Korrelation. *Erdöl-Zeitschrift*, **76**: 364–369.

Bukry, D. 1971a. Cenozoic calcareous nannofossils from the Pacific Ocean. *San Diego Society of Natural History Transactions*, **16**: 303–327.

Bukry, D. 1971b. *Discoaster* evolutionary trends. *Micropaleontology*, **17**: 43–52.

Bukry, D. 1973. Coccolith stratigraphy, eastern equatorial Pacific, Leg 16, Deep Sea Drilling Project. *Initial Reports of the DSDP*, **16**: 653–711.

Bukry, D. 1985. Mid-Atlantic Ridge coccolith and silicoflagellate biostratigraphy, Deep Sea Drilling Project Sites 558 and 563. *Initial Reports of the DSDP*, **82**: 591–603.

Bukry, D. & Bramlette, M.N. 1969. Some new and stratigraphically useful calcareous nannofossils of the Cenozoic. *Tulane Studies in Geology and Paleontology*, **7**: 131–142.

Bybell, L.M. & Self-Trail, J.M. 1997. Late Paleocene and Early Eocene calcareous nannofossils from three boreholes in an onshore–offshore transect from New Jersey to the Atlantic Continental Rise. *Proceedings of the ODP, Scientific Results*, **150X**: 91–110.

Deflandre, G. 1952. Classe des coccolithophoridés (Coccolithophoridae Lohmann, 1902). *In*: P.-P. Grassé (Eds). *Traité de Zoologie, Anatomie, Systématique, Biologie*, **1**(1): 439–470.

Deflandre, G. 1953. Hétérogénéité intrinsèque et pluralité des éléments dans les coccolithes actuels et fossiles. *Comptes rendus Académie des Sciences, Paris*, **237**: 1785–1787.

Deflandre, G. & Fert, C. 1954. Observations sur les coccolithophoridés actuels et fossiles en microscopie ordinaire et électronique. *Annales de Paléontologie*, **40**: 115–176.

Denne, R.A. 2007. Paleogene calcareous nannofossil bioevents from the fold belts of the central Gulf of Mexico. *In*: L. Kennan, J. Pindel & N.C. Rosen (Eds). *The Paleogene of the Gulf of Mexico and Caribbean basins: Processes, events, and petroleum systems*. Proceedings of the 27th Annual Gulf Coast Section of the Society of Economic Paleontologists and Mineralogists (Society for Sedimentary Geology) Foundation Bob F. Perkins Research Conference, Houston, Texas:

211–231.

Fioroni, C., Villa, G., Persico, D. & Jovane, L. 2015. Middle Eocene–Lower Oligocene calcareous nannofossil biostratigraphy and paleoceanographic implications from Site 711 (equatorial Indian Ocean). *Marine Micropaleontology*, **118**: 50–62.

Firth, J.V. 1989. Eocene and Oligocene calcareous nannofossils from the Labrador Sea, ODP Leg 105. *Proceedings of the ODP, Scientific Results*, **105**: 263–286.

Fornaciari, E. & Agnini, C. 2009. Taxonomic note: *Sphenolithus pseudoheteromorphus,* a new Miocene calcareous nannofossil species from the equatorial Indian Ocean. *Journal of Nannoplankton Research*, **30**(2): 97–101.

Fornaciari, E., Raffi, I., Rio, D., Villa, G., Backman, J. & Olafsson, G. 1990. Quantitative distribution patterns of Oligocene and Miocene calcareous nannofossils from the western equatorial Indian Ocean. *Proceedings of the ODP, Scientific Results*, **115**: 237–254.

Gartner, S., Jr. 1971. Calcareous nannofossils from the JOIDES Blake Plateau cores, and revision of Paleogene nannofossil zonation. *Tulane Studies in Geology and Paleontology*, **8**: 101–121.

Gennari, R., Persico, D., Turco, E., Villa, G., Iaccarino, S.M., Florindo, F., Lurcock, P.C. & de Santana dos Anjos Zerfass, G. 2017. High-resolution integrated calcareous plankton biostratigraphy and magnetostratigraphy at the Oligocene–Miocene transition in southwestern Atlantic Ocean. *Geological Journal*, **53**(3): 1079–1101.

Haq, B.U. 1971. Paleogene calcareous nannoflora. Parts I–IV. *Stockholm Contributions in Geology*, **25**: 1–158.

Haq, B.U. & Berggren, W.A. 1978. Late Neogene calcareous plankton biochronology of the Rio Grande Rise (South Atlantic Ocean). *Journal of Paleontology*, **52**(6): 1167–1194.

Jiang, S., Wang, Y., Varol, O., da Gama, R.O.B.P. & Blaj, T. 2016. A new early Miocene *Sphenolithus* species from the South China Sea. *Journal of Nannoplankton Research*, **36**(1): 61–63.

de Kaenel, E. & Villa, G. 1996. Oligocene–Miocene calcareous nannofossil biostratigraphy and paleoecology from the Iberian Abyssal Plain. *Proceedings of the ODP, Scientific Results*, **149**: 79–145.

Khalil, H. & Al Sawy, S. 2014. Integrated biostratigraphy, stage boundaries and paleoclimatology of the Upper Cretaceous–Lower Eocene successions in Kharga and Dakhala Oases, Western Desert, Egypt. *Journal of African Earth Sciences*, **96**: 220–242.

Knüttel, S. 1986. Calcareous nannofossil biostratigraphy of the central East Pacific Rise, Deep Sea Drilling Project Leg 92: Evidence for downslope transport of sediments. *Initial Reports of the DSDP*, **92**: 255–290.

Locker, S. 1967. Neue Coccolithophoriden (Flagellata) aus dem Alttertiär Norddeutschlands. *Geologie*, **16**: 361–365.

Lupi, C. & Wise, S.W., Jr. 2006. Calcareous nannofossil biostratigraphic framework for middle Eocene sediments from ODP Hole 1260A, Demerara Rise. *Revue de Micropaléontologie*, **49**(4): 245–253.

Mai, H. 2001. New coccolithophorid taxa from the Guelhemmerberg airshaft, Lower Paleocene, The Netherlands. *Micropaleontology*, **47**: 144–154.

Maiorano, P. & Monechi, S. 1997. New early Miocene species of *Sphenolithus* Deflandre, 1952 from the North Atlantic Ocean. *Journal of Nannoplankton Research*, **19**(2): 103–107.

Maiorano, P. & Monechi, S. 1998. Revised correlations of Early and Middle Miocene calcareous nannofossil events and magnetostratigraphy from DSDP Site 563 (North Atlantic Ocean). *Marine Micropaleontology*, **35**: 235–255.

Martini, E. 1965. Mid-Tertiary calcareous nannoplankton from Pacific deep sea cores. *In*: W.F. Whittard & R. Bradshaw (Eds). *Submarine geology and geophysics*. Proceedings of the 17th Symposium of the Colston Research Society. Butterworths, London: 393–411.

Martini, E. 1971. Standard Tertiary and Quaternary calcareous nannoplankton zonation. *In*: A. Farinacci (Ed.). *Proceedings of the II Planktonic Conference, Roma, 1970*. *Edizione Tecnoscienzia*, **2**: 737–785.

Martini, E. 1976. Cretaceous to Recent calcareous nannoplankton from the central Pacific Ocean (DSDP Leg 33). *Initial Reports of the DSDP*, **33**: 383–423.

Martini, E. 1986. Paleogene calcareous nannoplankton from the southwest Pacific Ocean, Deep Sea Drilling Project, Leg 90. *Initial Reports of the DSDP*, **90**: 747–761.

Okada, H. 1990. Quaternary and Paleogene calcareous nannofossils, Leg 115. *Proceedings of the ODP, Scientific Results*, **115**: 129–174.

Okada, H. & Bukry, D. 1980. Supplementary modification and introduction of code numbers to the low-latitude coccolith biostratigraphic zonation (Bukry, 1973; 1975). *Marine Micropaleontology*, **5**: 321–325.

Olafsson, G. 1989. Quantitative calcareous nannofossil biostratigraphy of upper Oligocene to middle Miocene sediment from ODP Hole 667A and middle Miocene sediment from DSDP site 574. *Proceedings of the ODP, Scientific Results*,

108: 9–22.

Perch-Nielsen, K. 1971a. Einige neue Coccolithen aus dem Paläozän der Bucht von Biskaya und dem Eozän der Labrador See. *Bulletin of the Geological Society of Denmark*, **21**: 347–361.

Perch-Nielsen, K. 1971b. Neue Coccolithen aus dem Paläozän von Dänemark, der Bucht von Biskaya und dem Eozän der Labrador See. *Bulletin of the Geological Society of Denmark*, **21**: 51–66.

Perch-Nielsen, K. 1972. Remarks on Late Cretaceous to Pleistocene coccoliths from the North Atlantic. *Initial Reports of the DSDP*, **12**: 1003–1069.

Perch-Nielsen, K. 1977. Albian to Pleistocene calcareous nannofossils from the western south Atlantic, DSDP Leg 39. *Initial Reports of DSDP*, **39**: 699–823.

Perch-Nielsen, K. 1980. New Tertiary calcareous nannofossils from the South Atlantic. *Eclogae Geologicae Helvetiae*, **73**(1): 1–7.

Perch-Nielsen, K. 1985. Cenozoic calcareous nannofossils. *In*: H.M. Bolli, J.B. Saunders & K. Perch-Nielsen (Eds). *Plankton Stratigraphy*. Cambridge University Press, Cambridge: 427–555.

Perch-Nielsen, K., Sadek, A., Barakat, M.G. & Teleb, F. 1978. Late Cretaceous and Early Tertiary calcareous nannofossil and planktonic foraminifera zones from Egypt. Actes du 6e Colloque Africain de Micropaléontologie, Tunis, 1979. *Annales des Mines et de la Géologie Tunis*, **28**(2): 337–403.

Proto Decima, F., Medizza, F. & Todesco, L. 1978. Southeastern Atlantic, Leg 40, calcareous nannofossils. *Initial Reports of the DSDP*, **40**: 571–634.

Quinterno, P.J. 1994. Calcareous nannofossil biostratigraphy: Sites 840 (Tonga Ridge) and 841 (Tonga Trench). *Proceedings of the ODP, Scientific Results*, **135**: 267–284.

Romein, A.J.T. 1979. Lineages in Early Paleogene calcareous nannoplankton. *Utrecht Micropaleontological Bulletins*, **22**: 1–231.

Roth P. H. 1970. Oligocene calcareous nannoplankton biostratigraphy. *Eclogae Geologicae Helvetiae*, **63**(3): 799–881.

Roth, P.H., Franz, H.E. & Wise, S.W., Jr. 1971. Morphological study of selected members of the genus *Sphenolithus* Deflandre (Incertae sedis, Tertiary). *In*: A. Farinacci (Ed.). *Proceedings of the II Planktonic Conference, Roma. Edizione Tecnoscienzia*, **2**: 1099–1119.

Shamrock, J.L. 2010. A new calcareous nannofossil species of the genus *Sphenolithus* from the Middle Eocene (Lutetian) and its biostratigraphic significance. *Journal of Nannoplankton Research*, **31**: 5–10.

Steurbaut, E. & Sztrákos, K. 2008. Danian/Selandian boundary criteria and North Sea Basin–Tethys correlations based on calcareous nannofossil and foraminiferal trends in SW France. *Marine Micropaleontology*, **67**: 1–29.

Towe, K.M. 1979. Variation and systematics in calcareous nannofossils of the genus *Sphenolithus*. *American Zoologist*, **19**: 555–572.

Wade, B.S., Pearson, P.N., Berggren, W.A. & Pälike, H. 2011. Review and revision of Cenozoic tropical planktonic foraminiferal biostratigraphy and calibration to the geomagnetic polarity and astronomical time scale. *Earth-Science Reviews*, **104**: 111–142.

Wilcoxon, J.A. 1970. *Sphenaster*, new genus, a Pliocene calcareous nannofossil from the tropical Indo-Pacific. *Tulane Studies in Geology and Paleontology*, **8**: 78–81.

Young, J.R., Bergen, J.A., Bown, P.R., Burnett, J.A., Fiorentino, A., Jordan, R.W., Kleijne, A., van Niel, B.E., Romein, A.J.T. & von Salis, K. 1997. Guidelines for coccolith and calcareous nannofossil terminology. *Palaeontology*, **40**: 875–912.

Young, J.R., Bown P.R. & Lees J.A. 2018. '*Ilselithina*'. Nannotax3 website. Accessed 1 August 2018. https://archive.is/SIOB4